Title
On the theory of core-mantle coupling

Journal
Geophysical & Astrophysical Fluid Dynamics, 106(2)

ISSN
0309-1929

Authors
Roberts, Paul H
Aurnou, Jonathan M

Publication Date
2012-04-01

DOI
10.1080/03091929.2011.589028

Peer reviewed

Geophysical & Astrophysical Fluid Dynamics

Publication details, including instructions for authors and subscription information:
http://www.tandfonline.com/loi/ggaf20

On the theory of core-mantle coupling

Paul H. Roberts [a] & Jonathan M. Aurnou [b]

[a] Department of Mathematics, University of California, Los Angeles, CA 90095, USA

[b] Department of Earth and Space Sciences, University of California, Los Angeles, CA 90095, USA

Available online: 01 Aug 2011

To cite this article: Paul H. Roberts & Jonathan M. Aurnou (2012): On the theory of core-mantle coupling, Geophysical & Astrophysical Fluid Dynamics, 106:2, 157-230

To link to this article: http://dx.doi.org/10.1080/03091929.2011.589028

Geophysical and Astrophysical Fluid Dynamics
Vol. 106, No. 2, April 2012, 157–230

On the theory of core-mantle coupling

PAUL H. ROBERTS*† and JONATHAN M. AURNOU‡

†Department of Mathematics, University of California, Los Angeles, CA 90095, USA
‡Department of Earth and Space Sciences, University of California, Los Angeles, CA 90095, USA

(*Received 19 July 2010; in final form 14 April 2011; first published online 1 August 2011*)

This article commences by surveying the basic dynamics of Earth's core and their impact on various mechanisms of core-mantle coupling. The physics governing core convection and magnetic field production in the Earth is briefly reviewed. Convection is taken to be a small perturbation from a hydrostatic, "adiabatic reference state" of uniform composition and specific entropy, in which thermodynamic variables depend only on the gravitational potential. The four principal processes coupling the rotation of the mantle to the rotations of the inner and outer cores are analyzed: viscosity, topography, gravity and magnetic field. The gravitational potential of density anomalies in the mantle and inner core creates density differences in the fluid core that greatly exceed those associated with convection. The implications of the resulting "adiabatic torques" on topographic and gravitational coupling are considered. A new approach to the gravitational interaction between the inner core and the mantle, and the associated gravitational oscillations, is presented. Magnetic coupling through torsional waves is studied. A fresh analysis of torsional waves identifies new terms previously overlooked. The magnetic boundary layer on the core-mantle boundary is studied and shown to attenuate the waves significantly. It also hosts relatively high speed flows that influence the angular momentum budget. The magnetic coupling of the solid core to fluid in the tangent cylinder is investigated. Four technical appendices derive, and present solutions of, the torsional wave equation, analyze the associated magnetic boundary layers at the top and bottom of the fluid core, and consider gravitational and magnetic coupling from a more general standpoint. A fifth presents a simple model of the adiabatic reference state.

Keywords: Geostrophic and magnetostrophic flow; Torsional waves; Taylor's constraint; Ekman–Hartmann layers; Gravitational oscillations

1. Introduction

The Earth is not a perfect timekeeper, and the spectrum of the variations in the mantle's angular velocity $\widehat{\boldsymbol{\Omega}}$ spans a wide range of frequencies. Of particular interest here are the comparatively large amplitude *sub-decadal variations* in which changes in length of day (LOD) of up to 2 ms occur (Abarca del Rio *et al*. 2000); see figure 1(a). The changes are so rapid that the atmosphere and oceans cannot be responsible as becomes clear when we consider the following extreme case.

*Corresponding author. Email: roberts@math.ucla.edu

Geophysical and Astrophysical Fluid Dynamics
ISSN 0309-1929 print/ISSN 1029-0419 online © 2012 Taylor & Francis
http://dx.doi.org/10.1080/03091929.2011.589028

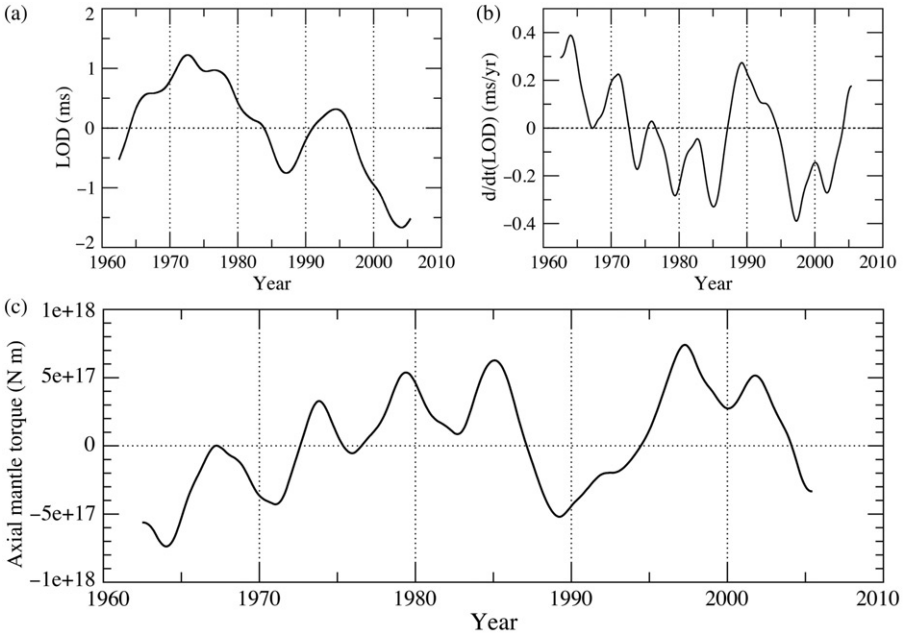

Figure 1. (a) Smoothed LOD time series data, $\delta P(t)$, from Holme and de Viron (2005). (b) Temporal derivative of the LOD time series, $\mathrm{d}P/\mathrm{d}t$. (c) Axial torque on the mantle, $\widehat{\Gamma}_z = -(2\pi\widehat{C}/P^2)\mathrm{d}P/\mathrm{d}t$, necessary to generate the LOD's temporal variations over the past half century.

Suppose that all motions in the atmosphere and oceans relative to the mantle ceased, their angular momentum δM $(=\delta M_{\mathrm{atm}} + \delta M_{\mathrm{ocm}})$ being shared by the entire Earth, so leading to a change in the LOD, P $(= 2\pi/\widehat{\Omega})$, of $\delta P = -P\delta M/C_{\mathrm{tot}}\widehat{\Omega}$, where $C_{\mathrm{tot}} \approx 8.04 \times 10^{37}\,\mathrm{kg\,m^2}$ is the total moment of inertia of the Earth about its polar axis. Although the moment of inertia C_{ocn} $(\approx 300 C_{\mathrm{atm}})$ of the oceans is large compared with that of the atmosphere, ocean currents are much slower than atmospheric motions. For example, applying the models of Gross (2007) to data from 2009 yields root-mean-square estimates of $|\delta M_{\mathrm{atm}}| = 1.8 \times 10^{25}\,\mathrm{kg\,m^2\,s^{-1}}$ and $|\delta M_{\mathrm{oc}}| = 2.1 \times 10^{24}\,\mathrm{kg\,m^2\,s^{-1}}$. Then $|\delta M| = 2.0 \times 10^{25}\,\mathrm{kg\,m^2\,s^{-1}}$, so that $|\delta P|$ is at most 0.3 ms. Therefore, extinguishing, or even reversing, the global wind and ocean circulations would not be able to account for the largest sub-decadal variations in LOD.

The origin of the sub-decade variations must be sought in the Earth's interior, and figure 1 suggests that the task of finding the origin will not be a light one. Figure 1(a) shows smoothed LOD data, δP, from the last half century, with the atmospheric, and tidal signals removed (Holme and de Viron 2005). Figure 1(b) shows the temporal derivative of the LOD time series, $\mathrm{d}P/\mathrm{d}t$; strong oscillations occur on sub-decadal time scales. From the temporal derivative, it is then possible to reconstruct $\widehat{\Gamma}_z$ as a function of time t in figure 1(c); here $\widehat{\Gamma}_z$ is the component parallel to the polar axis Oz of the torque $\widehat{\boldsymbol{\Gamma}}$ exerted by the core on the mantle (assumed a rigid body).

The equation of motion for the mantle's axial rotation is $\widehat{C}(\mathrm{d}\widehat{\Omega}/\mathrm{d}t) = \widehat{\Gamma}_z$, where $\widehat{C} = 7.12 \times 10^{37}\,\mathrm{kg\,m^2}$ is the mantle's axial moment of inertia. From figure 1(b), let the LOD change by $\delta P = 2 \times 10^{-3}\,\mathrm{s}$ over a time T equal to a decade $(\sim \pi \times 10^8\,\mathrm{s})$, corresponding to $0.2\,\mathrm{ms\,yr^{-1}}$. Then $\delta\widehat{\Omega} = -2\pi\,\delta P/P^2 = -8.4 \times 10^{-13}\,\mathrm{s^{-1}}$ and $\mathrm{d}\widehat{\Omega}/\mathrm{d}t \approx \delta\widehat{\Omega}/T = -5.4 \times 10^{-21}\,\mathrm{s^{-2}}$. Multiplying by $\widehat{C}$ yields a torque of $\widehat{\Gamma}_z = -4 \times 10^{17}\,\mathrm{Nm}$ that

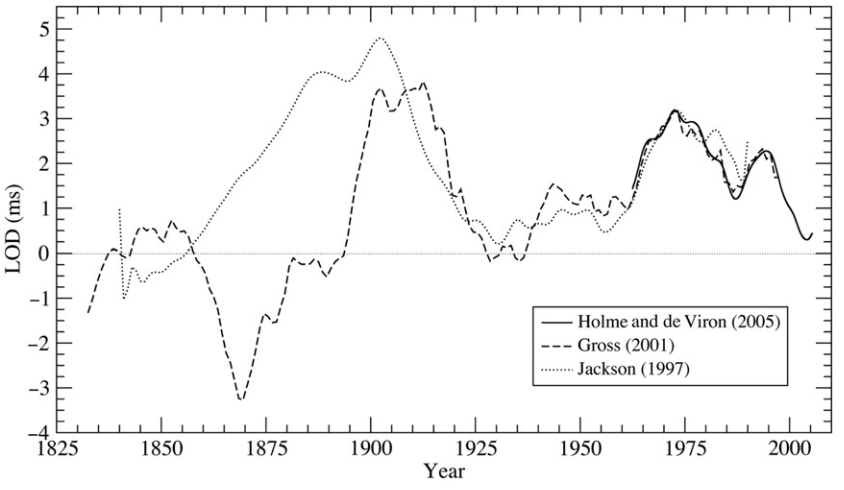

Figure 2. Comparison of LOD time series data, $\delta P(t)$, from Holme and de Viron (2005) and Gross (2001) against modeled LOD variations from the "smooth" core flow inversion of Jackson (1997). The qualitative agreement after 1900, when the data quality becomes relatively high, implies that axial angular momentum is exchanged between core and mantle on sub-decadal time scales. The time series include the variation due to lunar tidal drag. The mean LOD values are arbitrary, and, thus, have been selected to agree with that of Gross (2001) at 1972.5.

acts on the mantle on decadal time scales. Thus, the LOD data in figure 1 sets a target magnitude for theorists: how can torques as large as 10^{18} Nm be generated in the interior of the Earth?

The time scale of the variations in LOD shown in figure 1(b) has a dominant periodicity of nearly 6 years. However, lower resolution, longer time period LOD models suggest a possible periodicity of 60 years; see e.g., Roberts *et al.* (2007). The existence of this 60 year periodicity is controversial, mainly because records of the required length and accuracy are unavailable to establish it unequivocally. Thus, we will focus mainly here on explanations of the sub-decadal, 6 year oscillation.

The LOD fluctuations are so strongly reminiscent of that of the secular variation of the geomagnetic field, $\boldsymbol{B}$, that it is natural to seek a common cause for each in MHD processes in the core. This is made clear in figure 2, which shows the LOD data from figure 1 and the longer LOD time series of Gross (2001) plotted versus the estimated LOD variations inferred from the core flow models of Jackson (1997). Since the core flow models are obtained by inversion of geomagnetic secular variation data, the qualitative agreement amongst these data sets implies that the sub-decadal variations in LOD are due to core-mantle angular momentum exchange and that these decadal exchanges are associated with the MHD processes occurring in Earth's core.

The existence of the sub-decadal variations in LOD betrays the existence of angular momentum exchanges between the Earth's mantle, fluid outer core (FOC) and solid inner core (SIC). The core-mantle interactions are communicated via stresses on the base of the mantle. The LOD variations establish, further, that these stresses are large enough to be detectable via variations in the mantle's angular velocity $\boldsymbol{\Omega}$. Challenging questions arise such as, what does the changing LOD teach us about the deep interior of the Earth and the physical state of the core?

This article will focus on variations in LOD, i.e., changes in $\widehat{\Omega}_z$ ($\approx \widehat{\Omega}$). Precession and nutation of the Earth's axis, which describe variations in $\widehat{\Omega}_x$ and $\widehat{\Omega}_y$, are phenomena that cannot be satisfactorily explained without invoking torques, $\widehat{\boldsymbol{\Gamma}}$, on the core-mantle boundary (CMB) that have nonzero x- and y-components. These topics are beyond the scope of this article. We will however pay attention to the torques acting across the inner core boundary (ICB); it will become apparent that these are relevant to variations in LOD. Sections 2 and 3 presents the background physics, which is necessary to make this article self-contained. Technical issues are dealt with in five appendices. Throughout, variables in the SIC are distinguished by a tilde ($\widetilde{\ }$) and those in the mantle by a hat ($\widehat{\ }$). Unadorned letters are either used in general statements or refer to FOC variables. When however there seems to be a risk of ambiguity, a breve sign ($\breve{\ }$) is added to FOC quantities.

2. Background physics

2.1. *Thermal core-mantle coupling*

Discussion of the thermal coupling of the FOC to the mantle and the SIC provides a way of introducing physical concepts, governing equations, boundary conditions and the notation required for the remainder of this article.

The core and mantle are thermally coupled by two boundary conditions on the CMB. These are continuity of the temperature T and the normal component of the heat flux $\boldsymbol{q}$. Since the CMB is not perfectly spherical, its unit normal, $\boldsymbol{n}$, is not exactly parallel to the radius vector, $\boldsymbol{r}$. We assume $\boldsymbol{n}$ points *from* the core *into* the mantle, and denote by $\breve{q}_n$ ($= \boldsymbol{n}\cdot\breve{\boldsymbol{q}}$) the outward heat flux from the FOC. The boundary conditions are then

$$\breve{T} = \widehat{T}, \quad \breve{q}_n = \widehat{q}_n, \quad \text{on the CMB.} \tag{1a,b}$$

In principle, the core and mantle form one system, and T should be found by solving for core and mantle convection simultaneously, using (1a,b) to link them together. It would be much more convenient to divorce them by considering the core and mantle as separate systems, but there is a difficulty: even if T and q_n were known on the CMB, only one of them could be specified when seeking T in either system in isolation. To apply both conditions would overdetermine the mathematical problem. So the question arises, if the core and mantle are considered separately, which of the two conditions should be applied to each, or should some combination of the two conditions be used? Fortunately a clearcut answer is available which exploits the fact that a typical mantle velocity, $\widehat{\mathcal{V}} \sim 10^{-9}\,\mathrm{m\,s^{-1}}$, is very much smaller than a typical fluid core velocity, $\breve{\mathcal{V}} \sim 10^{-4}\,\mathrm{m\,s^{-1}}$. We shall show that a boundary condition of uniform CMB temperature is the correct condition to apply in a simulation of mantle dynamics (see (5e)). The mantle simulation then determines $\widehat{q}_n$ which transforms (1b) into the boundary condition to be applied in simulations of core dynamics.

In order to develop this argument in detail, it is necessary to discuss the thermodynamics and chemical composition of the core. The core is known from seismology to be lighter than iron would be at the same T and pressure p. Although the core is an uncertain combination of all the elements, the essential physics is adequately represented here by a core that is a ferric binary alloy in which the mass fraction of the

principal unknown light constituent (possibly Si, O or S) is denoted by X (e.g., Frost *et al.* 2010). Convection mixes the FOC so well that, except in thin boundary layers at the CMB and ICB, it is chemically and thermodynamically homogeneous. It is therefore isentropic, i.e., its specific entropy, S, is uniform. Except in boundary layers,

$$S = S_a = \text{constant}, \quad X = X_a = \text{constant}, \quad \text{in the FOC}, \tag{2a,b}$$

where the subscript $_a$ stands for "adiabatic"; (2a) makes S a more natural variable to use than T in describing FOC convection.

Pressure differences in a convective flow of characteristic speed $\mathcal{V}$ influences the primary dynamical balance if $\mathcal{V}$ is as large as the speed of sound, u_s. But $u_s \approx 10^4\,\mathrm{m\,s^{-1}}$ in the FOC while $\mathcal{V}$ is at most of order $10^{-3}\,\mathrm{m\,s^{-1}}$. The dynamical balance is therefore primarily hydrostatic. The differences in density, ρ, are mainly due to gravitational compression and are significant. Hydrostatic balance, including the centrifugal acceleration, requires that

$$\boldsymbol{\nabla} p_a = \rho_a(\boldsymbol{g}_a - \boldsymbol{\Omega} \times (\boldsymbol{\Omega} \times \boldsymbol{r})) = \rho_a[\boldsymbol{g}_a + \tfrac{1}{2}\boldsymbol{\nabla}(\boldsymbol{\Omega}\times\boldsymbol{r})^2], \tag{2c}$$

where $\boldsymbol{r}$ is the radius vector from the geocenter O. Newtonian gravitation theory requires that $\boldsymbol{g}$ is everywhere continuous and

$$\boldsymbol{\nabla}\times\boldsymbol{g} = \boldsymbol{0}, \quad \boldsymbol{\nabla}\cdot\boldsymbol{g} = -4\pi G\rho, \quad \boldsymbol{g} = -\boldsymbol{\nabla}\Phi, \quad \nabla^2\Phi = 4\pi G\rho, \tag{2d,e,f,g}$$

where G is the constant of gravitation, $\boldsymbol{g}$ is the gravitational field, and Φ is the gravitational potential. Equations (2a–g) are the basis of two reference models described below.

Adequate for most geophysical purposes is the *spherical reference model*, in which the core is taken to be non-rotating and spherically symmetric about O. Hydrostatic balance then requires that $p = p_a^s(r)$, $\rho = \rho_a^s(r)$ and $g = g_a^s(r)$, where $g = |\boldsymbol{g}| = -g_r$ and

$$\mathrm{d}p_a^s/\mathrm{d}r = \rho_a^s g_a^s. \tag{3a}$$

The superscript ^{s} distinguishes variables in the spherical reference model from those in the aspherical model introduced in section 2.2, which depend on all three polar coordinates (r, θ, ϕ). In appendix A, a simple example satisfying (2d,e) and (3a) is presented that mimics the core satisfactorily.

In the spherical model, the density ρ, temperature T and chemical potential μ (the conjugate variable to X; e.g., see Chapt. IX of Landau and Lifshitz (1980)) increase with depth, and define the *adiabatic gradients*

$$\mathrm{d}T_a^s/\mathrm{d}r = -\alpha_S g_a^s, \quad \mathrm{d}\rho_a^s/\mathrm{d}r = -\rho_a^s g_a^s/u_s^2, \quad \mathrm{d}\mu_a^s/\mathrm{d}r = -\alpha_X g_a^s. \tag{3b,c,d}$$

Here, α_S and α_X are the entropic and compositional expansion coefficients analogous to the thermal expansion coefficient, α:

$$\alpha_S = -\rho^{-1}(\partial\rho/\partial S)_{p,X} = \alpha T/c_p, \quad \alpha_X = -\rho^{-1}(\partial\rho/\partial X)_{p,S}, \tag{3e,f}$$

and c_p ($\approx 800\,\mathrm{J\,kg^{-1}K^{-1}}$) is the specific heat at constant pressure, p. Other typical values are $\alpha = 10^{-5}\,\mathrm{K^{-1}}$, $\alpha_S = 6\text{–}8 \times 10^{-5}\,\mathrm{kg\,J^{-1}\,K^{-1}}$ and $\alpha_X = 0.6$ (e.g., Stacey and Davis 2008). (The subscript $_a$ and superscript ^{s} are omitted from u_s, α, α_S, α_X and c_p in (3b–e) but are implied.)

A state of uniform S and X is neutrally buoyant, even though its density increases downwards; e.g. see §4 of Landau and Lifshitz (1987). If the FOC were in this state when the CMB suddenly became impervious to heat, convective motions would transport S and X upward on a turnover time scale. This would quickly carry the FOC toward an isothermal state of uniform μ, in which S and X increase upwards and which is buoyantly stable. This follows from the general thermodynamic inequality

$$\left(\frac{\partial \rho}{\partial p}\right)_{T,\mu} > \left(\frac{\partial \rho}{\partial p}\right)_{S,X}, \tag{4a}$$

i.e. density increases more rapidly with depth than in the neutrally buoyant adiabatic state. As this bottom heavy state is created, convection would cease and the geodynamo would shut down. This extreme "end member" example makes the point that the vigor of core convection and the generation of magnetic field by dynamo action are decided by the flow of heat, Q, from core to mantle, which in turn is controlled by the efficiency of mantle convection. The mantle is the valve that controls the core engine. Sufficient radioactivity in the core could alone supply Q at the CMB; even more would raise the core temperature, melt the inner core and the base of the mantle. The reality seems to be the opposite: the core is cooling, and the inner core is growing through the freezing of core fluid (e.g. Jacobs 1953, Davies 2007, Lay *et al.* 2008). The downward melting point gradient exceeds the downward adiabatic gradient, resulting in the unfamiliar situation of a fluid being cooled at the top (CMB) but freezing at the bottom (ICB). Conditions similar to (1a,b) apply:

$$\breve{T} = \widetilde{T} = T_{\mathrm{PhE}}, \quad \breve{q}_n = \widetilde{q}_n + \widetilde{\rho} L \dot{r}_i, \quad \text{on the ICB}, \tag{4b,c}$$

where $T_{\mathrm{PhE}}(p, X)$ is the temperature for phase equilibrium. The last term in (4c) expresses the rate of release of latent heat as the ICB advances into the FOC through freezing; r_i is the inner core radius and L is latent heat per unit SIC mass. Although very uncertain, $L = 10^6\,\mathrm{J\,kg^{-1}}$ is a common estimate.

The release of latent heat at the ICB creates a buoyancy source that helps to drive convection in the core, but it is not the only source. Buoyancy is also created compositionally. Generally when an alloy freezes, it partially ejects some of its constituents. It is known from seismology that $\widetilde{\rho} > \breve{\rho}$ at the ICB. The density jump, $\widetilde{\Delta} = \widetilde{\rho} - \breve{\rho} \approx 600\,\mathrm{kg\,m^{-3}}$, exceeds what is expected from thermal contraction on freezing. It seems more likely that $\breve{X} > \widetilde{X}$. The light material ejected on freezing provides a compositional buoyancy source at the ICB that is thermodynamically very efficient. If $\boldsymbol{K}$ is the mass flux of light constituent

$$K_n = \widetilde{\rho}(\breve{X} - \widetilde{X})\dot{r}_i, \quad \text{on the ICB}, \tag{4d}$$

which is the analog for X of (4c).

The heat flow, Q, from the core to the mantle is uncertain (e.g. Lay *et al.* 2008). Estimates of order 10 TW are common; some are as low as 3 TW and some as high as 20 TW, which we shall take as an upper bound. An important part of Q is Q_a, the heat flow down the adiabat. On taking $\alpha = 1.76 \times 10^{-5}\,\mathrm{K^{-1}}$, $c_p = 850\,\mathrm{J\,kg^{-1}\,K^{-1}}$, $T_a = 4000\,\mathrm{K}$ and $g_a = 10.68\,\mathrm{m\,s^{-2}}$ at the CMB (e.g. Stacey and Davis 2008), we obtain from (3b) an adiabatic temperature gradient of about $0.9\,\mathrm{K\,km^{-1}}$.

Assuming a thermal conductivity, K, of $40\,\mathrm{W\,m^{-1}\,K^{-1}}$, the resulting adiabatic heat flux, $I_{r,a} = -K\partial_r T_a$, is about $3.6\times10^{-2}\,\mathrm{W\,m^{-2}}$ at the CMB. This implies that $Q_a \approx 5.4\,\mathrm{TW}$. The uncertainty in Q is mainly an uncertainty in the convective heat flow, Q_c, which might even be negative in a regime that is dominantly compositionally driven (Loper 1978). We shall assume that Q_c is less than 15 TW, so that $q_{r,c} < 0.1\,\mathrm{W\,m^{-2}}$.

Convection creates deviations from the reference model, and the next step is to quantify these through a parameter $\epsilon_c = T_c/T_a$. We here use the notation

$$T = T_a + T_c, \tag{5a}$$

and similarly for other variables. The outward convective heat flux within the FOC is

$$q_{r,c} = \rho c_p \overline{T_c V_r} - K\partial_r T_c, \tag{5b}$$

where the overline denotes an average over the turbulence. The ratio of the two terms on the right-hand side of this equation is the Péclet number, $Pe = \mathcal{V}\mathcal{L}/\kappa$, where $\kappa = K/\rho c_p$ is the molecular thermal diffusivity, which is about $5\times10^{-6}\,\mathrm{m^2\,s^{-1}}$. In the main bulk of the core, (5b) is well-approximated for $\mathcal{L} \gtrsim 1\,\mathrm{m}$ by

$$q_{r,c} = \rho c_p \overline{T_c V_r}, \quad \text{and similarly } K_{r,c} = \rho_a \overline{X_c V_r}, \tag{5c,d}$$

for the compositional flux. These fail as the CMB is approached and $\breve{V}_r$ tends to zero. Thermal conduction increasingly carries the heat until, on the CMB itself, $q_{r,c} = -K\partial_r T_c$. Since Q_c is probably several TW, $\nabla_r T$ must be large too, both at the CMB and in a thin, non-adiabatic, thermal boundary layer not discussed here. As $q_{r,c}$ is nearly constant through the boundary layer, (5c) can be used even at the CMB, provided V_r refers to the flow beneath the boundary layer, typically estimated as $10^{-4}\,\mathrm{m\,s^{-1}}$. Then (5c) gives $q_{r,c} \approx (840\ T_c/\mathrm{K})\mathrm{W\,m^{-2}}$. Since $q_{r,c} < 0.1\,\mathrm{W\,m^{-2}}$ according to our earlier estimate, $T_c < 10^{-4}\,\mathrm{K}$. As $T_a \geq \widehat{T}_a \approx 4000\,\mathrm{K}$ (e.g. Kawai and Tscuchiya 2009), $\epsilon_c < 3\times10^{-8}$. The smallness of ϵ_c confirms that the FOC is very close to an adiabatic state so that, to an excellent approximation, (1a) gives

$$\widehat{T} = T_a, \quad \text{on the CMB.} \tag{5e}$$

Equation (5e) is the appropriate bottom thermal boundary condition when studying the mantle in isolation. Strictly, it is wrong to use this boundary condition when solving core convection in isolation, although this is "standard practice" in the majority of geodynamo simulations. This may be because it is slightly easier to implement and because it is believed that this choice does not fundamentally alter the solution (cf. Johnson and Doerring 2010, but see Sakuraba and Roberts 2009). Having solved the mantle convection equations with the $\widehat{T}$ prescribed by (5e) and appropriate upper boundary conditions, the heat flux $\widehat{\boldsymbol{q}}$ is determined everywhere, and $\widehat{q}_n$ is known at the CMB as a function of colatitude, θ, and longitude, ϕ. The only way in which (1b) can be satisfied is by imposing it, with its now known right-hand side, on the FOC, i.e. it provides the required upper thermal boundary condition for solving core magnetoconvection.

These arguments have essentially divorced the mantle and core, as far as their thermal states are concerned. We say "essentially" because it is still necessary to select the adiabat, S_a, for the core, that gives the appropriate T_a on the CMB, a task not discussed here.

2.2. *The aspherical reference model*

As deviations from spherical symmetry will be significant in sections 6 and 7, we need to define an *aspherical reference model*, which includes the effects of the Earth's rotation and of density anomalies in the mantle and SIC. This also satisfies (2a,b) and is therefore neutrally buoyant too.

Consider first the effect of rotation. Equations (2c,f) show that hydrostatic balance requires

$$\nabla p_a = \rho_a \boldsymbol{g}_{\rm e}, \quad \text{i.e. } \nabla p_a = -\rho_a \nabla \Phi_{\rm e}, \tag{6a,b}$$

where $\boldsymbol{g}_{\rm e}$ and $\Phi_{\rm e}$ are the "effective" gravitational field and potential:

$$\boldsymbol{g}_{\rm e} = -\nabla \Phi_{\rm e}, \quad \Phi_{\rm e} = \Phi_a - \frac{1}{2}(\boldsymbol{\Omega}\times\boldsymbol{r})^2. \tag{6c,d}$$

Equation (6b) requires the thermodynamic variables to be constant on equipotential surfaces $\Phi_{\rm e} =$ constant. In particular,

$$p_a = p(\Phi_{\rm e}, S_a, X_a), \quad \rho_a = \rho(\Phi_{\rm e}, S_a, X_a) = -\partial p(\Phi_{\rm e}, S_a, X_a)/\partial \Phi_{\rm e}. \tag{6e,f}$$

It follows from (4b) that the ICB in the reference state is an equipotential surface too but, in the core's turbulent environment, the actual ICB is an equipotential surface only on average. In what follows, the constants S_a and X_a are omitted from (6e,f) but are implied.

Because the mantle and SIC are so much less mobile than the FOC, deviations from hydrostatic equilibrium may endure for times long compared with the sub-decadal periods described in section 1. In fact, we shall treat the mantle, and usually the inner core too, as rigid bodies, with their density distributions, $\widehat{\rho}$ and $\widetilde{\rho}$, "frozen" to their co-moving reference frames. Their density distributions create gravity fields $\widehat{\boldsymbol{g}}_a^{\,\rm m}$ and $\widetilde{\boldsymbol{g}}_a^{\,\rm i}$, that are frozen in too, but these are only parts of the total gravitational fields, $\widehat{\boldsymbol{g}}_a$ and $\widetilde{\boldsymbol{g}}_a$, in the mantle and SIC, e.g. the mantle gravity field comprises the three components originating, respectively, in the mantle, fluid core and inner core:

$$\widehat{\boldsymbol{g}} = \widehat{\boldsymbol{g}}^{\,\rm m} + \widehat{\boldsymbol{g}}^{\,\rm f} + \widehat{\boldsymbol{g}}^{\,\rm i}. \tag{7a}$$

Note that the FOC and SIC contributions, $\widehat{\boldsymbol{g}}^{\,\rm f}$ and $\widehat{\boldsymbol{g}}^{\,\rm i}$, are not frozen to the mantle frame and may change on sub-decadal time scales. It will become clear later that these changes, though small, are significant.

We shall use the term *gravity anomaly* to mean that $\widehat{\rho}_a\widehat{\boldsymbol{g}}_{\rm e} - \nabla\widehat{p}_a$ and $\widetilde{\rho}_a\widetilde{\boldsymbol{g}}_{\rm e} - \nabla\widetilde{p}_a$ are nonzero, and we shall argue that they fluctuate about zero on sub-decadal time scales. This motivates the introduction of the following deviation measures:

$$\widehat{\boldsymbol{d}} = \int_{\widehat{\rm V}} (\widehat{\rho}_a\widehat{\boldsymbol{g}}_{\rm e} - \nabla\widehat{p}_a)\mathrm{d}v, \quad \widetilde{\boldsymbol{d}} = \int_{\widetilde{\rm V}} (\widetilde{\rho}_a\widetilde{\boldsymbol{g}}_{\rm e} - \nabla\widetilde{p}_a)\mathrm{d}v, \tag{7b,c}$$

$$\widehat{\boldsymbol{D}} = \int_{\widehat{\rm V}} \boldsymbol{r}\times(\widehat{\rho}_a\widehat{\boldsymbol{g}}_{\rm e} - \nabla\widehat{p}_a)\mathrm{d}v, \quad \widetilde{\boldsymbol{D}} = \int_{\widetilde{\rm V}} \boldsymbol{r}\times(\widetilde{\rho}_a\widetilde{\boldsymbol{g}}_{\rm e} - \nabla\widetilde{p}_a)\mathrm{d}v. \tag{7d,e}$$

Analogous integrals for the FOC are clearly zero by (6a).

The measures $\widehat{\boldsymbol{d}}$ and $\widetilde{\boldsymbol{d}}$ are relevant to linear momentum, as for example when the SIC is displaced relative to the mantle in the Slichter mode; the measures $\widehat{\boldsymbol{D}}$ and $\widetilde{\boldsymbol{D}}$

concern the balance of angular momentum and are relevant to LOD variations. Ignoring sources of $\boldsymbol{g}_a$ external to the Earth,

$$\widehat{\boldsymbol{d}}+\widetilde{\boldsymbol{d}}=\boldsymbol{0}, \quad \widehat{\boldsymbol{D}}+\widetilde{\boldsymbol{D}}=\boldsymbol{0}, \tag{7f,g}$$

because of conservation of linear and angular momentum; section 7.1 will give more details. We shall require that the aspherical reference model obeys not only (6a) but also

$$\widehat{\boldsymbol{d}}=\boldsymbol{0}, \quad \widetilde{\boldsymbol{d}}=\boldsymbol{0}, \quad \widehat{\boldsymbol{D}}=\boldsymbol{0}, \quad \widetilde{\boldsymbol{D}}=\boldsymbol{0}. \tag{7h,i,j,k}$$

These may be regarded as generalized isostasy statements, generalized because $\widehat{\boldsymbol{g}}_{\mathrm{e}}$, for example, includes the time-varying $\widehat{\boldsymbol{g}}_{\mathrm{e}}^{\mathrm{f}}$ and $\widehat{\boldsymbol{g}}_{\mathrm{e}}^{\mathrm{i}}$ which alter when the position and orientation of the SIC change. Then all four measures become nonzero, though (7f,g) continue to hold. Additionally, we assume that (7h–k) refer to a state of minimum gravitational energy for which the total linear and angular momentum of the core-mantle system is given and for which S_a and X_a for the FOC are assigned. This is the state to which the Earth seeks to return when the measures are nonzero.

To assess the difference between the spherical and aspherical models, we define

$$\Phi'_{\mathrm{e}}(r,\theta,\phi)=\Phi_{\mathrm{e}}(r,\theta,\phi)-\Phi^s_a(r), \tag{8a}$$

and similarly for p'_a, ρ'_a, etc. When Φ_{e} is expanded in spherical harmonics,

$$\Phi_{\mathrm{e}}(r,\theta,\phi)=\sum_{\ell=0}^{\infty}\sum_{m=0}^{\ell}[\mathcal{G}^m_\ell(r)\cos m\phi+\mathcal{H}^m_\ell(r)\sin m\phi]P^m_\ell(\theta), \tag{8b}$$

where the $\ell=m=0$ term is Φ^s_a, and the remaining terms define Φ'_{e}. The $\ell=2$, $m=0$ part is dominated by centrifugal forces, whose importance is quantified by the dimensionless parameter $\epsilon_\Omega=\Omega^2 r/g$. This varies from 1.7×10^{-3} at the CMB to 1.5×10^{-3} at the ICB.

The next most significant gravity anomaly, from $\ell=m=2$, is created by density inhomogeneities in the mantle so that, by (2g), $\nabla^2\Phi'_{\mathrm{e}}=0$ for $r\lesssim r_o$. Therefore, by choice of the zero of ϕ,

$$\Phi'_{\mathrm{e}}=\widehat{\mathcal{A}}(r/r_o)^2\sin^2\theta\cos 2\phi, \quad (\widehat{\mathcal{A}}>0). \tag{8c}$$

See Wahr and deVries (1989) and Forte *et al.* (1994). The value of the constant $\widehat{\mathcal{A}}$ is about $1300\,\mathrm{m^2\,s^{-2}}$, according to Defraigne *et al.* (1996) and about $2300\,\mathrm{m^2\,s^{-2}}$ according to Forte *et al.* (1994). We compromise by taking $\widehat{\mathcal{A}}=1800\,\mathrm{m^2\,s^{-2}}$, a value assumed below without further comment. Approximating p'_a as a small perturbation of p^s_a, (3a) gives

$$p'_a\approx-\rho^s_a\Phi'_a. \tag{8d}$$

The importance of the anomaly (8c) is quantified by $\epsilon_a=p'_a/p^s_a$, which reaches 10^{-4} on the CMB equator and 10^{-5} on the ICB equator. As ϵ_Ω exceeds ϵ_a by one or two orders of magnitude, rotation creates the larger difference between the spherical and aspherical models, but the torques that can change the LOD depend on asymmetries ($m\neq0$). It may also be seen that even ϵ_a greatly exceeds ϵ_c.

3. More background physics

3.1. *On representing sub-grid scales*

Equations (5b,c) raise a very significant modeling issue: the representation of turbulence in core dynamics. It is an unfortunate fact that the computational hardware needed to resolve significant length and time scales of core motion does not exist today nor apparently for the foreseeable future. A computer can only deal with the large length, time, and velocity scales that it can resolve; we denote these by $\mathcal{L}$, $\mathcal{T}$, and $\mathcal{V}$ and call them "the macroscales". Unfortunately the macroscale fields are greatly influenced by the unresolvable small length, time, and velocity scales, which we denote by ℓ, τ, and v, and call "the microscales", though ℓ and τ greatly exceed the molecular scales.

No completely satisfactory way of representing the effect of the microscales on the macroscales is known. Several approximate methods have been devised however that have been partially successful. Here we focus on the simplest, which is known as *mixing length theory*. It exists at several levels of sophistication, and is widely used in astrophysics and geophysics e.g. Bradshaw (1974) and Cushman-Roisin (2008). Promising alternatives to mixing length theory have been developed over the past three decades (Bardina *et al.* 1980) and have been applied to core turbulence during the past decade (e.g. Matsui and Buffett 2005).

It was recognized even in the nineteenth century that the most important effect to parametrize is the transport of macroscale variables by the microscale velocities. This can be vastly greater than their transport by molecular motions. In mixing length theory this is recognized by a similar diffusive process, but using eddy diffusivities that are much larger than their molecular counterparts.

To be more specific, we separate quantities into their resolved macroscale and unresolved microscale parts by

$$\boldsymbol{V} = \langle \boldsymbol{V} \rangle + \boldsymbol{v}, \quad S_c = \langle S_c \rangle + s_c, \quad X_c = \langle X_c \rangle + x_c, \ldots, \tag{9a,b,c}$$

where angle brackets surround a quantity averaged over the microscales. The averages that concern (5b,c) are the r-components of

$$\langle S_c \boldsymbol{V} \rangle = \langle S_c \rangle \langle \boldsymbol{V} \rangle + \langle s_c \boldsymbol{v} \rangle, \quad \langle X_c \boldsymbol{V} \rangle = \langle X_c \rangle \langle \boldsymbol{V} \rangle + \langle x_c \boldsymbol{v} \rangle. \tag{9d,e}$$

The mixing length approach approximates the last terms in (9d,e) by

$$\langle s_c \boldsymbol{v} \rangle = -\kappa_T \boldsymbol{\nabla} \langle S_c \rangle, \quad \langle s_c \boldsymbol{v} \rangle = -\kappa_T \boldsymbol{\nabla} \langle X_c \rangle, \tag{9f,g}$$

where κ_T is a turbulent diffusivity which is the same for S_c and X_c because S is an extensive thermodynamic variable that is transported by motion in the same way as X. It is therefore convenient (except in boundary layers) to combine thermal and compositional buoyancies together in

$$\rho_c = u_s^{-2} p_c + \rho_a C, \tag{10a}$$

where C is the *codensity* (Braginsky and Roberts 1995):

$$C = -\alpha_S S_c - \alpha_X X_c. \tag{10b}$$

Equation (10a) follows from the thermodynamic relation

$$\mathrm{d}\rho = u_s^{-2} \mathrm{d}p - \rho \alpha_S \, \mathrm{d}S - \rho \alpha_X \, \mathrm{d}X, \tag{10c}$$

since ρ_c/ρ_a, p_c/p_a, S_c/S_a, and X_c/X_a are all of order 10^{-8}, which determines the accuracy to which (10a) holds.

When applied to the transport of macroscale momentum by the microscale motions, the turbulent mixing ansatz (9f,g) introduces a turbulent kinematic viscosity, ν_T, very much greater than the molecular kinematic viscosity, ν. If it is supposed that s_c/S_c and x_c/X_c are $O(\ell/\mathcal{L})$, (9f,g) indicate that $\kappa_T = O(\nu\ell)$, and this is a common estimate for both κ_T and ν_T. Faced with lack of information about how the fluid velocity depends on its length scale, we take $\nu = 10^{-4}\,\mathrm{m\,s^{-1}}$, which is typical of what we call *the inferred core surface velocity*, as deduced by downward extrapolation of magnetic field data taken at or near the Earth's surface. It is also hard to estimate ℓ. We take $\ell \sim E^{1/3} r_o \approx 100\,\mathrm{m}$, where E is the Ekman number; see (15b). We choose this because it is a characteristic length scale in rapidly rotating convective systems of scale r_o (e.g. Stellmach and Hansen 2004, Sprague *et al.* 2006). We then obtain turbulent diffusivity estimates of

$$\kappa_T \approx \nu_T \approx 0.01\,\mathrm{m^2\,s^{-1}}. \tag{10d}$$

The simplistic belief that microscale motions act on all macroscale processes in the same way in a particular physical system encourages the assumption that all turbulent diffusivities in that system are the same. When a molecular diffusivity exceeds the corresponding turbulent diffusivity, as appears to be true for the magnetic diffusivity, it determines the total diffusivity. The molecular magnetic diffusivity in the FOC is $\eta = 1/\mu_0\sigma \approx 2\,\mathrm{m^2\,s^{-1}}$, based on $\sigma \approx 4 \times 10^5\,\mathrm{S\,m^{-1}}$ for the electrical conductivity, and $\mu_0 = 4\pi \times 10^{-7}\,\mathrm{H\,m^{-1}}$ for the magnetic permeability, assumed to be that of free space. Since this η exceeds the η_T given by (10d) by a factor of 200, the introduction of a turbulent magnetic diffusivity in simulating core MHD is superfluous.

Approximations such as (9f,g) implicitly assume that turbulent diffusion is an isotropic process at all length scales. This too is highly questionable. In numerical models, the length scale separating the macroscales from microscales is not a physical one; it is computational, dictated by the available computing hardware. Many of the processes controlling the unresolved scales are anisotropic (e.g. Ishihara *et al.* 2009). For example, consider again the estimate of κ_T and ν_T made above. The ratio of the microscale lengths perpendicular and parallel to the angular velocity, $\boldsymbol{\Omega}$, of a rapidly rotating system is typically $E^{1/3}$, indicating that the turbulence diffuses macroscale quantities at different rates in these directions. This strongly suggests that the sub-grid-scale diffusion processes are anisotropic as well. The ansatz can be improved by replacing κ_T and ν_T by tensor diffusivities. See Matsushima *et al.* (1999), Matsui and Buffett (2005), and Hejda and Reshetnyak (2009).

The application of mixing length theory to the core is discussed further by Braginsky and Meytlis (1990) and by Braginsky and Roberts (1995); see their §4.3 and appendix C. In what follows, we discuss only macrodynamics with isotropic turbulent diffusivities only. Although angle brackets are omitted, they should be understood to be present.

3.2. *Overview of core dynamics*

We have now assembled enough background to be able to summarize core dynamics. In the mantle frame, mass and momentum conservation require

$$\partial_t \rho + \boldsymbol{\nabla}\cdot(\rho \boldsymbol{V}) = 0, \tag{11a}$$

$$\rho[\partial_t \boldsymbol{V} + \boldsymbol{V}\cdot\boldsymbol{\nabla}\boldsymbol{V} + 2\boldsymbol{\Omega}\times\boldsymbol{V} + \dot{\boldsymbol{\Omega}}\times\boldsymbol{r}] = -\boldsymbol{\nabla}p + \rho\boldsymbol{g}_e + \boldsymbol{J}\times\boldsymbol{B} + \boldsymbol{F}^{\nu}. \tag{11b}$$

The four forces per unit mass on the left-hand side of (11b) are inertial [$\partial_t \boldsymbol{V}$ ($= \partial \boldsymbol{V}/\partial t$) and $\boldsymbol{V}\cdot\boldsymbol{\nabla}\boldsymbol{V}$], Coriolis ($2\boldsymbol{\Omega}\times\boldsymbol{V}$), and Poincaré ($\dot{\boldsymbol{\Omega}}\times\boldsymbol{r}$), the last of which is associated with variations in the rotational state of the mantle and is negligibly small on the LOD time scale. The centrifugal force $-\boldsymbol{\Omega}\times(\boldsymbol{\Omega}\times\boldsymbol{r})$ does not appear in (11b) because it has already been absorbed into the gravitational force $\boldsymbol{g}_{\rm e}$ (see (6d)). The four forces per unit volume on the right-hand side are the pressure gradient, the buoyancy force $\rho\boldsymbol{g}_{\rm e}$, the Lorentz force $\boldsymbol{J}\times\boldsymbol{B}$, and the viscous force $\boldsymbol{F}^{\nu}$, usually approximated by $\rho\nu_T\nabla^2\boldsymbol{V}$. According to pre-Maxwell EM theory (Davidson 2001), the electric current density is given by Ampère's law,

$$\boldsymbol{J} = \mu_0^{-1}\boldsymbol{\nabla}\times\boldsymbol{B}, \quad \text{where } \boldsymbol{\nabla}\cdot\boldsymbol{B} = 0. \tag{11c,d}$$

The electric field, $\boldsymbol{E}$, is subject to Ohm and Faraday's laws:

$$E = -\boldsymbol{V}\times\boldsymbol{B} + \eta\boldsymbol{\nabla}\times\boldsymbol{B}, \quad \boldsymbol{\nabla}\times\boldsymbol{E} = -\partial_t\boldsymbol{B}, \tag{11e,f}$$

from which the induction equation follows:

$$\partial_t\boldsymbol{B} = \boldsymbol{\nabla}\times(\boldsymbol{V}\times\boldsymbol{B}) + \eta\nabla^2\boldsymbol{B}, \tag{11g}$$

where we have assumed that η is uniform. (When a variable mantle conductivity, $\widehat{\sigma}$, is envisaged, $\eta\nabla^2\boldsymbol{B}$ is replaced by $-\boldsymbol{\nabla}\times(\widehat{\eta}\,\boldsymbol{\nabla}\times\widehat{\boldsymbol{B}})$.) According to (11c),

$$\boldsymbol{\nabla}\cdot\boldsymbol{J} = 0. \tag{11h}$$

As before, we separate variables into adiabatic and convective parts. In what follows, we adopt the spherical reference model but omit ^{s}. Since $\rho_c/\rho_a \approx 10^{-8}$, (11a,b) can be accurately approximated by the *anelastic approximation* (e.g. Braginsky and Roberts 2007):

$$\boldsymbol{\nabla}\cdot(\rho_a\boldsymbol{V}) = 0, \tag{12a}$$

$$\rho_a[\partial_t\boldsymbol{V} + \boldsymbol{V}\cdot\boldsymbol{\nabla}\boldsymbol{V} + 2\boldsymbol{\Omega}\times\boldsymbol{V}] = -\boldsymbol{\nabla}p_c + \rho_c\boldsymbol{g}_{\rm e} + \rho_a\boldsymbol{g}_c + \boldsymbol{J}\times\boldsymbol{B} + \rho_a\nu_T\nabla^2\boldsymbol{V}. \tag{12b}$$

An attractive simplification of (12b) makes use of a *reduced* "*pressure*" defined by

$$\Pi_c = \frac{p_c}{\rho_a}, \quad \text{so that } -\boldsymbol{\nabla}p_c = -\rho_a\boldsymbol{\nabla}\Pi_c - \frac{p_a}{u_s^2}\boldsymbol{g}_{\rm e}, \tag{13a,b}$$

using (3c). Therefore, by (10c),

$$-\boldsymbol{\nabla}p_c + \rho_c\boldsymbol{g}_{\rm e} = \rho_a(-\boldsymbol{\nabla}\Pi_c + C\boldsymbol{g}_e). \tag{13c}$$

If the $\rho_a\boldsymbol{g}_c$ part of the total buoyancy force, $\rho_c\boldsymbol{g}_{\rm e} + \rho_a\boldsymbol{g}_c$ is ignored, (12b) becomes

$$\partial_t\boldsymbol{V} + \boldsymbol{V}\cdot\boldsymbol{\nabla}\boldsymbol{V} + 2\boldsymbol{\Omega}\times\boldsymbol{V} = -\boldsymbol{\nabla}\Pi_c + C\boldsymbol{g}_{\rm e} + \rho_a^{-1}\boldsymbol{J}\times\boldsymbol{B} + \nu_T\nabla^2\boldsymbol{V}. \tag{14}$$

This form makes it plain that the density changes created by pressure differences, the first term on the right-hand sides of (10a,c), does not influence convection. Whether the $\rho_a\boldsymbol{g}_c$ part of the buoyancy force can be ignored without making a significant error is an open question; see, for example, §7.02.2.5.2 of Ricard (2007). Braginsky and Roberts (1995) pointed out that, by a minor modification to the definitions of ρ_c and p_c, a variant of (14) holds even when $\rho_a\boldsymbol{g}_c$ is retained in (12b).

The fact that the dipole axis of the geomagnetic field is currently nearly antiparallel to Earth's rotation axis, and has been either parallel or antiparallel over most of Earth's

history (e.g. Merrill *et al.* 1998), indicates that the Coriolis force, $2\boldsymbol{\Omega} \times \boldsymbol{V}$, strongly affects core motions. That it is generally more significant than the inertial and viscous forces is confirmed by the smallness of the *Rossby number* and *Ekman number*, respectively,

$$Ro = \frac{\mathcal{V}}{\Omega r_o}, \quad E = \frac{\nu}{\Omega r_o^2}. \tag{15a,b}$$

Taking $\mathcal{V} = 10^{-4}\,\mathrm{m\,s^{-1}}$ and $\nu = 10^{-6}\,\mathrm{m^2\,s^{-1}}$, we obtain $Ro \approx 10^{-6}$ and $E \approx 10^{-15}$. Even if ν in (15b) were replaced by the turbulent viscosity $\nu_T \approx 10^{-2}\,\mathrm{m^2\,s^{-1}}$, E would be about 10^{-11}. This suggests that the inertial and viscous terms can be safely omitted from (14) except on very small length scales. (The omission of the inertial force will be questioned later.) When the viscosity is dropped, the differential order of the system is lowered and the no-slip boundary condition on $\boldsymbol{V}$ must be replaced by

$$\boldsymbol{n} \cdot \boldsymbol{V} = 0, \quad \text{on CMB and ICB.} \tag{16a}$$

After applying this, the tangential components

$$\boldsymbol{V}_\mathrm{H} = \boldsymbol{V} - (\boldsymbol{n} \cdot \boldsymbol{V})\boldsymbol{n} \tag{16b}$$

are generally nonzero on these boundaries.

A measure of the vigor of core convection is the *Rayleigh number*,

$$Ra = \frac{g_o \mathcal{L}^3 C_r}{\nu\kappa}, \tag{17a}$$

where C_r is a typical radial gradient of C in the FOC. We here selected one of the many ways that the Rayleigh numbers can be defined; it has no special merit. No matter how it is defined, it is a very large number (cf. Christensen and Aubert 2006, Aurnou 2007). If we take $C_r = 3 \times 10^{-16}\,\mathrm{m^{-1}}$, a very uncertain estimate based on $\alpha_S = 10^{-4}\,\mathrm{kg\,J^{-1}\,K}$ and an entropy difference across the FOC of $10^{-5}\,\mathrm{J\,kg^{-1}\,K^{-1}}$, we obtain $\mathrm{Ra} \approx 10^{23}$ using molecular diffusivity estimates and $\mathrm{Ra} \approx 5 \times 10^{14}$ using the turbulent diffusivity estimates of (10d).

For convection to be possible, the Rayleigh number must exceed a critical value, Ra_c. The value of Ra_c is sensitive to the strength of Coriolis and Lorentz forces, as measured by E and the *Elsasser number*, defined as

$$\Lambda = \frac{V_\mathrm{A}^2}{2\Omega\eta}, \quad \text{where } V_\mathrm{A} = \frac{\mathcal{B}}{\sqrt{(\mu_0 \rho_a)}} \tag{17b,c}$$

is the Alfvén velocity based on a typical magnitude, $\mathcal{B}$, of $\boldsymbol{B}$. The Elsasser number is independent of $\mathcal{L}$ and plays an important role in theoretical models of core magnetoconvection. Another dimensionless parameter, relevant later, is the *Alfvén number*,

$$A = \mathcal{V}/V_\mathrm{A}. \tag{17d}$$

For $\mathcal{B} = 1\,\mathrm{mT}$, $V_\mathrm{A} \approx 1\,\mathrm{cm\,s^{-1}}$. Taking $\mathcal{V} = 10^{-4}\,\mathrm{m\,s^{-1}}$ as before, $A \approx 0.01$.

If $\Lambda \ll \mathrm{O}(1)$, $\mathrm{Ra}_c = \mathrm{O}(E^{-4/3})$. Molecular values for ν and κ give $E^{-4/3} = 10^{20}$ and $\mathrm{Ra}/\mathrm{Ra}_c \approx 10^3$. Turbulent values ν_T and κ_T of (10d) give $E^{-4/3} = 5 \times 10^{14}$ and $\mathrm{Ra}/\mathrm{Ra}_c \approx 1$. This would mean that convection would be weak or non-existent, which is inconsistent with the assumption of strong turbulence and eddy diffusivities.

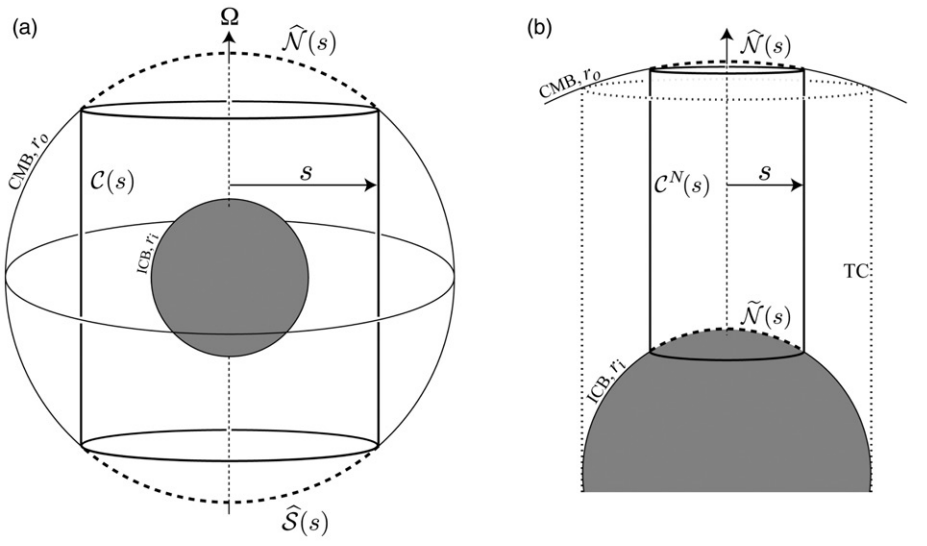

Figure 3. Geostrophic cylinders (a) $\mathcal{C}(s)$ located outside the tangent cylinder (TC), $s > r_i$, and (b) $\mathcal{C}^N(s)$ located inside the TC, $s < r_i$. The thick dashed lines denote a given cylinders' spherical caps. The TC is shown dotted in panel (b).

However, magnetic field strongly affects these estimates. If $\Lambda \geq \mathrm{O}(1)$, $\mathrm{Ra}_c = \mathrm{O}(E^{-1})$. Molecular diffusivities give $E^{-1} = 10^{15}$ and $\mathrm{Ra}/\mathrm{Ra}_c \approx 10^8$, while turbulent diffusivities give $E^{-1} = 10^{11}$ and $\mathrm{Ra}/\mathrm{Ra}_c \approx 10^4$. From these estimates, it seems probable that $\mathrm{Ra}/\mathrm{Ra}_c \gg 1$. Thus, it can be argued that the magnetic field makes the convection highly *supercritical*, such that the flow is sufficiently turbulent to homogenize S and X in the core.

In assessing the plausibility of these conclusions, it should be remembered that Ra is extremely uncertain in the core. Furthermore, the value of Ra_c for $\boldsymbol{B} \neq \boldsymbol{0}$ is derived from analyses in which $\boldsymbol{B}$ is not self-generated but has a source outside the fluid (cf. Zhang and Schubert 2000, King *et al.* 2010).

In section 8 and appendices B–D, an even simpler description of core magneto-convection will be adopted, the so-called *Boussinesq approximation* in which the density is assumed constant:

$$\rho_a = \rho_0 = \text{constant}, \quad \text{so that } \boldsymbol{\nabla} \cdot \boldsymbol{V} = 0, \tag{18a,b}$$

by (12a). The equation of motion (14) is virtually unchanged:

$$\partial_t \boldsymbol{V} + \boldsymbol{V} \cdot \boldsymbol{\nabla} \boldsymbol{V} + 2\boldsymbol{\Omega} \times \boldsymbol{V} = -\boldsymbol{\nabla} \Pi_c + C \boldsymbol{g}_{\mathrm{e}} + \rho_0^{-1} \boldsymbol{J} \times \boldsymbol{B} + \nu_T \nabla^2 \boldsymbol{V}, \tag{18c}$$

where the reduced pressure is now $\Pi_c = p_c/\rho_0$.

A flow $\boldsymbol{v}$ in which only the Coriolis force and the gradient of the reduced pressure ϖ_c are significant is said to be *geostrophic*. Then, by (18c),

$$2\boldsymbol{\Omega} \times \boldsymbol{v} = -\boldsymbol{\nabla} \varpi_c. \tag{19a}$$

On operating on this with $\nabla\times$ and combining with (18b), the *Proudman-Taylor theorem* emerges: $(\boldsymbol{\Omega}\cdot\nabla)\boldsymbol{v}=\boldsymbol{0}$, which implies that $\boldsymbol{v}$ is independent of z. For an axisymmetric boundary such as $\widehat{\mathcal{S}}$ where (16a) applies, it follows that

$$\boldsymbol{v} = v(s,t)1_\phi, \quad \varpi_c(s,t) = 2\Omega\int v(s,t)\mathrm{d}s, \tag{19b,c}$$

where (s,ϕ,z) are cylindrical coordinates. This is a motion in which each *geostrophic cylinder*, $\mathcal{C}(s)$ of radius s, rotates as a solid body about Oz with an angular velocity,

$$\zeta(s,t) = v(s,t)/s, \tag{19d}$$

independent of $\zeta(s,t)$ for every other $\mathcal{C}(s)$, see figure 3. The geostrophic cylinder, $\mathcal{C}(r_i)$, that touches the SIC is called the *tangent cylinder* (TC). The TC is particularly significant because the fluid dynamics inside and outside the TC are quite dissimilar (e.g. Hide and James 1983, Heimpel *et al*. 2005). It has been pointed out by Jault (2003) that, in the presence of bumps on the SIC, geostrophic cylinders generally do not exist for a small range of s surrounding $s=r_i$, but for simplicity we shall suppose that the FOC can be filled with geostrophic cylinders.

The smallness of Ro and E does not justify as drastic an approximation as (19a) but it encourages ejection of the inertial and viscous forces from (18c), leaving

$$2\boldsymbol{\Omega}\times\boldsymbol{V} = -\nabla\Pi_c + C\boldsymbol{g}_\mathrm{e} + \rho_0^{-1}\boldsymbol{J}\times\boldsymbol{B}. \tag{20a}$$

This form of the momentum equation is called the *magnetostrophic approximation*. One has a reasonable expectation that the macroscales of core MHD will be well-approximated by combining (20a) with (11d,g), (12a), and the boundary conditions. For $\boldsymbol{V}$, these are (16a); for the EM field they are

$$\boldsymbol{B}=\widehat{\boldsymbol{B}},\ \boldsymbol{E}_\mathrm{H}=\widehat{\boldsymbol{E}}_\mathrm{H}, \quad \text{on } r=r_o, \quad \boldsymbol{B}=\widetilde{\boldsymbol{B}},\ \boldsymbol{E}_\mathrm{H}=\widetilde{\boldsymbol{E}}_\mathrm{H},\ \text{on } r=r_i, \tag{20b,c,d,e}$$

where $\boldsymbol{E}$, $\widehat{\boldsymbol{E}}$ and $\widetilde{\boldsymbol{E}}$ are determined from $\boldsymbol{B}$, $\widehat{\boldsymbol{B}}$ and $\widetilde{\boldsymbol{B}}$ by (11e,f).

Because the inertial terms have been abandoned in (20a), there are no Alfvén waves and their timescale $\tau_\mathrm{A}=\mathcal{L}/V_\mathrm{A}$ does not feature in solutions of the magnetostrophic system. Alfvén waves are replaced by MAC waves that define the time scale:

$$\tau^\mathrm{m} = \frac{2\Omega\mathcal{L}^2}{V_\mathrm{A}^2} = \frac{\tau_\eta}{\Lambda}, \quad \text{where } \tau_\eta = \frac{\mathcal{L}^2}{\eta} \approx 10^5\,\mathrm{yr} \tag{20f,g}$$

is the free decay time for magnetic fields of scale $\mathcal{L}=r_o$. The acronym "MAC" and our index $^\mathrm{m}$ recognize that magnetostrophic motions and MAC waves are controlled as much by **M**agnetic and **A**rchimedean (buoyancy) forces as by **C**oriolis forces; inertial forces are conspicuous in the acronym by their absence. The magnetostrophic approximation is good only for macroscales for which $\mathcal{L}\gg V_\mathrm{A}/\Omega$ and on time periods that greatly exceed a day. For $V_\mathrm{A}\approx 1\,\mathrm{cm\,s^{-1}}$, this inequality is satisfied for $\mathcal{L}\gg 1\,\mathrm{km}$.

As $g_{\mathrm{e},\phi}=0$, the ϕ-component of (20a) is

$$2\Omega V_s = -\partial_\phi\Pi_c + \rho_0^{-1}(\boldsymbol{J}\times\boldsymbol{B})_\phi. \tag{21a}$$

This is integrated over the surface, $\mathcal{C}(s)$. To evaluate the resulting left-hand side of (21a), integrate (18b) over the interior, $\widehat{\mathcal{I}}(s)$, of $\mathcal{C}(s)$:

$$\int_{\mathcal{C}(s)} \boldsymbol{V}\cdot\boldsymbol{n}\,\mathrm{d}a + \int_{\widehat{\mathcal{N}}(s)} \boldsymbol{V}\cdot\boldsymbol{n}\,\mathrm{d}a + \int_{\widehat{\mathcal{S}}(s)} \boldsymbol{V}\cdot\boldsymbol{n}\,\mathrm{d}a = 0, \tag{21b}$$

where $\widehat{\mathcal{N}}(s)$ and $\widehat{\mathcal{S}}(s)$ are the spherical caps on the CMB completing the boundary of $\widehat{\mathcal{I}}(s)$. The second and third terms in (21b) vanish by (16a). The left-hand side of (21a) therefore vanishes on integration, as does the first-term on the right-hand side, leaving

$$\int_{\mathcal{C}(s)} (\boldsymbol{J}\times\boldsymbol{B})_\phi\,\mathrm{d}a = 0. \tag{21c}$$

If $s<r_i$, there are two cylinders, $\mathcal{C}^N(s)$ and $\mathcal{C}^S(s)$, of radius s to the north and south of the SIC, and two more spherical caps, $\widetilde{\mathcal{N}}(s)$ and $\widetilde{\mathcal{S}}(s)$, on the ICB across which no fluid flows either; see figure 3(b). Results analogous to (21c) hold:

$$\int_{\mathcal{C}^N(s)} (\boldsymbol{J}\times\boldsymbol{B})_\phi\,\mathrm{d}a = 0, \quad \int_{\mathcal{C}^S(s)} (\boldsymbol{J}\times\boldsymbol{B})_\phi\,\mathrm{d}a = 0. \tag{21d,e}$$

Equations (21c–e) are known as *Taylor's constraints* (Taylor 1963).

An arbitrary flow $\boldsymbol{V}$ can be separated into geostrophic and non-geostrophic parts: $\boldsymbol{V}=\boldsymbol{v}+\boldsymbol{V}^n$, and similarly $\Pi_c = \varpi_c + \Pi_c^{\mathrm{n}}$. To introduce these, we at first ignore the existence of the SIC. Then the *geostrophic average*, of a quantity such as V_ϕ is defined by

$$\{\!\{V_\phi\}\!\}(s,t) = \frac{1}{\widehat{A}(s)}\int_{\mathcal{C}(s)} V_\phi(s,\phi,z,t)\mathrm{d}a, \tag{22a}$$

where $\widehat{A}(s) = 4\pi s z_1$ is the surface area of $\mathcal{C}(s)$ and $z_1 = \sqrt{(r_o^2 - s^2)}$ is half the length of its sides. The geostrophic velocity is written as $\boldsymbol{v} = v(s,t)\mathbf{1}_\phi$ where $v(s,t) = \{\!\{V_\phi\}\!\}$. The non-geostrophic velocity, which carries the superscript $^{\mathrm{n}}$, is

$$\boldsymbol{V}^{\mathrm{n}}(s,\phi,z,t) = \boldsymbol{V}(s,\phi,z,t) - v(s,t)\mathbf{1}_\phi. \tag{22b}$$

It follows that the angular momentum of core flow about Oz is

$$\breve{M}_z(t) = \rho_0\int_{\mathrm{V}} sV_\phi\,\mathrm{d}v = \rho_0\int_0^{r_o} sv(s,t)\widehat{\mathcal{A}}(s)\,\mathrm{d}s, \quad \text{so that } \int_{\mathrm{V}} sV_\phi^{\mathrm{n}}\,\mathrm{d}v = 0, \tag{22c,d}$$

where $\mathrm{d}v$ is the volume element. Although derived for a core lacking an SIC, these results are easily generalized; see section 8.4 and appendix B. In confirmation of (22c), it is found that the geostrophic part of $\boldsymbol{V}$ carries all the axial angular momentum of the FOC.

Both v and $\breve{M}_z$ can be estimated from LOD data and the zonal part of the inferred core surface flow. In so far as the SIC is locked to the mantle (see section 7.2), $\widetilde{M}_z$ is a part of $\widehat{M}_z$ so that variations in LOD determine $(\widehat{M}_z + \widetilde{M}_z)$. Conservation of $\breve{M}_z + (\widehat{M}_z + \widetilde{M}_z)$ can therefore be checked, with generally gratifying agreement (Jault *et al.* 1988, Jackson 1997); see also our description of figure 1(c) above.

In the new notation just introduced, (21c–e) can be collectively written

$$\{\!\{\boldsymbol{J}\times\boldsymbol{B}\}\!\}_\phi = 0. \tag{23a}$$

For given $\boldsymbol{J}\times\boldsymbol{B}$, (20a), (18b) and (16a) determine $\boldsymbol{V}^{\rm n}$ but not v. That is the task of Taylor's constraint (23a). The class of $\boldsymbol{B}$ satisfying (23a) is so narrow that it is hard to find a single member. Having found one, it is necessary to preserve it as $\boldsymbol{B}$ evolves, by requiring

$$\partial_t\{\!\{\boldsymbol{J}\times\boldsymbol{B}\}\!\}_\phi = 0, \quad \text{i.e. } \{\!\{(\partial_t\boldsymbol{J})\times\boldsymbol{B}+\boldsymbol{J}\times(\partial_t\boldsymbol{B})\}\!\}_\phi = 0. \tag{23b,c}$$

The induction equation provides $\partial_t\boldsymbol{B}$ and Ampère's law (11c) supplies $\boldsymbol{J}$ and $\partial_t\boldsymbol{J}$. After reductions (relegated to the end of appendix B), it is found that (23b) is equivalent to

$$s^{-1}\mu_0\partial_t\{\!\{\boldsymbol{J}\times\boldsymbol{B}\}\!\}_\phi \equiv \alpha(s,t)\frac{\partial^2\zeta}{\partial s^2}+\beta(s,t)\frac{\partial\zeta}{\partial s}-R(s,t)=0, \tag{23d}$$

where

$$\alpha(s,t)=\{\!\{B_s^2\}\!\}, \quad \beta(s,t)=\{\!\{\boldsymbol{B}\cdot\boldsymbol{\nabla}B_s+2B_s^2/s\}\!\}, \tag{23e,f}$$

$$sR(s,t)=-\{\!\{(\boldsymbol{\nabla}\times\mathcal{S})\times\boldsymbol{B}+(\boldsymbol{\nabla}\times\boldsymbol{B})\times\mathcal{S}\}\!\}_\phi, \quad \mathcal{S}=\boldsymbol{\nabla}\times(\boldsymbol{V}^{\rm n}\times\boldsymbol{B})+\eta\nabla^2\boldsymbol{B}. \tag{23g,h}$$

Equations (23d–f) were derived by Taylor (1963). He pointed out that, if $\breve{M}_z$ is assigned, (23d) determines ζ uniquely from $R(s,t)$, i.e. from the evolving $\boldsymbol{V}^{\rm n}$ and $\boldsymbol{B}$. Since these obey the magnetostrophic equations, they evolve on the slow MAC time scale, $\tau^{\rm m}$, as therefore do $R(s,t)$ and ζ. This solution of (23d) will therefore be denoted by $\zeta^{\rm m}$ below, If the equations (20a) and (23a) are satisfied initially,

$$\boldsymbol{V}^{\rm m}=\boldsymbol{V}^{\rm n}+\boldsymbol{v}^{\rm m} \tag{23i}$$

satisfies them always. It is therefore the required solution of (20a).

An arbitrarily assigned $\boldsymbol{J}$ in general creates a $\boldsymbol{B}$ that contradicts (23a), at least initially. This shows that (20a) is an oversimplification of (18c) as is its consequence (21a); the inertial term, $\partial_t\boldsymbol{V}+\boldsymbol{V}\cdot\boldsymbol{\nabla}\boldsymbol{V}$, must be restored to (20a), resulting in the addition of $\{\!\{\rho_0(\partial_t\boldsymbol{v}+\boldsymbol{V}^{\rm n}\cdot\boldsymbol{\nabla}\boldsymbol{v}+\boldsymbol{v}\cdot\boldsymbol{\nabla}\boldsymbol{V}^{\rm n})\}\!\}_\phi$ to the right-hand side of (23a). As shown below, $\{\!\{\partial_t v_\phi\}\!\}_\phi=\mathrm{O}(V_{\rm A}\zeta)$ while $\{\!\{\boldsymbol{V}^{\rm n}\cdot\boldsymbol{\nabla}\boldsymbol{v}+\boldsymbol{v}\cdot\boldsymbol{\nabla}\boldsymbol{V}^{\rm n}\}\!\}_\phi\approx V_s^{\rm n}(s\partial_s\zeta+\zeta)=\mathrm{O}(V^{\rm n}\zeta)$. As $V_{\rm A}/V_{\rm n}=\mathrm{O}(100)$, only the $\partial_t\boldsymbol{V}$ of the inertial acceleration is significant; because $E\ll1$, the viscous term can be omitted as before. The geostrophic average of (18b) becomes

$$\rho_0\partial_t v=\{\!\{\boldsymbol{J}\times\boldsymbol{B}\}\!\}_\phi. \tag{24a}$$

On differentiating with respect to t and using (23d), it is seen that

$$\mu_0\rho_0\frac{\partial^2\zeta}{\partial t^2}-\alpha(s,t)\frac{\partial^2\zeta}{\partial s^2}-\beta(s,t)\frac{\partial\zeta}{\partial s}=-R(s,t). \tag{24b}$$

Another, perhaps more transparent, way of writing (24b) is

$$\frac{\partial^2\zeta^{\rm A}}{\partial t^2}=\frac{1}{s^2\widehat{A}}\frac{\partial}{\partial s}\left(s^2\widehat{A}V_{\rm A}^2\frac{\partial\zeta^{\rm A}}{\partial s}\right)+\widehat{N}s\frac{\partial\zeta^{\rm A}}{\partial s}-\frac{R(s,t)}{\mu_0\rho_0}, \tag{24c}$$

where $V_{\rm A}(s,t)$ is the Alfvén velocity defined by $V_{\rm A}^2=\{\!\{B_s^2\}\!\}/\mu_0\rho_0$, and

$$\widehat{N}(s,t)=\frac{r_o}{\mu_0\rho_0\widehat{A}z_1}\oint[(B_sB_r)(s,\phi,z_1)+(B_sB_r)(s,\phi,-z_1)]\mathrm{d}\phi. \tag{24d}$$

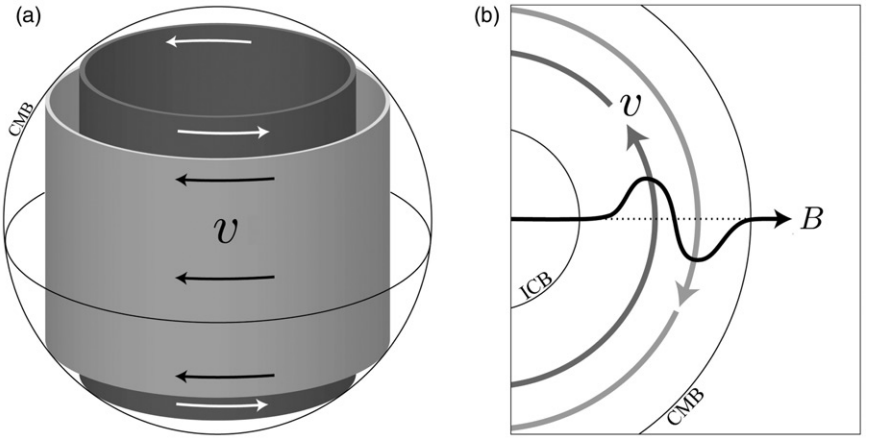

Figure 4. Schematics showing (a) a geostrophic flow in the core, $\boldsymbol{V}^{\mathrm{g}}$, and (b) a plan view of an initially cylindrical magnetic field (dashed line) distorted by $\boldsymbol{v}$. The restoring Lorentz torque on the distorted magnetic field, $\boldsymbol{B}$ (solid line), lead to the cylindrical propagation of torsional waves. Adapted from Dumberry 2007.

(The derivation of (24c) from (23d), though lengthy, is direct; it is included at the end of appendix B. The reduction does not discard the effects of magnetic diffusion which continues to be locked into the definition (23g) of $R(s, t)$.)

The essence of (24c) is contained in

$$\frac{\partial^2 \zeta^{\mathrm{A}}}{\partial t^2} = \frac{1}{s^2 \widehat{A}} \frac{\partial}{\partial s}\left(s^2 \widehat{A} V_{\mathrm{A}}^2 \frac{\partial \zeta^{\mathrm{A}}}{\partial s}\right), \tag{25}$$

which we call the *canonical wave equation*. (The additional $\widehat{N} s \partial_s \zeta^{\mathrm{A}}$ is one of two terms that are new to the subject and are discussed later; see section 8.3 and appendix B.) Equation (25) recovers something very similar to an Alfvén wave, called the *torsional wave* in which ζ^{A} evolves on the fast Alfvénic time scale

$$\tau_{\mathrm{A}} = r_o / V_{\mathrm{A}} \approx \ 6\,\mathrm{yr}. \tag{26a}$$

This is why $^{\mathrm{A}}$ was added to ζ in (24c) and (25). Because τ_{A} is so similar to the time-scales τ_{LOD} seen in figure 1, it is plausible that torsional waves are responsible for the LOD variations, as argued by Gillet *et al.* (2010). Because it is so dissimilar to τ^{m}, it is sensible to base discussions of torsional waves on representations of the form

$$\boldsymbol{V} = \boldsymbol{V}^{\mathrm{m}} + \boldsymbol{v}^{\mathrm{A}}. \tag{26b}$$

Then, when studying the waves, mac variables ($^{\mathrm{m}}$) can be assumed to be constant. In section 8 and appendices B–D, we shall use (26b) but omit the $^{\mathrm{A}}$ on wave variables such as ζ^{A}. We shall consider only the case when (23a) is nearly satisfied, and the wave amplitude is so small that quantities such as $(v^{\mathrm{A}})^2$ are negligible.

In a torsional wave, the geostrophic cylinders are in relative angular motion about their common (polar) axis; see figure 4(a). The response $\boldsymbol{b}^{\mathrm{A}}$ of $\boldsymbol{B}$ to the motion $\boldsymbol{v}^{\mathrm{A}}$ is not the geostrophic average of $\boldsymbol{B}$, but is determined by solving (11d,g) and boundary conditions (20b–e). It can, as for an Alfvén wave, be visualized by using the frozen

flux theorem, the field lines behaving like elastic strings threading the cylinders together and opposing their relative motion; see figure 4(b). The resulting torque on the cylinder supplies the restoring force for a wave that travels in the $\pm s$-direction, the mass of the cylinders providing the inertia. Whenever $\boldsymbol{J}$ and $\boldsymbol{B}$ contradict (23a), a torsional wave is launched.

Torsional waves open a window onto the dynamics of the core (e.g. Braginsky 1970, Jault and Le Mouël 1991, Jackson 1997, Zatman and Bloxham 1997, Gillet *et al*. 2010). They describe a basic dynamical response of core fluid in a rapidly rotating planet.

We have now completed a basic description of the thermal and dynamical states of Earth's core that will be needed in the following sections, where we discuss the various ways in which the core exchanges angular momentum with the mantle and inner core.

4. The four coupling mechanisms

The torque about O on the mantle, is

$$\widehat{\boldsymbol{\Gamma}} = \oint_{\widehat{\mathrm{S}}} \boldsymbol{r} \times \widehat{\boldsymbol{T}} \, \mathrm{d}a, \tag{27a}$$

where $\widehat{\boldsymbol{T}}$, sometimes called the *surface traction*, is the stress associated with the normal:

$$\widehat{T}_i = -\widehat{S}_{ij}\widehat{n}_j, \tag{27b}$$

where $\widehat{S}_{ij}$ $(= \widehat{S}_{ji})$ is the total stress tensor. The minus sign arises in (27b) because the unit normal, $\boldsymbol{n}$, points into the mantle. The component of $\widehat{\boldsymbol{\Gamma}}$ parallel to Oz is

$$\widehat{\Gamma}_z = -\oint_{\widehat{\mathrm{S}}} s \, \widehat{S}_{\phi n} \, \mathrm{d}a. \tag{27c}$$

Similar expressions hold for the torque on the SIC

$$\widetilde{\boldsymbol{\Gamma}} = \oint_{\widetilde{\mathrm{S}}} \boldsymbol{r} \times \widetilde{\boldsymbol{T}} \, \mathrm{d}a, \quad \widetilde{\Gamma}_z = \oint_{\widetilde{\mathrm{S}}} s \, \widetilde{S}_{\phi n} \mathrm{d}a, \quad \widetilde{T}_i = \widetilde{S}_{ij}\widetilde{n}_j. \tag{27d,e,f}$$

There is no minus sign in (27e,f) because $\boldsymbol{n}$ points out of the SIC.

Equation (27a) tacitly assumes that the core alone exerts a torque on the mantle; sources of torque from outside the Earth are ignored, and therefore

$$\breve{\boldsymbol{\Gamma}} + \widehat{\boldsymbol{\Gamma}} + \widetilde{\boldsymbol{\Gamma}} = \boldsymbol{0}, \tag{28a}$$

where $\breve{\boldsymbol{\Gamma}}$ is the torque on the FOC. Since

$$\mathrm{d}_t \widehat{\boldsymbol{M}} = \widehat{\boldsymbol{\Gamma}}, \quad \mathrm{d}_t \widetilde{\boldsymbol{M}} = \widetilde{\boldsymbol{\Gamma}}, \quad \mathrm{d}_t \breve{\boldsymbol{M}} = -\widehat{\boldsymbol{\Gamma}} - \widetilde{\boldsymbol{\Gamma}}, \tag{28b,c,d}$$

the angular momenta, $\widehat{\boldsymbol{M}}$, $\widetilde{\boldsymbol{M}}$ and $\breve{\boldsymbol{M}}$, of mantle, SIC and FOC are conserved in total:

$$\boldsymbol{M}_{\mathrm{tot}} = \widehat{\boldsymbol{M}} + \widetilde{\boldsymbol{M}} + \breve{\boldsymbol{M}} = \text{constant}. \tag{28e}$$

Equation (28e) implies that, if one of these three torques changes, so do(es) one or two of the others, in the opposite sense. The system is, in this respect, self-regulating.

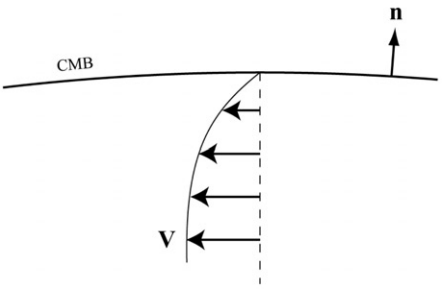

Figure 5. Schematic representation of how viscous core-mantle torques arise due to the normal gradient of the flow field on the CMB, $\partial \boldsymbol{V}/\partial \mathrm{n}$.

Stress is exerted on the CMB in four ways: through viscosity, topography, gravity and magnetic field, and there are correspondingly four parts to each of S_{ij}, $\boldsymbol{T}$ and $\widehat{\boldsymbol{\Gamma}}$, e.g.

$$\widehat{\boldsymbol{\Gamma}} = \widehat{\boldsymbol{\Gamma}}^V + \widehat{\boldsymbol{\Gamma}}^T + \widehat{\boldsymbol{\Gamma}}^G + \widehat{\boldsymbol{\Gamma}}^M. \tag{29}$$

We shall assess the magnitudes of the torques in turn. This requires some care since overestimation is all too easy. For example, we shall find below that the magnetic stress scales as $S_{ij}^M = \mathrm{O}(\mathcal{B}^2/\mu_0)$. It might therefore seem that $\widehat{\boldsymbol{\Gamma}}^M = \mathrm{O}(\widehat{\mathcal{B}}^2 r_o^3/\mu_0)$, but clearly this is false since $\widehat{\boldsymbol{\Gamma}}^M$ is proportional to the Lorentz force, $\widehat{\boldsymbol{J}}\times\widehat{\boldsymbol{B}}$, and $\widehat{\boldsymbol{J}}$ vanishes if the mantle is electrically insulating. Although $\widehat{S}_{ij}^M = \mathrm{O}(\widehat{\mathcal{B}}^2/\mu_0)$ is still a good estimate of the magnetic stress at each point of the CMB, there is complete cancellation of the integral of $\boldsymbol{r}\times\widehat{\boldsymbol{T}}^M$ over the CMB.

Apart from $\widehat{\boldsymbol{\Gamma}}^T$, $\widehat{\boldsymbol{\Gamma}}^G$, $\widetilde{\boldsymbol{\Gamma}}^T$, and $\widetilde{\boldsymbol{\Gamma}}^G$, negligible error is made by replacing the CMB and ICB in (27a–f) by spheres, $\widehat{\mathrm{S}}_\bullet$ and $\widetilde{\mathrm{S}}_\bullet$, of radius r_o and r_i; these are written $\widehat{\mathrm{S}}$ and $\widetilde{\mathrm{S}}$ in sections 5 and 8.

5. The viscous torque

The components of the viscous stress tensor are

$$S_{ij}^V = \rho_0\nu\left(\nabla_j V_i + \nabla_i V_j - \frac{2}{3}\nabla_k V_k \delta_{ij}\right), \tag{30a}$$

the last term of which is ignored because in this section it is assumed that core fluid has a uniform fluid density, ρ_0 ($\approx 10^4\,\mathrm{kg\,m^{-3}}$), so that $\boldsymbol{\nabla}\cdot\boldsymbol{V}=0$. In the mantle frame, the no slip condition on the CMB (assumed spherical) is $\boldsymbol{V}=0$ so that the surface traction on the mantle is

$$\widehat{\boldsymbol{T}}^V = -\rho_0\nu(\partial_r \boldsymbol{V} + \boldsymbol{\nabla} V_r), \tag{30b,c}$$

in which the final term contributes to $\widehat{T}_r^V$ only, because $V_r=0$ on the CMB. Therefore, assuming that the kinematic viscosity ν is uniform, (27c,d) give

$$\widehat{\boldsymbol{\Gamma}}^V = -\rho_0\nu \oint_{\widehat{\mathrm{S}}_\bullet} \boldsymbol{r}\times\partial_r \boldsymbol{V}\,\mathrm{d}a, \quad \widehat{\Gamma}_z^V = -\rho_0\nu \oint_{\widehat{\mathrm{S}}_\bullet} s\,\partial_r V_\phi\,\mathrm{d}a. \tag{31a,b}$$

The traction acts to drag the mantle in the direction of the subsurface flow, see figure 5.

The viscosity of core fluid is hard to estimate. First principles calculations (e.g. de Wijs *et al*. 1998) suggest that ν at the CMB is $10^{-6}\,\mathrm{m^2\,s^{-1}}$, to within a factor of 3. Assuming $\boldsymbol{V}$ is laminar, an upper bound on $\boldsymbol{\Gamma}^V$ is obtained by assuming that $\partial_r \boldsymbol{V} = \mathrm{O}(\mathcal{V}/d_\nu)$, where d_ν is the thickness of the Ekman layer at the CMB: $d_\nu = E^{-1/2} r_o \approx 0.1\,\mathrm{m}$. Assuming $\mathcal{V} \approx 10^{-4}\,\mathrm{m\,s^{-1}}$, the surface traction, $\widehat{T}^V \approx \rho_0 \nu \mathcal{V}/d_\nu$, is about $10^{-5}\,\mathrm{N\,m^{-2}}$, implying that $\widehat{\Gamma}^V \approx 5 \times 10^{14}\,\mathrm{Nm}$.

One may argue that the core is highly turbulent, so that a turbulent viscosity, ν_T, should replace the molecular value, ν, in this estimate. Although it is strictly inconsistent to assume that $\mathcal{L}$ is the microscale length, $\ell \sim E^{1/3} r_o \approx 100\,\mathrm{m}$, used in deriving (10d), an upper bound on $\boldsymbol{\Gamma}^V$ is obtained by doing so. This gives $\widehat{T}^V \approx \rho_0 \nu_T v/\ell \approx \rho_0 (\nu \ell v/\ell) \approx \rho_0 v^2 \approx 10^{-4}\,\mathrm{N\,m^{-2}}$, implying $\widehat{\Gamma}^V_z \approx 5 \times 10^{15}\,\mathrm{N\,m}$.

These arguments may overestimate $\widehat{\boldsymbol{\Gamma}}^V$ for another reason: according to Braginsky (1999), Loper (2007), and Buffett (2010) there may be a low density layer at the top of the FOC. Braginsky (1999) pointed out that the light material released during the freezing of the SIC may tend to congregate near the ICB, and that this may answer unresolved questions about the geomagnetic secular variation (Braginsky 1984). Turbulent motions in a buoyantly stable layer tend to be damped preferentially in the direction of stratification, and this reduces the macroscale momentum transport across the layer (e.g. Duck and Foster 2001, Davidson 2004). Waves in such a layer may increase what ν alone can do in transporting macroscale momentum (e.g. Rogers and Glatzmaier 2006). But it is doubtful if they can transport it as effectively as the fully convective turbulence that exists far from boundaries.

Though these and similar arguments lack rigor, the upper bounds on $\widehat{\Gamma}^V$ derived above are consistently less than the target torque, though not by a large factor (cf. Deleplace and Cardin 2006, Buffett and Christensen 2007).

6. The topographic torque

The likelihood that there are inverted mountains and valleys on the CMB, and that these might create topographic torques large enough to explain the observed changes in LOD, was first suggested by Hide (1969). These irregularities in the figure of the CMB are often collectively called "bumps", and their study was jokingly christened *Geophrenology* by the late Keith Runcorn. Hide's suggestion generated significant interest and much literature, e.g. Anufriyev and Braginsky (1977), Jault and Le Mouël (1989), Kuang and Bloxham (1993, 1997), Buffett (1998), and Kuang and Chao (2001).

Topographic coupling between the FOC and its boundaries depends on deviations from sphericity in the shape of the CMB and ICB. The fluid pressure, p, creates a surface traction, $\boldsymbol{T}^T = p\boldsymbol{n}$, that is not purely radial. The resulting topographic torques on the mantle and SIC are

$$\widehat{\boldsymbol{\Gamma}}^T = \oint_{\widetilde{\mathrm{S}}} p\,\boldsymbol{r} \times \boldsymbol{n}\,\mathrm{d}a, \quad \widetilde{\boldsymbol{\Gamma}}^T = -\oint_{\widetilde{\mathrm{S}}} p\,\boldsymbol{r} \times \boldsymbol{n}\,\mathrm{d}a. \tag{32a,b}$$

Equal but opposite torques act on the FOC, so that (cf. (28a))

$$\check{\boldsymbol{\Gamma}}^T = -\widehat{\boldsymbol{\Gamma}}^T - \widetilde{\boldsymbol{\Gamma}}^T = -\int_{\check{\mathrm{V}}} \boldsymbol{r} \times \nabla p\,\mathrm{d}v. \tag{32c}$$

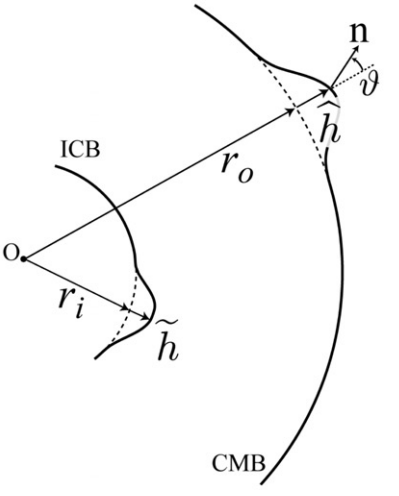

Figure 6. Schematic showing stresses acting on non-axisymmetric topography, $\widehat{h}(\theta,\phi)$, that rests atop a spherical CMB. A varying core fluid pressure field, $p(\mathbf{x})$, may then exert a net topographic torque on the mantle, $\widehat{\boldsymbol{\Gamma}}^T$. Similarly, non-axisymmetric topography on the ICB, $\widetilde{h}(\theta,\phi)$, can lead to torques, $\widetilde{\boldsymbol{\Gamma}}^T$, being exerted on the SIC. The bumps shown are greatly exaggerated in scale; for small-scale bumps such that $\widehat{h} \ll r_o$, note that $\widehat{\vartheta} \approx \tan\widehat{\vartheta} \approx |\nabla\widehat{h}|$.

In what follows, we take the equations of the CMB and ICB to be

$$r = r_o + \widehat{h}(\theta,\phi), \quad r = r_i + \widetilde{h}(\theta,\phi). \tag{33a,b}$$

There is a good way of approximating the torques (32a,b). To derive it, we focus on the CMB; application to the ICB is similar. Two assumptions are made. First it is supposed that $|\widehat{h}| \ll r_o$. This is supported by seismic studies that indicate that the typical height $\mathcal{H}$ of bumps on the CMB is of order 1 km; see e.g. Tanaka (2010). Second, it is supposed that the horizontal scale of the topography is significantly greater than $\mathcal{H}$, so that the angle $\vartheta(\approx |\nabla\widehat{h}|)$ between $\boldsymbol{r}$ and $\boldsymbol{n}$ is small at most points on the CMB, see figure 6. (For a discussion of the effects of small-scale topography, see Le Mouël *et al.* (2006).) As $\widehat{h}$ is a function of only θ and ϕ, its gradient $\nabla\widehat{h}$ is necessarily horizontal, and $\nabla\widehat{h}\times\boldsymbol{r} = r|\nabla\widehat{h}|\boldsymbol{t} = r\vartheta\boldsymbol{t}$, where $\boldsymbol{t}$ is the horizontal unit vector parallel to $\boldsymbol{r}\times\boldsymbol{n}$. As $\boldsymbol{r}\times\boldsymbol{n}$ is also $r\vartheta\boldsymbol{t}$, it follows that $\boldsymbol{r}\times\boldsymbol{n} = -\boldsymbol{r}\times\nabla\widehat{h}$. Because $|\vartheta| \ll 1$, the areas of da and its projection on the sphere $\widehat{\mathrm{S}}_\bullet$ are approximately equal. Therefore $\boldsymbol{r}\times\boldsymbol{n}\,\mathrm{d}a \approx -\boldsymbol{r}\times\nabla\widehat{h}\,\mathrm{d}a$ and (32a) becomes

$$\widehat{\boldsymbol{\Gamma}}^T = -\oint_{\widehat{\mathrm{S}}_\bullet} p\,\boldsymbol{r}\times\nabla\widehat{h}\,\mathrm{d}a, \quad \text{or} \quad \widehat{\boldsymbol{\Gamma}}^T = \oint_{\widehat{\mathrm{S}}_\bullet} \widehat{h}\,\boldsymbol{r}\times\nabla p\,\mathrm{d}a. \tag{34a,b}$$

The equality of the z-components of these torques, i.e.

$$\widehat{\Gamma}^T_z = -\oint_{\widehat{\mathrm{S}}_\bullet} p\,\partial_\phi\widehat{h}\,\mathrm{d}a, \quad \text{or} \quad \widehat{\Gamma}^T_z = \oint_{\widehat{\mathrm{S}}_\bullet} \widehat{h}\,\partial_\phi p\,\mathrm{d}a \tag{34c,d}$$

is apparent by an integration by parts. Since this argument does not depend on how Oz is chosen, the equality of the x- and y-components is also verified, so that the equivalence of (34a) and (34b) is established.

Equations (34a) can also be derived from (32a) by first noticing that the torques are O($\mathcal{H}$) and that extrapolation of the integrand onto $\widehat{\mathrm{S}}_\bullet$ only makes negligible corrections

of order $\mathcal{H}^2$. On writing (33a) as $f(r,\theta,\phi)=0$, where $f(r,\theta,\phi)\equiv r-\widehat{h}(\theta,\phi)$, it is clear that ∇f is parallel to $\boldsymbol{n}$. If $|\nabla\widehat{h}|^2 \ll 1$, then $(\nabla f)^2\approx 1$ so that $\boldsymbol{n}\approx \mathbf{1}_r-\nabla\widehat{h}$. This implies that $\boldsymbol{r}\times\boldsymbol{n}\approx -\boldsymbol{r}\times\nabla\widehat{h}$, as before. Analogous approximations apply for (32b).

In the aspherical reference model of section 2.2, the equipotential surfaces in the FOC deviate from spheroidal form not only because of convection, but also because of the bumpiness of Φ_{e}, created primarily by density anomalies in the mantle. The induced density variations, ρ_a', in the FOC were estimated in section 2.2 to be of order $10^{-4}\rho_a$; see also Wahr and deVries (1989), Forte *et al.* (1994), and Defraigne *et al.* (1996). This greatly exceeds the convective variations, $\rho_c=\mathrm{O}(10^{-8}\rho_a)$. Similarly, the pressure variations, p_a, are of order 10^4 times larger than the pressure differences, p_c, associated with convection. Potentially, the largest parts of (32a–c) are the *adiabatic topographic torques*:

$$\widehat{\boldsymbol{\Gamma}}_a^{\,T}=\oint_{\widehat{\mathrm{S}}} p_a\,\boldsymbol{r}\times\boldsymbol{n}\,\mathrm{d}a,\quad \widetilde{\boldsymbol{\Gamma}}_a^{\,T}=-\oint_{\widetilde{\mathrm{S}}} p_a\,\boldsymbol{r}\times\boldsymbol{n}\,\mathrm{d}a,\quad \check{\boldsymbol{\Gamma}}_a^{\,T}=-\int_{\check{\mathrm{V}}}\boldsymbol{r}\times\nabla p_a\,\mathrm{d}v, \qquad (35\mathrm{a,b,c})$$

which should therefore be examined first.

If the CMB and ICB were equipotential surfaces, p_a on them would be constant, and could be withdrawn through the integral signs, leaving integrals that vanish. But relative motions in the mantle and SIC are slow, and in these bodies thermodynamic variables such as the pressure are not constant on equipotential surfaces. In particular, the CMB and ICB are not equipotentials. Also, as they are not perfectly spherical, $\boldsymbol{r}\times\boldsymbol{n}\neq 0$. There is therefore no *a priori* reason to suppose that the adiabatic topographic torques should be zero, although, as mentioned in section 4, the system mantle-FOC-SIC is self-regulating. If the adiabatic torques cause the angular velocities of mantle and SIC relative to the FOC to change, other torques will grow in opposition and establish a new torque balance.

The density anomalies in the mantle evolve on such a long time scale that their contributions to the gravitational potential Φ_{e} can be regarded as nearly time independent. Similarly, the shape and structure of the SIC can change significantly only over long time spans. Nevertheless, the orientation of the SIC and even its center of mass can alter on much shorter, sub-decadal time scales as it responds to its turbulent environment. This modifies the equipotential surfaces in the FOC and therefore alters p_a. The torques $\widehat{\boldsymbol{\Gamma}}_a^{\,T}$ and $\widetilde{\boldsymbol{\Gamma}}_a^{\,T}$ therefore fluctuate about their means. We postpone further discussion of adiabatic torques until section 7.

Consider next the torques associated with the convective motions in the FOC, e.g.

$$\widehat{\boldsymbol{\Gamma}}_c^{\,T}=\oint_{\widehat{\mathrm{S}}_\bullet}\widehat{h}\,\boldsymbol{r}\times\nabla p_c\,\mathrm{d}a,\quad \widehat{\Gamma}_{c,z}^{\,T}=\oint_{\widehat{\mathrm{S}}_\bullet}\widehat{h}\,\partial_\phi p_c\,\mathrm{d}a. \qquad (36\mathrm{a,b})$$

Reasons were given in section 3.2 why core flow is well-described by the magnetostrophic approximation (20a), and why Coriolis and Lorentz forces are comparable deep in the core, implying a magnetic field strength $\mathcal{B}$ there of about 2 mT, or about 40 times greater than the typical field strength $\mathcal{B}_o$ on the CMB. The Lorentz force in (20a) is therefore negligible on the CMB and, as g_ϕ is small, $\partial_\phi p_c\approx -2\Omega\rho_0 r_o V_\theta\cos\theta\sin\theta$ on the CMB. Therefore (Speith *et al.* 1986, Hide *et al.* 1993), by (34d),

$$\widehat{\Gamma}_{c,z}^{\,T}=-2\Omega\rho_0 r_o\oint_{\widehat{\mathrm{S}}_\bullet}\widehat{h}(\theta,\phi)V_\theta(r_o,\theta,\phi)\cos\theta\sin\theta\;\mathrm{d}a. \qquad (36\mathrm{c})$$

In principle, $\widehat{\Gamma}^{T}_{c,z}$ can be estimated by extracting $\widehat{h}$ from seismological analysis, and by using the $V_\theta(r_o,\theta,\phi)$ inferred from the core surface motion. In practice, this is difficult and has led to controversy. Equation (36c) suggests that

$$\widehat{\Gamma}^{T}_{c,z} = \mathrm{O}(2\Omega\rho\,\mathcal{V}_c\mathcal{H}r_o^3), \tag{36d}$$

which is of order 10^{18} Nm for $\mathcal{H} = 100$ m. Such a bump height is well within the bounds set by recent seismic investigations (e.g. Tanaka 2010). Equation (36b) superficially confirms (36d) but highlights a serious concern: because p_c is a single-valued function, $\partial_\phi p_c$ is as often positive as negative for any θ in the integrand of (36b). Though $\pm 2\Omega\rho\mathcal{V}_c r_o$ is a reasonable estimate of $\partial_\phi p_c$ at most points on the CMB, considerable cancellation is possible when evaluating the integral in (36b). There is even a remote possibility that the cancellation is complete; see Anufriyev and Braginsky (1977).

Reliable estimation of the convective topographic torque must probably await careful experiments and allied theory. No argument has so far convincingly demonstrated that topography can create torques of the target magnitude of 10^{18} Nm but, equally, nothing has shown that it cannot.

7. The gravitational torque

7.1. *Initial considerations*

The gravitational force and torque about O on a body V of density $\rho(\boldsymbol{r})$ in a gravitational field $\boldsymbol{g}(\boldsymbol{r})$ are

$$\boldsymbol{F}^G = \int_{\mathrm{V}} \rho\boldsymbol{g}\,\mathrm{d}v, \quad \boldsymbol{\Gamma}^G = \int_{\mathrm{V}} \rho\boldsymbol{r}\times\boldsymbol{g}\,\mathrm{d}v. \tag{37a,b}$$

These integrals over volume can be transformed into surface integrals by introducing the gravitational stress tensor S^G_{ij}. It is shown in appendix E that

$$\rho g_i = \nabla_j S^G_{ij}, \quad \text{where } S^G_{ij} = -(4\pi G)^{-1}\left(g_i g_j - \frac{1}{2}g^2\delta_{ij}\right). \tag{37c,d}$$

Equations (37c,d) enable (37a,b) to be written as integrals over the surface, A, of V:

$$\boldsymbol{F}^G = -\frac{1}{4\pi G}\oint_{\mathrm{A}} [(\boldsymbol{n}\cdot\boldsymbol{g})\boldsymbol{g} - \tfrac{1}{2}g^2\boldsymbol{n}]\mathrm{d}a, \tag{37e}$$

$$\boldsymbol{\Gamma}^G = -\frac{1}{4\pi G}\oint_{\mathrm{A}} \boldsymbol{r}\times[(\boldsymbol{n}\cdot\boldsymbol{g})\boldsymbol{g} - \tfrac{1}{2}g^2\boldsymbol{n}]\mathrm{d}a, \tag{37f}$$

where $\boldsymbol{n}$ points out of V. These general results can be applied to the gravitational interactions between SIC, FOC and mantle. As in the last section, the unit normals to the CMB and ICB are directed approximately away from O. Because the self-gravitational force and torque of the Earth on itself are zero (see appendix E),

$$\widehat{\boldsymbol{\Gamma}}^G + \widetilde{\boldsymbol{\Gamma}}^G + \check{\boldsymbol{\Gamma}}^G = \boldsymbol{0}. \tag{37g}$$

If the FOC were in a quiescent state, the ICB would be an equipotential surface in phase equilibrium, but turbulent flow in the FOC exerts torques on the SIC that continually change its orientation, so that it is no longer an equipotential surface. Phase equilibrium can be re-established only very slowly and, before that can happen, the torques will again change the SIC orientation. The ICB is in phase equilibrium only in an average sense. As the ICB departs from phase equilibrium, two processes constantly try to re-establish it: internal flow and change of phase. In the former, the stresses exerted on the ICB by the FOC set up slow internal motions within the SIC that tend to restore its equilibrium form (Yoshida *et al.* 1996, Buffett 1997). In the latter, the thermodynamic disequilibrium created by the misalignment is removed by new freezing of the FOC or new melting of the SIC at the ICB (cf. Fearn *et al.* 1981, Morse 1986).

The mechanical properties of iron at high pressures and temperatures strongly depend on grain size and history, and on stress state and history (Bergman 1998, van Orman 2004, Venet *et al.* 2009). Models make widely different predictions. For example, in contrast to the results of Bergman (1998) and Venet *et al.* (2009), van Orman (2004) argues, based on a Harper–Dorn creep mechanism, that the SIC has such a small viscosity that it may be restored to equilibrium in a time of order 60 s. To satisfy anomalous seismic observations pertaining to the bottom 200 km of the FOC, Gubbins *et al.* (2008) argue that this fluid may not be on an adiabat but on the liquidus. This implies that, in super-saturated regions, iron would tend to rain out preferentially onto the ICB (e.g. Chen *et al.* 2008). Such a phase change process might act to return the SIC to its equilibrium form on a time scale controlled by the dynamics of the flow at the base of the FOC.

The results of van Orman (2004) and Gubbins *et al.* (2008) may imply such a fast relaxation that the gravitational torque between the mantle and the SIC is weak. We will now consider consequences of the opposite assumption, that the equilibration processes are very slow relative to semi-decadal time scales of interest here. The SIC then well-approximates a rigid body whose orientation is determined by the torques that act on it. The mantle will be treated as a solid too. (Its elasticity is included in the analysis of Dumberry 2008.)

By (37b), the gravitational torque on the fluid core due to the mantle and SIC is

$$\check{\boldsymbol{\Gamma}}^{G} = \int_{\check{\mathrm{V}}} (\rho_a + \rho_c)\boldsymbol{r} \times (\boldsymbol{g}_{\mathrm{e}} + \boldsymbol{g}_c)\,\mathrm{d}v = \check{\boldsymbol{\Gamma}}_a^{G} + \check{\boldsymbol{\Gamma}}_c^{G}, \tag{38a}$$

where $\check{\boldsymbol{\Gamma}}_a^{G}$ and $\check{\boldsymbol{\Gamma}}_c^{G}$ are the adiabatic and convective parts of $\check{\boldsymbol{\Gamma}}^{G}$:

$$\check{\boldsymbol{\Gamma}}_a^{G} = \int_{\check{\mathrm{V}}} \rho_a \boldsymbol{r} \times \boldsymbol{g}_{\mathrm{e}}\,\mathrm{d}v, \quad \check{\boldsymbol{\Gamma}}_c^{G} = \int_{\check{\mathrm{V}}} \boldsymbol{r} \times (\rho_c \boldsymbol{g}_{\mathrm{e}} + \rho_a \boldsymbol{g}_c + \rho_c \boldsymbol{g}_c)\,\mathrm{d}v. \tag{38b,c}$$

It was pointed out in section 2.2 that $\rho_c = \mathrm{O}(10^{-4}\,\rho_a)$. Similarly, Φ_c is smaller than the Φ_a contained in Φ_e by a similar factor. Potentially, $\check{\boldsymbol{\Gamma}}^{G}$ is dominated by its adiabatic part, which should therefore be examined first. By (6a), (35c) and (38b)

$$\check{\boldsymbol{\Gamma}}_a^{G+T} \equiv \check{\boldsymbol{\Gamma}}_a^{G} + \check{\boldsymbol{\Gamma}}_a^{T} = \int_{\check{\mathrm{V}}} \boldsymbol{r} \times (\rho_a \boldsymbol{g}_{\mathrm{e}} - \boldsymbol{\nabla} p_a)\,\mathrm{d}v = \boldsymbol{0}. \tag{38d}$$

The integrals, $\widehat{\boldsymbol{\Gamma}}_a^{G+T}$ and $\widetilde{\boldsymbol{\Gamma}}_a^{G+T}$, that correspond to (38d) for the mantle and SIC are the measures $\widehat{\boldsymbol{D}}$ and $\widetilde{\boldsymbol{D}}$ already introduced in (7d,e) and are in general nonzero.

By (34a,b), (37f) and the continuity of $\boldsymbol{g}$ and p, we may write these as

$$\widehat{\boldsymbol{D}} = \oint_{\widehat{\mathrm{A}}} \boldsymbol{r} \times \left\{ p_a \boldsymbol{n} + (4\pi G)^{-1} [(\boldsymbol{n} \cdot \boldsymbol{g}_\mathrm{e}) \boldsymbol{g}_\mathrm{e} - \tfrac{1}{2} g_\mathrm{e}^2 \boldsymbol{n}] \right\} \mathrm{d}a, \tag{39a}$$

$$\widetilde{\boldsymbol{D}} = -\oint_{\widetilde{\mathrm{A}}} \boldsymbol{r} \times \left\{ p_a \boldsymbol{n} + (4\pi G)^{-1} [(\boldsymbol{n} \cdot \boldsymbol{g}_\mathrm{e}) \boldsymbol{g}_\mathrm{e} - \tfrac{1}{2} g_\mathrm{e}^2 \boldsymbol{n}] \right\} \mathrm{d}a, \tag{39b}$$

from which, in agreement with (7g) and (38d),

$$\widehat{\boldsymbol{D}} + \widetilde{\boldsymbol{D}} = \boldsymbol{0}, \quad \text{i.e. } \widehat{\boldsymbol{\Gamma}}_a^{G+T} + \widetilde{\boldsymbol{\Gamma}}_c^{G+T} = \boldsymbol{0}. \tag{39c,d}$$

This expresses the dominant, adiabatic part of the torque balance.

If the torques $\widehat{\boldsymbol{\Gamma}}_a^{G+T}$ and $\widetilde{\boldsymbol{\Gamma}}_a^{G+T}$ are nonzero, $\widehat{\boldsymbol{\Omega}}$ and $\widetilde{\boldsymbol{\Omega}}$ change, and the relative orientation of the mantle and SIC is altered, so that $\boldsymbol{g}_a$ and p_a in (39a,b) change. This tends to return the system to its minimum energy configuration, in which

$$\widehat{\boldsymbol{\Gamma}}_a^{G+T} = \boldsymbol{0}, \quad \widetilde{\boldsymbol{\Gamma}}_a^{G+T} = \boldsymbol{0}. \tag{40a,b}$$

This is why (7f,g) were imposed on the aspherical reference state. If this torque-free state is perturbed, these restoring torques set up a *gravitational oscillation* of the SIC relative to the mantle.

This discussion has centered on conservation of angular momentum and the measures $\widehat{\boldsymbol{D}}$ $(=\widehat{\boldsymbol{\Gamma}}_a^{G+T})$ and $\widetilde{\boldsymbol{D}}$ $(=\widetilde{\boldsymbol{\Gamma}}_a^{G+T})$. Closely parallel statements can be made concerning conservation of linear momentum and the measures $\widehat{\boldsymbol{d}}$ $(=\widehat{\boldsymbol{F}}_a^{G+T})$ and $\widetilde{\boldsymbol{d}}$ $(=\widetilde{\boldsymbol{F}}_a^{G+T})$. These bear on phenomena such as the Slichter mode, but are beyond the scope of this article.

7.2. *Gravitational oscillations*

We start with a simple model of a gravitational oscillation and then elaborate on it. Suppose that the gravitational anomaly (8c) is created by sources entirely within the mantle, the CMB having no bumps, so that $\widehat{\Gamma}_{a,z}^{G+T} = \widehat{\Gamma}_{a,z}^{G}$. Similarly, suppose the SIC is spherical but has internal sources that above the ICB produce the gravitational anomaly

$$\Phi_\mathrm{e}'' = \widetilde{\mathcal{A}} (r_i/r)^3 \sin^2\theta \cos 2(\phi - \varphi), \quad (\widetilde{\mathcal{A}} > 0), \tag{41a}$$

where φ is the angular displacement of the system from the stable equilibrium state $\varphi = 0$. This is sometimes called the *misalignment angle*. Equations (39a,b) show that

$$\widehat{\Gamma}_{a,z}^{G} = -\widetilde{\Gamma}_{a,z}^{G} = \Gamma_0^G \sin 2\varphi, \quad \text{where } \Gamma_0^G = 8\widehat{\mathcal{A}}\,\widetilde{\mathcal{A}}\, r_i^3/3Gr_o^2 \ (>0) \tag{41b,c}$$

with $\widehat{\mathcal{A}}$ defined in (8c). These torques vanish for the stable minimum energy states $\varphi = 0$, π (and also for the unstable states $\varphi = \pm\frac{1}{2}\pi$). Small departures from a stable state satisfy

$$\widehat{C}\mathrm{d}_t^2\widehat{\varphi} = 2\Gamma_0^G(\widetilde{\varphi} - \widehat{\varphi}), \quad \widetilde{C}\mathrm{d}_t^2\widetilde{\varphi} = -2\Gamma_0^G(\widetilde{\varphi} - \widehat{\varphi}), \tag{41d,e}$$

where $\widehat{C}$ $(=7.12 \times 10^{37}\,\mathrm{kg\,m^2})$ and $\widetilde{C}$ $(= 5.87 \times 10^{34}\,\mathrm{kg\,m^2})$ are the polar moments of inertia of mantle and SIC, respectively. These equations imply

$$\widehat{C}\widetilde{C}\mathrm{d}_t^2(\widehat{\phi} - \widetilde{\phi}) = -2\Gamma_0^G(\widehat{C} + \widetilde{C})(\widehat{\phi} - \widetilde{\phi}), \tag{41f}$$

which has a solution (for some constant t_0)

$$\widehat{\phi} - \widetilde{\phi} = (\widehat{\phi} - \widetilde{\phi})_{\max} \cos \omega^G (t - t_0), \tag{41g}$$

where the frequency, ω^G, of the gravitational oscillation is

$$\omega^G = [2(\widehat{C} + \widetilde{C})\Gamma_0^G / \widehat{C}\widetilde{C}]^{1/2} \approx [2\Gamma_0^G / \widetilde{C}]^{1/2}. \tag{41h}$$

This example can be generalized to the case where the CMB and/or the ICB have bumps. Suppose the anomaly defined by (8c) is created entirely by CMB topography, $\widehat{h} = \widehat{\epsilon} \sin^2\theta \cos 2\phi$. Since $|\widehat{h}| \ll r_o$, the gravitational potential produced by the topography $\widehat{h}$ is, for $|r - r_o| \gg |\widehat{h}|$, the same as that of a surface mass distribution whose mass per unit area is $\widehat{m} = \widehat{h}\,\widehat{\Delta}$, where $\widehat{\Delta} = \rho - \widehat{\rho} \approx 4.34 \times 10^3\,\mathrm{kg\,m^{-3}}$ is the density jump across the CMB. Using the fact [see(2e)] that $\widehat{g}_r(r_o) - \breve{g}_r(r_o) = -4\pi G\widehat{m}$, for the surface mass distribution, the gravitational potential it creates is continuous and may be written

$$\Phi' = \begin{cases} \mathcal{A}(r_o/r)^3 \sin^2\theta \cos 2\phi, & r \geq r_o, \\ \mathcal{A}(r/r_o)^2 \sin^2\theta \cos 2\phi, & r \leq r_o, \end{cases} \tag{42a}$$

where $\mathcal{A} = -4\pi G r_o \widehat{m}/5$. This agrees with (8c) if

$$\widehat{h} = \widehat{\epsilon} \sin^2\theta \cos 2\phi, \quad \text{where } \widehat{\epsilon} = -5\widehat{\mathcal{A}}/4\pi G r_o \widehat{\Delta}. \tag{42b,c}$$

This shows that the $\widehat{\mathcal{A}}$ in (8c) can be explained by topography on the CMB with a maximum bump height, $|\widehat{\epsilon}|$, of about 0.7 km. The anomaly is however usually attributed to deviations in $\widehat{\rho}\,'$ within the mantle that are "frozen in" because of its high viscosity; $\widehat{\nu} \approx 5 \times 10^{19}\,\mathrm{m^2\,s^{-1}}$ in the deep mantle (e.g. Schubert *et al.* 2001).

In a similar way, the anomaly of (41a) could be produced entirely by topography on the ICB:

$$\widetilde{h} = \widetilde{\epsilon} \sin^2\theta \cos 2(\phi - \varphi), \quad \text{where } \widetilde{\epsilon} = -5\widetilde{\mathcal{A}}/4\pi G r_i \widetilde{\Delta}. \tag{42d,e}$$

This result will be useful below, although bumps on the CMB will be ignored: $\widehat{h} = 0$.

Interest in gravitational torques and oscillations was sparked by Buffett (1996). He envisaged an SIC in thermodynamic equilibrium with its environment, so that the gravitational potential, $\Phi_a^s(r) + \Phi_a'(r, \theta, \phi)$, is constant over its surface. Since $\epsilon_a \ll 1$ according to section 2.2, $|\Phi_a'/\Phi_a^s| \ll 1$ so that $\widetilde{h}$ can be derived by Taylor expansion. This shows that $\Phi_a^s(r_i) + \widetilde{g}\widetilde{h}(\theta, \phi) + \Phi_a'(r_i, \theta, \phi)$ is approximately constant, where $\widetilde{g} = -g^s_{\mathrm{e},r}(r_i) = \partial_r \Phi_a^s(r_i)$ (>0) is gravity at the ICB. It follows that

$$\widetilde{h} = -\Phi_a'(r_i, \theta, \phi)/\widetilde{g} = \widetilde{\epsilon} \sin^2\theta \cos 2\phi, \quad \widetilde{\epsilon} = -\widehat{\mathcal{A}}(r_i/r_o)^2/\widetilde{g}. \tag{43a,b}$$

It has been assumed that (8c) is the only anomaly present, except for the gravity anomaly created by the topography $\widetilde{h}$. Because $\widetilde{\Delta}/\widetilde{\rho}$ is small ($\approx$0.047), and

$$\widetilde{\mathcal{A}}/\widehat{\mathcal{A}} = 4\pi G r_i^3 \widetilde{\Delta}/5 r_o^2 \widetilde{g} \approx 0.0034, \tag{43c}$$

this only slightly perturbs the $\widetilde{h}$ given by (43a), for which the maximum bump height, $|\widetilde{\epsilon}|$, is only 50 m for $\widehat{\mathcal{A}} = 1800\,\mathrm{m^2\,s^{-2}}$.

Now suppose that the SIC turns through an angle φ. Its frozen-in topography turns with it, to produce the gravitational anomaly (41a); see figure 7. As $\widehat{h} = 0$, the torque on

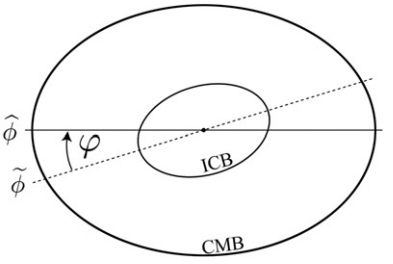

Figure 7. Schematic showing an equatorial plan view through the core. The symmetry axis of the SIC (dashed line) is displaced by the misalignment angle, $\varphi = \widehat{\phi} - \widetilde{\phi}$, from the equilibrium orientation defined by the mantle gravity field (solid line). The displacement φ results in a restoring gravitational torque between mantle and SIC.

the mantle is only gravitational, i.e. $\widehat{\Gamma}^G_{a,z}$ with Γ^G_0 given by (41c) and (43c):

$$\Gamma^G_0 = 32\pi r_i^6 \widetilde{\Delta}\widehat{\mathcal{A}}^2/15 r_o^4 \widetilde{g} \approx 6.7 \times 10^{19}\,\mathrm{Nm}. \tag{43d}$$

By (43d), the frequency of the gravitational oscillations is $\omega^G \approx 4.8 \times 10^{-8}\,\mathrm{s}^{-1}$, with a period of

$$\tau^G = 2\pi/\omega^G \approx 4.1\mathrm{yr}. \tag{43e}$$

(It should perhaps be mentioned that ω^G is derived from $\widetilde{\Gamma}^{G+T}_{a,z}$ $(= -\widehat{\Gamma}^{G+T}_{a,z})$, where the topographic parts are not easily evaluated. If however one or other of these parts is small, because the topography of that body can be neglected, the required torque on that body is the gravitational torque alone, which is more easily evaluated. Therefore, when $\widetilde{\Gamma}^{G+T}_{a,z}$ was required above in deriving (43d), it could be obtained from $-\widehat{\Gamma}^G_{a,z}$, because the CMB had been supposed bumpless.)

One of the limitations of these estimates arises from the discrepancy in the estimated values of $\widehat{\mathcal{A}}$. We have taken $\widehat{\mathcal{A}} = 1800\,\mathrm{m}^2\,\mathrm{s}^{-2}$, but Buffett (1996) used values of $\widehat{\mathcal{A}} = 1300$ and $2300\,\mathrm{m}^2\,\mathrm{s}^{-2}$, taken from Defraigne *et al.* (1996) and Forte *et al.* (1994), respectively. These differ by a factor of almost 2, which is unfortunate in view of the quadratic dependence of (43d) on $\widehat{\mathcal{A}}$. If we take $\widehat{\mathcal{A}} = 1800 \pm 500\ \mathrm{m}^2\,\mathrm{s}^{-2}$, we obtain $|\widetilde{\epsilon}| = 50 \mp 14\,\mathrm{m}$, $\Gamma^G_0 = (6.8 \pm 3.4) \times 10^{19}\,\mathrm{N\,m}$, $\omega^G = (4.8 \pm 1.5) \times 10^{-8}\,\mathrm{s}^{-1}$, and a period of gravitational oscillation, $P^G = 2\pi/\omega^G$, of $4.1 \mp 1.5\,\mathrm{yr}$. These estimates show that gravitational torques are of sufficient amplitude to explain the observed sub-decadal scale of the LOD variations. According to Buffett *et al.* (2009), gravitational oscillations are mainly responsible for the LOD variations shown in figure 1.

Equations (41d,g) imply

$$\widehat{\Omega} = \frac{\mathrm{d}\widehat{\phi}}{\mathrm{d}t} = \widehat{\Omega}_0 + \frac{2\Gamma^G_0}{\widehat{C}\omega^G}(\widetilde{\phi} - \widehat{\phi})_{\max} \sin \omega^G (t - t_0). \tag{44a}$$

Since the second term on the right-hand side is small compared with the first, the LOD, $P = 2\pi/\widehat{\Omega}$, is

$$P = P_0 \left[1 - \frac{2\Gamma^G_0}{\widehat{C}\omega^G \widehat{\Omega}_0}(\widetilde{\phi} - \widehat{\phi})_{\max} \sin \omega^G (t - t_0) \right]. \tag{44b}$$

The amplitude of the gravitational oscillation is therefore

$$(\widetilde{\phi} - \widehat{\phi})_{\max} = \pi \widehat{C} \omega^G \Delta P / \Gamma_0^G P_0^2. \tag{44c}$$

For $\Delta P \simeq 1$ ms, our estimates of $\widehat{\mathcal{A}}$, Γ_0^G, and ω^G lead to an estimated maximum angular separation of approximately 1.2° between the mantle and SIC from their equilibrium alignment. This implies an inner core oscillation with a maximum angular velocity of $\omega^G(\widetilde{\phi} - \widehat{\phi})_{\max} \approx 2^\circ \, \mathrm{yr}^{-1}$. This angular velocity is comparable to early estimates of inner core rotation rate (e.g. Glatzmaier and Roberts 1996a, Song and Richards 1996) but is significantly larger than recent estimates (Souriau 2007).

The oscillation of the SIC creates a variation of the same frequency in the gravitational field at the Earth's surface, $r = r_E$. The peak-to-peak variation in the radial component is

$$\Delta g_r''(r_E) = \frac{12\widetilde{\mathcal{A}}}{r_i} \left(\frac{r_i}{r_E} \right)^4 (\widehat{\phi} - \widetilde{\phi})_{max}^2 \simeq 4 \, \mathrm{nGal}. \tag{44d}$$

This value is too small by roughly a factor of five to be detected by the GRACE satellite system (e.g. Wahr *et al.* 2006).

Because $\boldsymbol{\Gamma}_c^G$ and $\boldsymbol{\Gamma}_c^T$ are smaller than $\boldsymbol{\Gamma}_a^G$ and $\boldsymbol{\Gamma}_a^T$ by a factor of order 10^{-4}, our analyses centered first on $\boldsymbol{\Gamma}_a^G$ and $\boldsymbol{\Gamma}_a^T$. We demonstrated that the sum, $\boldsymbol{\Gamma}_a^{G+T}$, of these two torques vanishes for the minimum energy state, and is large only when the deviations from that state are sufficiently great. Earlier, the topographic and magnetic torques on the SIC associated with core turbulence were held responsible for changing the relative orientations of the SIC and mantle. This turbulent torque is convective, and is nullified by a tiny misalignment angle φ. Equating a turbulent torque of the target size and an adiabatic GT torque of $1.3 \times 10^{20} \varphi$ Nm (see (41b) and (43d)), we find $\varphi \approx 0.5^\circ$, This is in approximate agreement with the estimate $(\widetilde{\phi} - \widehat{\phi})_{\max} = 1.2^\circ$ obtained from (44c). To within this angle, the mantle and SIC are gravitationally locked together, over time scales short compared with those of the relaxation processes in the SIC described in the last section.

At first sight, the idea of gravitational locking appears to be contradicted by the geophysical facts. The early geodynamo simulations of Glatzmaier and Roberts (1995, 1996a,b) predicted that strong, prograde, zonal flows exist near the ICB; the EM stresses associated with these flows, create a magnetic torque that causes the SIC to rotate in the same direction as the adjacent flow and with a comparable angular velocity (Aurnou *et al.* 1996, 1998, Roberts and Glatzmaier 1996a, Hollerbach 1998). Following this, seismologists found evidence of a strong, prograde rotation of the SIC of roughly $1^\circ \, \mathrm{yr}^{-1}$ (e.g. Song and Richards 1996). Subsequent studies inferred rotation rates that are at most an order of magnitude smaller than this; see Souriau (2007). To accommodate a persistent drift between SIC and mantle, Buffett (1997) invoked the first of the two inner core relaxation processes described earlier; the effect of the second has never been properly assessed. However, any nonzero mean SIC rotation rate must be reconciled with seismic observations of hemispherical SIC structure (e.g. Tanaka and Hamaguchi 1997, Niu and Wen 2001, Cao and Romanowicz 2004, Deuss *et al.* 2010). Recent models suggest that inner core convection may be able to explain large-scale hemispherical structure (e.g. Alboussière *et al.* 2010, Monnereau *et al.* 2010). It is still unclear how such features can be reconstituted in the presence of a mean differential rotation of the SIC.

The most severe limitation of this analysis of gravitational oscillations may be the neglect of electromagnetic stresses that couple the fluid within the TC. This may be significant both because the frequency ω^G is high and because the SIC is probably as good an electrical conductor as the FOC or better; see Secco and Schloessin (1989). To examine the effect of this coupling, we make the extreme assumption that the fluid in the TC is locked to the SIC. Because the mantle is a poor electrical conductor, the fluid in the TC is not well-coupled to the mantle (see section 8), so the entire fluid column within the TC can rotate almost freely with the SIC about Oz. From the PREM model of Dziewonski and Anderson (1981), we find that the moment of inertia of the fluid within the TC is $2.12\times10^{35}\,\mathrm{kg\,m^2}$ which, when added to $\widetilde{C}$, gives $C^{\mathrm{TC}}=2.71\times10^{35}\,\mathrm{kg\,m^2}$. Using this instead of $\widetilde{C}$ in (41f), τ^G is lengthened from $4.1\mp1.5\,\mathrm{yr}$ to

$$\tau^{\,G}_{\mathrm{TC}}=2\pi/\omega^{\,G}_{\mathrm{TC}}\approx 8.9\mp3.2\,\mathrm{yr},\quad \text{where } \omega^{\,G}_{\mathrm{TC}}=[2(\widehat{C}+C^{\mathrm{TC}})\Gamma^{\,G}_{\,0}/\widehat{C}C^{\mathrm{TC}}]^{1/2}. \tag{44e,f}$$

The coupling of the SIC and the TC is considered further in section 8.4.

8. The magnetic torque

8.1. *Initial considerations*

The main aims of this section are to develop further the ideas of section 3.2 about torsional waves and to study their magnetic coupling to the mantle and SIC. Technical complications are relegated to appendices B–D.

The magnetic force and torque about O on a body V carrying a current $\boldsymbol{J}$ are

$$\boldsymbol{F}^M=\int_{\mathrm{V}}\boldsymbol{J}\times\boldsymbol{B}\,\mathrm{d}v,\quad \boldsymbol{\Gamma}^M=\int_{\mathrm{V}}\boldsymbol{r}\times(\boldsymbol{J}\times\boldsymbol{B})\,\mathrm{d}v=\int_{\mathrm{V}}r[B_r\boldsymbol{J}-J_r\boldsymbol{B}]\mathrm{d}v. \tag{45a,b}$$

It is shown in appendix E that

$$(\boldsymbol{J}\times\boldsymbol{B})_i=\nabla_j S^M_{ij},\quad \text{where } S^M_{ij}=\mu_0^{-1}(B_iB_j-\tfrac{1}{2}B^2\delta_{ij}) \tag{45c,d}$$

is the magnetic stress tensor. This enables $\boldsymbol{F}^M$ and $\boldsymbol{\Gamma}^M$ to be expressed as integrals over the surface, A, of V:

$$\boldsymbol{F}^M=\frac{1}{\mu_0}\oint_{\mathrm{A}}[(\boldsymbol{n}\cdot\boldsymbol{B})\boldsymbol{B}-\tfrac{1}{2}B^2\boldsymbol{n}]\mathrm{d}a,\quad \boldsymbol{\Gamma}^M=\frac{1}{\mu_0}\oint_{\mathrm{A}}[(\boldsymbol{n}\cdot\boldsymbol{B})\boldsymbol{r}\times\boldsymbol{B}-\tfrac{1}{2}B^2\boldsymbol{r}\times\boldsymbol{n}]\mathrm{d}a, \tag{45e,f}$$

where the unit normal $\boldsymbol{n}$ to A points out of V. By (45a,f), equivalent expressions for the axial torque are

$$\Gamma^M_z=\int_{\mathrm{V}}s(\boldsymbol{J}\times\boldsymbol{B})_\phi\mathrm{d}v,\quad \Gamma^M_z=\frac{1}{\mu_0}\oint_{\mathrm{A}}sB_\phi(\boldsymbol{n}\cdot\boldsymbol{B})\mathrm{d}a, \tag{45g,h}$$

the latter holding for axisymmetric A only; otherwise the magnetic pressure, $B^2/2\mu_0$, contributes. In the applications of (45h) below, A is assumed to be spherical and to be either the CMB, $\widehat{\mathrm{S}}$, or the ICB, $\widetilde{\mathrm{S}}$, so that $\boldsymbol{n}=\mathbf{1}_r$. Because the magnetic Rossby number

$$Ro_M=V_A/2\Omega r_o=\tau_{\mathrm{A}}/\tau^{\,\mathrm{m}}\approx 4\times10^{-5}, \tag{46}$$

is so small for the waves, it will be convenient to separate variables according to their time scales as in (26b).

To evaluate the axial torques from (45 h), it is necessary to determine $\widehat{\boldsymbol{B}}$ on the CMB and $\widetilde{\boldsymbol{B}}$ on the ICB from $\zeta(s,t)$. It will become clear that this is not a straightforward task. The first step is to solve the EM equations in the mantle and SIC.

The magnetic field, $\widehat{\boldsymbol{B}}$, electric field $\widehat{\boldsymbol{E}}$, and current density $\widehat{\boldsymbol{J}}$, in the mantle are related by the pre-Maxwell equations (e.g. Davidson 2001 and section 3.2),

$$\partial_t \widehat{\boldsymbol{B}} = -\boldsymbol{\nabla}\times\widehat{\boldsymbol{E}}, \quad \widehat{\boldsymbol{J}} = \widehat{\sigma}\widehat{\boldsymbol{E}}, \quad \mu_0\widehat{\boldsymbol{J}} = \boldsymbol{\nabla}\times\widehat{\boldsymbol{B}}, \quad \boldsymbol{\nabla}\cdot\widehat{\boldsymbol{B}} = 0, \tag{47a,b,c,d}$$

where $\widehat{\sigma}$ is the electrical conductivity of the mantle. In view of the changes in reference frame made below, it may be helpful to recall that $\boldsymbol{B}$ and $\boldsymbol{J}$ are frame-indifferent but that $\boldsymbol{E}$ is not. Equations (47b,c) apply only in the mantle's reference frame in which $\widehat{\boldsymbol{V}} = \boldsymbol{0}$. In a frame in which the mantle rotates with angular velocity $\widehat{\boldsymbol{\zeta}}$ $(= \widehat{\zeta}\mathbf{1}_z)$, (47b) is replaced by $\widehat{\boldsymbol{J}} = \widehat{\sigma}(\widehat{\boldsymbol{E}} + \widehat{\boldsymbol{V}}\times\widehat{\boldsymbol{B}})$, where $\widehat{\boldsymbol{V}} = \widehat{\boldsymbol{\zeta}}\times\boldsymbol{r}$. From (47a–c),

$$\mu_0\widehat{\sigma}\widehat{\boldsymbol{E}} = \boldsymbol{\nabla}\times\widehat{\boldsymbol{B}}, \quad \partial_t\widehat{\boldsymbol{B}} = -\boldsymbol{\nabla}\times[(\mu_0\widehat{\sigma})^{-1}\boldsymbol{\nabla}\times\widehat{\boldsymbol{B}}]. \tag{47e,f}$$

Since the CMB has been supposed spherical, solutions to (47e,f) must satisfy

$$\widehat{\boldsymbol{B}}_{\mathrm{H}} = \boldsymbol{B}_{\mathrm{H}}, \quad \widehat{\boldsymbol{E}}_{\mathrm{H}} = \boldsymbol{E}_{\mathrm{H}}, \quad \text{at } r = r_o. \tag{47g,h}$$

By (47a,h), $\partial_t(\boldsymbol{n}\cdot\widehat{\boldsymbol{B}}) = \partial_t(\boldsymbol{n}\cdot\boldsymbol{B}$ on $\widehat{\mathrm{S}}$. If (as we shall assume) $\boldsymbol{n}\cdot\widehat{\boldsymbol{B}} = \boldsymbol{n}\cdot\boldsymbol{B}$ holds at $t=0$, it holds for all t. However, this last condition is not included in (47g,h) in order to make its four scalar conditions independent. This is also why $\boldsymbol{n}\cdot\widehat{\boldsymbol{J}} = \boldsymbol{n}\cdot\boldsymbol{J}$ is not included; it is implied by (47c,g). We have ignored the possibility of thermoelectric or electrochemical potential differences on the contact surface $\widehat{\mathrm{S}}$, which would lead to discontinuities in $\boldsymbol{E}_{\mathrm{H}}$. In the context of torsional waves, (47g,h) are satisfied by means of boundary layers.

We shall assume that the mantle is electrically conducting in the layer

$$r_o < r < r_1 = r_o + d. \tag{47i}$$

In the insulating region V^* above this layer, the magnetic and electric fields are denoted by $\boldsymbol{B}^*$ and $\boldsymbol{E}^*$, where $\boldsymbol{B}^* = -\boldsymbol{\nabla}W$ is a potential field; W obeys Laplace's equation and is $\mathrm{O}(r^{-2})$ for $r\to\infty$. As for (47g,h),

$$\boldsymbol{B}^*_{\mathrm{H}} = \widehat{\boldsymbol{B}}_{\mathrm{H}}, \quad \boldsymbol{E}^*_{\mathrm{H}} = \widehat{\boldsymbol{E}}_{\mathrm{H}}, \quad \text{at } r = r_1. \tag{47j,k}$$

8.2. *Modeling conduction in the mantle and SIC*

To make progress, it is necessary both to model mantle conductivity and to consider the way its spatial distribution affects the relationship between $\widehat{\boldsymbol{E}}$ and $\widehat{\boldsymbol{B}}$ on the CMB. Some results will hold for general $\widehat{\sigma} = \widehat{\sigma}(r,\theta,\phi)$. In all cases, a significant quantity is the mantle conductance,

$$\widehat{\Sigma}(\theta,\phi) = \int_{r_o}^{r_1} \widehat{\sigma}(r,\theta,\phi)\mathrm{d}r, \tag{48}$$

which is a constant when $\widehat{\sigma}$ depends only on r.

So little is known with any degree of certainty about $\widehat{\sigma}$ that it is common practice to assume something simple and convenient; sometimes only the conductance is specified, usually in the range $10^7\,\mathrm{S} < \widehat{\Sigma} < 10^9\,\mathrm{S}$. But the spatial distribution of the conductivity

has a considerable effect on solutions of (47f). Suppose $\widehat{\boldsymbol{B}}$ on the CMB is characterized by horizontal time and length scales, $\mathcal{T}$ and $\mathcal{L}$. Associated with $\mathcal{L}$ is the EM diffusion time, $\widehat{\tau}_\eta$, quantifying how rapidly a field $\widehat{\boldsymbol{B}}$ of scale $\mathcal{L}$ in the mantle can change. Associated with $\mathcal{T}$ is the EM "skin depth", $\widehat{d}_\eta$, quantifying how far $\widehat{\boldsymbol{B}}$ and $\widehat{\boldsymbol{E}}$ varying on that time scale can penetrate from the FOC into the solid mantle; at high frequencies $|\omega| = 2\pi/\mathcal{T}$, this is only skin-deep, so giving $\widehat{d}_\eta$ its name. These quantities are defined here by

$$\widehat{d}_\eta = (\tfrac{1}{2}|\omega|\mu_0\widehat{\sigma}_o)^{-1/2} = (\widehat{\eta}_o\mathcal{T}/\pi)^{1/2}, \quad \widehat{\tau}_\eta = \mu_0\widehat{\sigma}_o\mathcal{L}^2 = \mathcal{L}^2/\widehat{\eta}_o, \tag{49a,b}$$

where $\widehat{\sigma}_o$ and $\widehat{\eta}_o = 1/\mu_0\widehat{\sigma}_o$ are values on the CMB.

The following discussion is intended to apply principally to $\mathcal{L}$ and $\mathcal{T}$ relevant to the magnetic coupling of torsional waves to the mantle and SIC. The principal wave modes have wavelengths comparable with r_o. Attention therefore focuses on $\mathcal{L} = \mathrm{O}(r_o)$. (Indeed, it was seen in section 3.2 that, unless $\mathcal{L} \gg V_A/\Omega \approx 0.3\,\mathrm{km}$, torsional waves do not exist.) This suggests that a useful approximate treatment of conduction in the mantle associated with torsional waves is the *long length scale approximation*:

$$d \ll \mathcal{L}, \quad \widehat{d}_\eta \ll \mathcal{L}, \tag{50a,b}$$

the second of which implies $\mathcal{T} \ll \widehat{\tau}_\eta$.

In the reference frame of the mantle, consider the Fourier component of $\widehat{\boldsymbol{b}}$ proportional to $\mathrm{e}^{-\mathrm{i}\omega t}$. By (50a,b), the horizontal derivatives in (11d) and (47f) are small and can be discarded in a first approximation, so that (suppressing the θ and ϕ dependences, which are implied)

$$\frac{\partial \widehat{b}_r}{\partial r} = 0, \quad \frac{\partial^2 \widehat{\boldsymbol{b}}_{\mathrm{H}}}{\partial r^2} = -\mathrm{i}\omega\mu_0\widehat{\sigma}_o\widehat{\boldsymbol{b}}_{\mathrm{H}} = -\frac{2\mathrm{i}\varsigma\widehat{\boldsymbol{b}}_{\mathrm{H}}}{\widehat{d}_\eta^2}, \tag{51a,b}$$

where $\varsigma = \mathrm{sgn}(\omega)$. In the same approximation, (47b,c) give

$$\mu_0\widehat{\sigma}\,\widehat{\boldsymbol{e}}_{\mathrm{H}} = \frac{\partial}{\partial r}\mathbf{1}_r \times \widehat{\boldsymbol{b}}_{\mathrm{H}}. \tag{51c}$$

These equations imply

$$\widehat{b}_r(r) = \widehat{b}_r(r_o), \tag{51d}$$

$$\widehat{\boldsymbol{b}}_{\mathrm{H}}(r) = \widehat{\boldsymbol{b}}_{\mathrm{H}}(r_o)\cosh\widehat{\xi} - (\mu_0\widehat{\Sigma}/\widehat{\varpi})\mathbf{1}_r \times \widehat{\boldsymbol{e}}_{\mathrm{H}}(r_o)\sinh\widehat{\xi}, \tag{51e}$$

$$\widehat{\boldsymbol{e}}_{\mathrm{H}}(r) = \widehat{\boldsymbol{e}}_{\mathrm{H}}(r_o)\cosh\widehat{\xi} + (\widehat{\varpi}/\mu_0\widehat{\Sigma})\mathbf{1}_r \times \widehat{\boldsymbol{b}}_{\mathrm{H}}(r_o)\sinh\widehat{\xi}, \tag{51f}$$

where

$$\widehat{\xi} = (1 - \mathrm{i}\varsigma)\left(\frac{r - r_o}{\widehat{d}_\eta}\right) = \widehat{\varpi}\left(\frac{r - r_o}{d}\right), \quad \widehat{\varpi} = \widehat{\xi}(r_1) = (1 - \mathrm{i}\varsigma)\frac{d}{\widehat{d}_\eta}. \tag{51g,h}$$

Further simplification is possible in two cases:

(i) The *thin wall approximation* $d \ll \widehat{d}_\eta$, i.e. $0 < |\widehat{\varpi}| \ll 1$
This is often used in modeling laboratory MHD experiments; see e.g. Müller and Bühler (2001). Starting with Glatzmaier and Roberts (1995), it has been

frequently adopted in studying mantle conduction. The approximation is easily understood. For $d \ll \widehat{d}_\eta$ the horizontal electric field, $\widehat{\boldsymbol{e}}_{\mathrm{H}}$, in the conducting layer is almost independent of r, and it creates a horizontal electric current of density $\widehat{\boldsymbol{j}} = \widehat{\sigma}\,\widehat{\boldsymbol{e}}_{\mathrm{H}}$ so that, in the layer of thickness d, a net current of $\widehat{\mathcal{J}} = d\widehat{\sigma}\,\widehat{\boldsymbol{e}}_{\mathrm{H}}\,\mathrm{A\,m^{-1}}$ is trapped across which there is a finite jump in $\widehat{\boldsymbol{b}}$.

It may be helpful to write $\widehat{\boldsymbol{b}} = \boldsymbol{b}^* + \widehat{\boldsymbol{b}}'$, etc., where $\boldsymbol{b}^* = -\nabla w$ is the magnetic field present everywhere in an insulating mantle, and $\widehat{\boldsymbol{b}}'$ is the magnetic field due to mantle conduction. Obviously the effect of the mantle's conducting layer disappears as $d \to 0$ unless simultaneously $\widehat{\sigma}$ becomes large. The thin layer approximation posits that $\widehat{\sigma} \to \infty$ as $d \to 0$, in such a way that $\widehat{\Sigma}$ remains finite. Then $\widehat{\mathcal{J}}$ becomes a surface current that, by (47c), creates a discontinuity in $\widehat{\boldsymbol{b}}_{\mathrm{H}}$ of $\mu_0\,\widehat{\mathcal{J}}\times\mathbf{1}_r = \mu_0\widehat{\Sigma}\,\widehat{\boldsymbol{e}}\,'_{\mathrm{H}}\times\mathbf{1}_r$. This follows directly from (51e,f) which show that, in the limit $\varpi \to 0$,

$$\widehat{\boldsymbol{e}}\,'_{\mathrm{H}}(r) = \widehat{\boldsymbol{e}}\,'_{\mathrm{H}}(0), \quad \widehat{\boldsymbol{b}}\,'_{\mathrm{H}}(r) = \widehat{\boldsymbol{b}}\,'_{\mathrm{H}}(0) - \mu_0\widehat{\Sigma}\mathbf{1}_r \times \widehat{\boldsymbol{e}}\,'_{\mathrm{H}}(0)(r - r_o)/d, \tag{52a,b}$$

apart from $\mathrm{O}(\varpi^2)$ errors. Therefore

$$\widehat{\boldsymbol{b}}(r_o) = -\nabla w(r_o) + \mu_0\widehat{\Sigma}\mathbf{1}_r \times \widehat{\boldsymbol{e}}_{\mathrm{H}}(r_o). \tag{52c}$$

We shall require this later in a reference frame in which the mantle rotates with angular velocity $\widehat{\zeta}$, so that (neglecting terms in the square of the wave amplitude)

$$\widehat{\boldsymbol{b}}(r_o) = -\nabla w(r_o) + \mu_0\widehat{\Sigma}[\mathbf{1}_r \times \widehat{\boldsymbol{e}}_{\mathrm{H}}(r_o) + sB_r^{\mathrm{m}}(r_o)\widehat{\zeta}\mathbf{1}_\phi]. \tag{52d}$$

The ohmic dissipation per unit area of CMB due to mantle conduction is $\widehat{q}_\eta = \frac{1}{2}|\widehat{\Sigma}(\widehat{\boldsymbol{e}}_{\mathrm{H}})^2|$. (In full, the horizontal electric field of the wave is $\mathrm{Re}(\widehat{\boldsymbol{e}}_{\mathrm{H}}(\boldsymbol{x})\mathrm{e}^{-\mathrm{i}\omega t}) = \frac{1}{2}[\widehat{\boldsymbol{e}}_{\mathrm{H}}(\boldsymbol{x})\mathrm{e}^{-\mathrm{i}\omega t} + \widehat{\boldsymbol{e}}^*_{\mathrm{H}}(\boldsymbol{x})\mathrm{e}^{\mathrm{i}\omega t}]$, where the star denotes the complex conjugate. Therefore $|\widehat{\boldsymbol{e}}^2_{\mathrm{H}}| = \frac{1}{2}|\widehat{\boldsymbol{e}}_{\mathrm{H}}(\boldsymbol{x})|^2$ + oscillatory terms. When averaged over t, this leads to the expression for $\widehat{q}_\eta$ above.)

(ii) The *high frequency approximation* $\widehat{d}_\eta \ll d$, i.e. $|\widehat{\varpi}| \gg 1$

We shall use this approximation in section 8.4 to evaluate the magnetic coupling of the SIC to the fluid in the TC. We therefore transfer to the reference frame of the SIC and introduce the analogues of (49a,b):

$$\widetilde{d}_\eta = (\tfrac{1}{2}|\omega|\mu_0\widetilde{\sigma})^{-1/2} = (\widetilde{\eta}\mathcal{T}/\pi)^{1/2}, \quad \widetilde{\tau}_\eta = \mu_0\widetilde{\sigma}\mathcal{L}^2 = \mathcal{L}^2/\widetilde{\eta}, \tag{53a,b}$$

where $\widetilde{\sigma}$ is the conductivity of the SIC, assumed uniform. For $\widetilde{\sigma} = \sigma$ and $\omega_A = 3 \times 10^{-8}\,\mathrm{s^{-1}}$, (53b) gives $\widetilde{d}_\eta \approx 10\,\mathrm{km}$. Since $\widetilde{d}_\eta \ll r_i$, the fields $\widetilde{\boldsymbol{b}}$ and $\widetilde{\boldsymbol{e}}$ induced in the SIC by the varying $\boldsymbol{b}$ and $\boldsymbol{e}$ on the ICB die out exponentially fast with increasing $r_i - r$ and have effectively completely disappeared when $r_i - r = \mathrm{O}(\widetilde{d}_\eta)$, a distance much less than d $(= r_i)$. Thus the results are independent of d; the relevant conductance, $\widetilde{\Sigma}$, of the SIC is complex and is defined by

$$\widetilde{\Sigma} = \tfrac{1}{2}(1 + \mathrm{i}\varsigma)\widetilde{\sigma}\widetilde{d}_\eta = (1 + \mathrm{i}\varsigma)(\widetilde{\sigma}/2\mu_0|\omega|)^{1/2}. \tag{53c}$$

It is helpful to write $\widetilde{\boldsymbol{B}} = \widetilde{\boldsymbol{B}}^{\mathrm{m}} + \widetilde{\boldsymbol{b}}$, etc., and again to think of the current, $\widetilde{\boldsymbol{j}}$, created by the wave as being trapped in a boundary layer whose thickness is

$\widetilde{d}_\eta$, and for which the stretched coordinate is $\widetilde{\xi} = (1 - \mathrm{i}\varsigma)(r_i - r)/\widetilde{d}_\eta$. Since $\widetilde{\boldsymbol{b}}, \widetilde{\boldsymbol{e}} \to \mathbf{0}$ as $\widetilde{\xi} \to \infty$,

$$\widetilde{\boldsymbol{b}}_{\mathrm{H}}(\widetilde{\xi}) = \widetilde{\boldsymbol{b}}_{\mathrm{H}}(0)\exp(-\widetilde{\xi}), \quad \widetilde{\boldsymbol{e}}_{\mathrm{H}}(\widetilde{\xi}) = \widetilde{\boldsymbol{e}}_{\mathrm{H}}(r_i)\exp(-\widetilde{\xi}), \tag{53d,e}$$

and (47b,c) give

$$\widetilde{\mathcal{J}} = \mu_0 \widetilde{\Sigma}\widetilde{\boldsymbol{e}}_{\mathrm{H}} = -\mathbf{1}_r \times d_\xi \widetilde{\boldsymbol{b}}_{\mathrm{H}} = \mathbf{1}_r \times \widetilde{\boldsymbol{b}}_{\mathrm{H}}. \tag{53f}$$

We shall require this later in a reference frame in which the SIC rotates with angular velocity $\widetilde{\zeta}$, so that (neglecting terms in the square of the wave amplitude)

$$\widetilde{\boldsymbol{b}}_{\mathrm{H}}(r_i) = -\mu_0 \widetilde{\Sigma}[\mathbf{1}_r \times \widetilde{\boldsymbol{e}}_{\mathrm{H}}(r_i) + sB_r^{\mathrm{m}}(r_i)\widetilde{\zeta}\mathbf{1}_\phi]. \tag{53g}$$

In contrast to the thin wall approximation (see (52d)), a complex constant relates $\widetilde{\boldsymbol{b}}_H$ to $\widetilde{\boldsymbol{e}}_H$; see (53f,g). This is because the coupling exists only through EM induction. In the thin wall approximation induction is unimportant; currents leaking from the core alone couple it to the mantle. The ohmic dissipation per unit area of ICB is $\widetilde{q}_\eta = \frac{1}{2}|\widetilde{\Sigma}(\widetilde{\boldsymbol{e}}_{\mathrm{H}})^2|$.

In sections 8.3 and 8.4, we shall meet boundary layers within the FOC in contact with the CMB and ICB; see appendix D. These have some similarity with the one considered above. Its thickness is d_η and its conductance is Σ, defined as in (53a,c) with σ replacing $\widetilde{\sigma}$, is complex:

$$d_\eta = (\tfrac{1}{2}|\omega|\mu_0\sigma)^{-1/2}, \quad \Sigma = \tfrac{1}{2}(1 + \mathrm{i}\varsigma)\sigma d_\eta = (1 + \mathrm{i}\varsigma)(\sigma/2\mu_0|\omega|)^{1/2}. \tag{53h,i}$$

It too hosts a similar surface current, $\breve{\mathcal{J}}$, that dissipates energy ohmically at the rate $\breve{q}_\eta = \mathrm{O}(|\Sigma(\breve{\boldsymbol{e}}_{\mathrm{H}})^2|)$, per unit area.

Intermediate between the two extremes of the thin wall and high frequency forms of the long length scale approximation is the case (51d–f) of nonzero but finite $d/\widehat{d}_\eta$, in which the fields induced in the solids by the fields on the boundary, partially penetrate and are partially absorbed by the conducting layer. The theory in this more general case follows the same lines as above, but will not be pursued here.

Several simple forms for $\widehat{\sigma}$ have been proposed in the literature, and we now contrast two of them. Buffett *et al.* (2002) inferred from their studies of diurnal nutation that d is only 200 m and that $\widehat{\sigma}_o \gtrsim 3 \times 10^5\,\mathrm{S\,m^{-1}}$, which is comparable to the core conductivity σ, so that for $\widehat{d}_\eta \lesssim 10\,\mathrm{km}$ for $\omega = 3 \times 10^{-8}\,\mathrm{s^{-1}}$. The long length scale approximation is good for most practical purposes and, as $d \ll \widehat{d}_\eta$, its simple thin layer form should also be accurate. In contrast, the laboratory experiments of Ohta *et al.* (2008) suggest $\widehat{\sigma}_o = 100\,\mathrm{S\,m^{-1}}$ and $d = 3 \times 10^5\,\mathrm{m}$; see also Yoshino (2010). This gives $\widehat{d}_\eta = 2 \times 10^6\,\mathrm{m}$, so that the long length scale approximation has dubious validity. Although these extreme models strongly differ, their conductances are similar: $\widehat{\Sigma} = 6 \times 10^7\,\mathrm{S}$ and $3 \times 10^7\,\mathrm{S}$. It is still unclear whether in reality the mantle conductance is as small as this.

As the thin layer approximation may be an inaccurate means of studying torsional wave coupling for mantle conductivities of Ohta *et al.* type, alternatives are worth considering. For some choices of $\widehat{\sigma}$, solutions to (47f) can be derived analytically (e.g. Roberts and Lowes 1961). For more general $\widehat{\sigma}$, accurate solutions require numerical integration. The common practice (also adopted below) is to apply the thin layer

approximation regardless of whether the conditions required for its validity are satisfied or not. This is based on the hope that, even if the conditions are unsatisfied, the resulting loss of accuracy is no greater than that due to the inherent uncertainty in $\widehat{\sigma}$. In contrast, there seems little doubt that the conditions required to validate the high frequency approximation for the coupling between torsional waves and the SIC are well-satisfied.

8.3. *Torsional wave coupling to the mantle*

We continue here the discussion of torsional waves initiated in section 3.2 where a simple form of the theory was presented; the full theory of small amplitude waves in a dissipative core is derived in appendix B. When the waves ride on a purely axisymmetric Taylor state ($\boldsymbol{B}^{\mathrm{m}} = \overline{\boldsymbol{B}}^{\mathrm{m}}$), and when ohmic dissipation is ignored, they are controlled by the canonical wave equation (25), which is the simplest form of the theory. It is however of limited interest here, as it excludes the coupling of the waves to the mantle that creates $\boldsymbol{\Gamma}^{M}$. We commence our discussion with (25) and its difficulties, and initially ignore the existence of the SIC.

Equation (25) also governs waves on a stretched string having a mass per unit length of $m(s) = \rho_0 s^2 \widehat{A}(s)/r_o^2$ and a tension of $m(s)\overline{V}_A^2(s)$, both of which vary along the string and vanish at its ends, because $m(0) = m(r_o) = 0$. As for the stretched string, one can hope to determine the natural frequencies, ω, of the torsional waves by seeking non-trivial "normal modes" in which $\zeta \propto \mathrm{e}^{-\mathrm{i}\omega t}$:

$$\mathrm{d}_s[s^2 \widehat{A}(s) V_A^2(s) \mathrm{d}_s \zeta] + \omega^2 s^2 \widehat{A}(s)\zeta = 0. \tag{54}$$

Since $m(0) = m(r_o) = 0$, (54) has regular singularities at both $s = 0$ and $s = r_o$. One can hope that one solution of (54) is bounded at $s = 0$, and that one is bounded at $s = r_o$. By finding ω^2 which makes these two solutions proportional to one another, one can hopefully determine the eigenvalues, ω, and eigenfunctions and then solve (25) as a sum of normal modes of (54).

The search for solutions to (54) was initiated by Braginsky in his famous 1970 paper. Since then, his numerical work has been greatly extended, e.g. see Zatman and Bloxham (1997), Hide *et al.* (2000), and Dickey and de Viron (2009). In particular, Hide *et al.* (2000) demonstrated that even a low order truncation of (54) can give useful information. So far most research has focused on torsional waves in a non-conducting mantle, but some authors have followed Braginsky (1970) by assuming $\widehat{\sigma} \neq 0$, e.g. Buffett (1998) and Jault (2003).

When magnetic diffusion is ignored so that magnetic coupling to the mantle does not exist, one solution of (54), which we call the "exceptional mode", is $\zeta = \zeta_0 =$ constant; its eigenvalue is $\omega = 0$. When a solution of (25) is expressed as a sum of normal modes, its exceptional part carries the entire axial angular momentum of the waves:

$$\breve{M}_z(t) = \rho_0 \int_0^{r_o} s^2 \widehat{A}(s)\zeta(s,t)\mathrm{d}s, \tag{55}$$

i.e. $\breve{M}_z = 0$ for all modes apart from the exceptional one. For these, solution of (54) encounters an inconvenient obstacle: no physically acceptable solution of (54) exists

when $\boldsymbol{B}$ is axisymmetric because then *both* solutions of (54) are unbounded at $s=0$; see appendix C. Two theoretical remedies have been advocated:

(a) Adding geometry. Assume that the SIC and the TC are locked together in solid-body rotation about Oz (Braginsky 1970). This excises the singularity of (54) at $s=0$ by applying that equation only in $r_i \le s \le r_o$;
(b) Adding physics. Restore core viscosity, ν or ν_T (Fearn and Proctor 1987). This diminishes the severity of the singularity though it does not remove it; see appendix C. Since $\nu/V_A r_0 \ll 1$, large ζ may exist in a narrow pencil surrounding Oz.

Although numerical solutions can be obtained if the singularity is ignored, they are valueless since, as the level of numerical truncation is increased, the answers they give become increasingly inaccurate instead of the reverse. Possibility (b) has not been fully investigated; most research has focused on option (a).

A geophysically more reasonable way of evading the obstacle is by returning to general, non-axisymmetric $\boldsymbol{B}^{\mathrm{m}}$. Then the planned solution of (54) succeeds. Appendix C gives two examples. Equation (25) is not, however, the correct equation governing ζ for general $\boldsymbol{B}^{\mathrm{m}}$, for which (25) is augmented by two additional terms, one of which already appeared in (24c); both are evaluated in appendix B. They exist because, when $\boldsymbol{B}^{\mathrm{m}}$ is not axisymmetric, $\boldsymbol{b}$ emerges from the core as $\widehat{\boldsymbol{b}}$. This couples every geostrophic cylinder to every other, creating a nonlocal angular momentum exchange between them. Most studies of torsional waves omit the additional terms. In an example analyzed in appendix C which ignores mantle conduction, they only have a small effect. Plausibly, this is generally true though it is has not been established. It is found below that the additional terms are significant when the mantle is a conductor.

Once magnetic diffusion is restored, further difficulties arise that will be investigated below. In view of all these theoretical obstacles, the reader may wonder whether computer simulation might not provide a simpler approach. It is difficult however to discern torsional waves in geodynamo simulations. This is because geophysically realistic magnetic Prandtl numbers, $P_m(=\nu/\eta)$, are still unattainable in geodynamo models. The importance of viscous damping of torsional waves can be assessed by the ratio

$$\tau_{\mathrm{A}}/\tau_{\mathrm{SU}} = (\nu\Omega)^{1/2}/V_A = \sqrt{(P_m/\Lambda)}. \tag{56}$$

This is the ratio of the Alfvén crossing time scale $\tau_{\mathrm{A}} = r_o/V_{\mathrm{A}}$ to the spin-up timescale $\tau_{\mathrm{SU}} = r_o/\sqrt{(\nu\Omega)}$; see Roberts and Soward (1972). Its value is small for the Earth, $\tau_{\mathrm{A}}/\tau_{\mathrm{SU}} = \mathrm{O}(10^{-3})$, but inconveniently large in simulations, $\tau_{\mathrm{A}}/\tau_{\mathrm{SU}} = \mathrm{O}(1)$. For recent numerical simulations, see Wicht and Christensen (2010).

When diffusion of $\boldsymbol{v}$ and $\boldsymbol{b}$ is included, the equation governing ζ is changed yet again, and its eigenvalues ω acquire negative imaginary parts, corresponding to decay. If electrical conduction in the mantle is also included, there is a magnetic torque, $\widehat{\boldsymbol{\Gamma}}^M$, coupling the core to the mantle, so that $\breve{M}$ is no longer conserved though $\breve{M} + \widehat{M}$ is, where $\breve{M}$ is the axial angular momentum of the mantle. Our next objective is to quantify the ohmic dissipation and to evaluate $\widehat{\Gamma}_z^M$.

The solutions described above and in section 3.2 do not obey physically realistic boundary conditions; $\boldsymbol{v}$ does not satisfy the no-slip conditions and $\boldsymbol{b}$ does not obey (20b,c). If viscosity is restored and the no-slip conditions are imposed, a thin Ekman layer is added at the CMB that traps a jet of fluid that travels along the CMB and exchanges mass with the main bulk of the core through Ekman pumping proportional to $E^{1/2}$. This creates viscous coupling to the mantle and causes the amplitude of the waves to be damped on the spin-up time scale, of order 10^4 yr; see Roberts and Soward (1972). This is so long compared with τ_A that viscosity and the no-slip conditions can be ignored.

More significantly, the waves are also damped by ohmic diffusion in the core. This creates a boundary layer of Ekman–Hartmann (EH) type; see e.g. Dormy and Soward (2007; §3.2.3). This layer is simplified here because $E=0$ has been assumed above. We distinguish it from the EH-layer by calling it a *magnetic diffusion layer* (MDL) though, like the EH layer, its structure is affected by Coriolis and Lorentz forces and depends on the Elsasser number (17b). See Braginsky (1970) and appendix D. The thickness of the MDL is d_η, given by (53h). It traps a jet of electric current that travels along the CMB. When the mantle is conducting, the layer passes current from the main bulk of the FOC to the mantle. A further time scale, $\widehat{\tau}_\eta$, emerges that is very much smaller than τ_{SU} and is estimated below. The Lorentz force of the current layer propels a surface mass flux that affects the angular momentum balance; see appendix B. This surface motion may tend to mask what is happening deeper in the core on torsional wave time scales, and may make the inferred core surface velocities untypical of the rest of the core.

The MDL plays a vital role in linking ζ in the main bulk of the FOC to $\widehat{\boldsymbol{b}}$ on the CMB. It is therefore indispensable in determining $\widehat{\Gamma}^M$. At the CMB, where $\mathcal{B}_o \approx 0.5\,\mathrm{mT}$ and $\Lambda \approx 0.07$, the prevailing magnetic field, $\boldsymbol{B}^m$, which defines Λ, therefore has very little effect on the MDL, which is controlled almost entirely by Coriolis forces and magnetic diffusion. In contrast, the ICB hosts an MDL in which $\mathcal{B}$ may be even an order of magnitude greater than $\mathcal{B}_o$, so that $\Lambda > 1$ and Lorentz forces are too significant to ignore; see section 8.4.

In the case of the CMB, it is shown in appendix D that $\widehat{\boldsymbol{e}}$ and $\widehat{\boldsymbol{b}}$ on the CMB are related to their counterparts, $\boldsymbol{e}$ and $\boldsymbol{b}$, beneath the MDL by (D.10b) and (D.11a) or equivalently:

$$\widehat{\boldsymbol{b}}_H + \mu_0 \Sigma\, \mathbf{1}_r \times \widehat{\boldsymbol{e}}_H = \boldsymbol{b}_H + \mu_0 \Sigma\, \mathbf{1}_r \times \boldsymbol{e}_H \quad \text{on } r = r_o, \tag{57}$$

where Σ is the (complex) core conductance defined by (53i). When (57) is combined with the thin layer approximation for mantle conduction (52d), it is found that

$$\widehat{\boldsymbol{b}}_H = [\Sigma \boldsymbol{b}_H^* + \widehat{\Sigma}\boldsymbol{b}_H - \mu_0 \Sigma \widehat{\Sigma} s B_r^m (\zeta - \widehat{\zeta})\mathbf{1}_\phi]/(\Sigma + \widehat{\Sigma}) \quad \text{on } r = r_o. \tag{58}$$

The first term on the right-hand side of (58) does not contribute to $\widehat{\Gamma}_z^M$, and for simplicity we retain only the last term on the right-hand side of (58), which creates

$$\widehat{\Gamma}_z^M = \int_0^{r_o} \rho_0 s^2 \widehat{A}(s)\widehat{D}(s)(\zeta - \widehat{\zeta})\,\mathrm{d}s, \tag{59a}$$

where

$$\widehat{D}(s) = \frac{r_o s}{\rho_0 \widehat{A} z_1} \frac{\Sigma \widehat{\Sigma}}{\Sigma + \widehat{\Sigma}} \oint [(B_r^{\mathrm{m}})^2]_{\widehat{\mathcal{N}} \& \widehat{\mathcal{S}}} \mathrm{d}\phi. \tag{59b}$$

In (59a), $\widehat{\mathcal{N}}\&\widehat{\mathcal{S}}$ signifies evaluation on the rims of $\widehat{\mathcal{C}}(s)$, where it joins the spherical caps $\widehat{\mathcal{N}}$ and $\widehat{\mathcal{S}}$; see section 3.2. Reciprocally, $\widehat{D}(s)$ creates a torque not only on the mantle but also on each $\mathcal{C}(s)$, so that (25) becomes

$$\frac{\partial^2 \zeta}{\partial t^2} + \widehat{D}(s) \frac{\partial}{\partial t}(\zeta - \widehat{\zeta}) \approx \frac{1}{s^2 \widehat{A}(s)} \frac{\partial}{\partial s} \left[s^2 \widehat{A}(s) V_A^2(s) \frac{\partial \zeta}{\partial s} \right]. \tag{59c}$$

The inclusion of the term involving $\widehat{D}(s)$ in (59c) adds what may be the most significant part of wave coupling to the mantle and to the ohmic losses. We use $\approx$ in (59c) to indicate that it is not the full wave equation of appendix B.

Partnering (59c) is the equation of motion of the mantle

$$\frac{\mathrm{d}\widehat{M}_z}{\mathrm{d}t} = \widehat{C} \frac{\mathrm{d}\widehat{\zeta}}{\mathrm{d}t} = \widehat{\Gamma}_z^M = \int_0^{r_o} \rho_0 s^2 \widehat{A}(s) \widehat{D}(s) (\zeta - \widehat{\zeta}) \mathrm{d}s. \tag{59d}$$

On multiplying (59c) by $\rho_0 s^2 \widehat{A}(s)$ and integrating over s, it is seen that

$$\frac{\mathrm{d}\breve{M}_z}{\mathrm{d}t} = -\int_0^{r_o} \rho_0 s^2 \widehat{A}(s) \widehat{D}(s) (\zeta - \widehat{\zeta}) \mathrm{d}s = -\widehat{\Gamma}_z^M. \tag{59e}$$

Evidently (59d,e) assure conservation of the total angular momentum $\breve{M}_z + \widehat{M}_z$.

One might have expected that the coupling of the waves to the mantle would depend solely on the mantle conductance, $\widehat{\Sigma}$, but in its place the combination $\widehat{\Sigma}\Sigma/(\Sigma + \widehat{\Sigma})$ has appeared in (59b), involving the complex core conductance Σ. This arises because of the intense currents flowing in the MDL whose Lorentz force reduces $|\widehat{\Gamma}_z^M|$ by a factor of $|\Sigma/(\Sigma + \widehat{\Sigma})|$. Numerically, $|\Sigma| \approx 3 \times 10^9$ S, which is comparable with $\widehat{\Sigma}$. The damping of torsional waves is often attributed to conduction in the mantle but, if we assume that $|\boldsymbol{e}_{\mathrm{H}}|^2$ is the same in our earlier estimates of $\breve{q}_\eta$ and $\widehat{q}_\eta$, they are in the ratio of the conductances, the total ohmic dissipation per unit area then being $\frac{1}{2}|(\Sigma + \widehat{\Sigma})\boldsymbol{e}_{\mathrm{H}}^2|$. The ohmic losses in the MDL may therefore be significant. As the effect of core conductance may be masked by other geophysical uncertainties, we shall use $\widehat{\Sigma}$ in place of $\Sigma\widehat{\Sigma}/(\Sigma + \widehat{\Sigma})$ in making rough estimates below. It is probable that, by doing so, the total ohmic damping will be underestimated and the torque on the mantle overestimated.

As already mentioned, the ohmic losses in the mantle and MDL impart negative imaginary parts to the frequencies, ω, of the normal modes of the coupled equations (59c,d) that cause the corresponding eigenfunctions to evanesce in the e-folding time, $\widehat{\tau}_\eta = 1/[\mathrm{Im}(\omega)]$. We make two approximations leading to a rough estimate of $\widehat{\tau}_\eta$. First, we take $B_r^{\mathrm{m}}(r_o, \theta, \phi) = B_0 \cos\theta$, corresponding to an axial dipole of polar strength B_0; second, we replace $\widehat{D}$ by its average over s so that the solutions of (59c,d) are functions of t alone. Then

$$\widehat{C} \mathrm{d}_t \widehat{\zeta} = \Gamma_z^M = \widehat{\Gamma}_0^M (\zeta - \widehat{\zeta}), \quad C \mathrm{d}_t \zeta = -\widehat{\Gamma}_0^M (\zeta - \widehat{\zeta}), \tag{60a,b}$$

where $C = 9.14 \times 10^{36}\,\mathrm{kg\,m^2}$ is the axial moment of inertia of the core when rotating as a solid body, and

$$\widehat{\Gamma}_0^M = 8\pi r_o^4 \widehat{\Sigma} B_0^2/15, \tag{60c}$$

which is $6 \times 10^{27}\,\mathrm{N\,ms}$ for $\widehat{\Sigma} = 10^8\,\mathrm{S}$ and $B_0 = 0.5\,\mathrm{mT}$, and leads to the estimate

$$\widehat{\tau}_\eta = \frac{C\widehat{C}}{\widehat{\Gamma}_0^M(C+\widehat{C})} \approx \frac{C}{\widehat{\Gamma}_0^M} \approx \frac{\rho_0 r_o}{\widehat{\Sigma} B_0^2} \approx 64\,\mathrm{yr}, \tag{60d}$$

which is much less than τ_{SU} and τ_η but is greater than the time taken by the waves to cross the core, which is $\tau_{\mathrm{A}} = r_o/V_{\mathrm{A}} \approx 6\,\mathrm{yr}$, for $\mathcal{B} = 2\,\mathrm{mT}$.

In section 1, LOD data led to the estimate $\delta\widehat{\zeta} \approx 3 \times 10^{-12}\,\mathrm{s^{-1}}$. If a torsional wave is responsible, (60a,b) suggest that $\zeta - \widehat{\zeta} \approx (\widehat{C}+C)\widehat{\zeta}/C \approx 2 \times 10^{-11}\,\mathrm{s^{-1}}$, so that $r_o(\zeta - \widehat{\zeta}) \approx 7 \times 10^{-5}\,\mathrm{m\,s^{-1}}$, which is less than, but comparable with, the inferred core surface flow. The ohmic dissipation, $\widehat{Q}^\eta$ of the waves is $\widehat{Q}^\eta = \frac{1}{2}\widehat{\Gamma}_0^M(\zeta - \widehat{\zeta})^2 \approx 1\,\mathrm{MW}$, which is far smaller than Q. According to this estimate of $\zeta - \widehat{\zeta}$ and (60c), $\widehat{\Gamma}_z^M \approx 10^{17}\,\mathrm{Nm}$. This can be increased to the target torque, by taking $\widehat{\Sigma}$ ten times bigger, but then $\widehat{\tau}_\eta$ is only 6 yr. This illustrates *the magnetic coupling paradox*. On the one hand, $\widehat{\Sigma}$ must be large enough to create a torque $\widehat{\Gamma}_z^M$ of target size, $10^{18}\,\mathrm{Nm}$. On the other hand, if $\widehat{\Sigma}$ is too large, mantle conduction will quench the waves before they can cross the core. We introduce the *paradox parameter*:

$$\Pi = \tau_A \widehat{\Sigma}\,\widehat{\mathcal{B}}_o^2/\rho_0 r_o = \tau_A/\widehat{\tau}_\eta. \tag{61}$$

There is a window for $\widehat{\Sigma}$, that may be narrow or non-existent, in which $\widehat{\Gamma}_z^M$ is large enough to explain variations in LOD by torsional waves, but simultaneously is small enough to ensure that $\Pi > 1$ so that the waves are not overdamped by ohmic dissipation. According to the admittedly imprecise, order of magnitude estimates made here, the window is non existent. For the target torque to be reached or exceeded, $\widehat{\Sigma} \gtrsim 1.2 \times 10^9\,\mathrm{S}$, but $\Pi > 1$ requires $\widehat{\Sigma} \lesssim 1.1 \times 10^9\,\mathrm{S}$. There is clearly a substantive issue, but one not convincingly resolved by the order of magnitude arguments made here.

One might hope that a more satisfactory treatment of the specific issues raised above will emerge in the near future through more complete data coverage, leading to a reliable torsional wave spectrum. This objective is complicated through the existence of gravitational oscillations of similar period, and interaction of the two wave motions is a strong possibility (Mound and Buffett 2003, 2005). Plausibly ohmic diffusion in the MDL and mantle damp the wave motions together. The recently discovered short time scales of core surface motions (Olsen and Mandea 2008, Finlay *et al.* 2010) may provide useful clues.

An even more puzzling question concerns torsional wave generation. If, as appears likely, the waves are heavily damped by both the MDL and the mantle, one must ask what power source makes good those losses. No definitive answer has been given to this key question. Core turbulence is often held responsible, directly or indirectly, through the Reynolds magneto-stresses it exerts on the SIC or TC. In the latter case, the driving of both torsional waves and gravitational oscillations is likely to be a complex, coupled process. Interestingly, Buffett *et al.* (2009) find evidence for torsional wave generation near the TC.

8.4. *Torsional wave coupling to the SIC*

The argument that led to (59c,d) supposed that the SIC did not exist. The following simplified discussion assumes conversely that there is no magnetic coupling to the mantle. See also appendices B and D.

As in the last section, the key is the simplified EH layer that links ζ in the main body of the FOC to the electric and magnetic fields, $\widetilde{\boldsymbol{e}}$ and $\widetilde{\boldsymbol{b}}$, in the SIC. It has already been pointed out that the Elsasser number, Λ, at the ICB plausibly exceeds unity. If it is large, appendix D shows that $\widetilde{\boldsymbol{b}}$ is simply related to $\boldsymbol{b}$. From (D.12f),

$$\widetilde{b}_\phi = b_\phi + \Lambda^{-1/2}\mu_0 \Sigma s B_r^{\mathrm{m}}(\zeta - \widetilde{\zeta}) \quad \text{on } r = r_i, \tag{62a}$$

where $\widetilde{\zeta}$ is the angular velocity of the SIC. The second term on the right-hand side makes a contribution to $\widetilde{\Gamma}_z^M$ of

$$\widetilde{\Gamma}_z^M = \Lambda^{-1/2}\Sigma \oint_{\widetilde{\mathrm{S}}} s^2 (B_r^{\mathrm{m}})^2 (\zeta - \widetilde{\zeta})\, \mathrm{d}a, \tag{62b}$$

where for simplicity it is assumed that both the geostrophic cylinders $\widehat{\mathcal{C}}^N$ and $\widehat{\mathcal{C}}^S$ introduced in section 3.2 have the same angular velocity, ζ. The balancing torque on these cylinders, required to ensure conservation of angular momentum, is

$$\widetilde{D}(s)(\zeta - \widetilde{\zeta}), \quad \text{where } \widetilde{D}(s) = \Lambda^{-1/2}\frac{r_i s \Sigma}{\widehat{A} z_1} \oint_{\widetilde{\mathcal{N}\&\mathcal{S}}} (B_r^{\mathrm{m}})^2\, \mathrm{d}\phi, \tag{62c,d}$$

where $\widetilde{\mathcal{A}} = 4\pi s(z_1 - z_2)$ is the combined areas of $\mathcal{C}^N$ and $\mathcal{C}^S$ and $z_2 = \sqrt{(r_i^2 - s^2)}$; similar to what appeared in (59b), $\widetilde{\mathcal{N}\&\mathcal{S}}$ signifies that the integral is taken over the rims of the spherical caps where $\widehat{\mathcal{C}}^S$ and $\widehat{\mathcal{C}}^N$ meet the SIC. For $s < r_i$, (59c) is replaced by

$$\frac{\partial^2 \zeta}{\partial t^2} + \widetilde{D}(s)\frac{\partial}{\partial t}(\zeta - \widetilde{\zeta}) \approx \frac{1}{s^2 \widetilde{\mathcal{A}}(s)} \frac{\partial}{\partial s}\left[s^2 \widetilde{\mathcal{A}}(s) V_A^2(s) \frac{\partial \zeta}{\partial s} \right], \tag{62e}$$

where V_A^2 is the geostrophic average of $(B_s^{\mathrm{m}})^2/\mu_0\rho_0$ over $\mathcal{C}^N$ or $\mathcal{C}^S$.

Equations (62b–d) can be used to shed light on a topic that has arisen several times in this article: the magnetic coupling of the SIC and the TC. For the same simple example of uniform ζ and a dipolar field, (62b) gives (omitting for simplicity a factor of $1 + \mathrm{i}\varsigma$ and taking $\Lambda = 1$)

$$\widetilde{\Gamma}_z^M = \widetilde{\Gamma}_0^M(\zeta - \widetilde{\zeta}), \quad \text{where } \widetilde{\Gamma}_0^M = 4\pi r_i^4 \widetilde{\sigma} \widetilde{d}_\eta B_0^2/15, \tag{63a,b}$$

so that, for $B_0 = 5\,\mathrm{mT}$, $\widetilde{\Gamma}_0^M \approx 2 \times 10^{29}\,\mathrm{Nms}$. This large torque acts on the SIC whose moment of inertia is less than $\widehat{C}/1000$. The corresponding coupling time, $\widetilde{\tau}_\eta$, is therefore very much less than $\widehat{\tau}_\eta$. An equation analogous to (60d) gives

$$\widetilde{\tau}_\eta = \frac{C^{\mathrm{TC}}\widetilde{C}}{\widetilde{\Gamma}_0^M(C^{\mathrm{TC}} + \widetilde{C})} \approx \frac{\widetilde{C}}{\widetilde{\Gamma}_0^M} \approx 4 \text{ days}. \tag{63c}$$

This geophysically short response time supports, but does not directly verify, the belief that the TC responds as a solid to torsional waves of sufficiently long period.

It is seems clear from (63c) that the magnetic coupling between TC and ICB is extremely tight at frequencies of order ω_{A} and smaller. There is also a good reason for believing that frictional coupling is strong too. Loper and Roberts (1981) argued that the freezing of the inner core described in section 2.1 is so rapid that the ICB is, in the language of metallurgy, *constitutionally supercooled*. Such a surface is rough, being

populated with channels (aka "chimneys"), where light material released by subsurface freezing is ejected into the FOC. The concomitant enhancement of momentum transfer has not been properly quantified but plausibly greatly enhances that of viscous traction. See particularly Le Mouël *et al.* (2006).

9. Synthesis

We have analyzed the various ways in which Earth's core is coupled to the mantle and have estimated the amplitudes of these couplings in order to show which may plausibly explain the available LOD data. In the first section, we provided observational evidence for core-mantle coupling. We showed that Earth's rotation rate has a roughly semi-decadal time variability, such that the LOD fluctuates at the ms level. To explain these LOD fluctuations, an internal coupling must exist between the mantle and the core that provides torques of order 10^{18} Nm. To explain the LOD observations, we need to make mechanistic models of core-mantle coupling. To build these models, it is necessary to understand the essential processes underlying core dynamics. These essentials are discussed in sections 2 and 3; they are used in the subsequent text to estimate the strength of various coupling mechanisms, including the viscous, topographic, gravitational and electromagnetic torques.

Analysis of the four coupling mechanisms reveals a complex picture. Three of the four are capable of producing the observed LOD variations. Only the viscous torque, Γ_z^T, seems to be too weak to explain the LOD signal. This is true even when we allow for the enhanced coupling that turbulence can provide.

Convective topographic torques, $\widehat{\Gamma}_{c,z}^T$, are created by flow over bumps on the core-mantle boundary. Their importance is uncertain. Within our present knowledge, $\Gamma_{c,z}^T$ may be 0 Nm or it may be $O(10^{18})$ Nm or greater (cf. Kuang and Bloxham 1997, Hide 1998, Jault and Le Mouël 1999). Currently, little is known about how core turbulence interacts with mantle topography. Two conflicting arguments have been advanced. One focuses on the smallness of the Ekman number E, a dimensionless number quantifying the ratio of viscous and Coriolis forces, estimated to be of order 10^{-15} in the core. It claims the flow around a topographic bump cannot create a torque when $E=0$, the inference being that the torque vanishes as $E\to 0$ and is therefore small for $E\sim 10^{-15}$. However, the other argument estimates large topographic torques even when $E\sim 10^{-15}$. These arise from the turbulent stresses that develop in the high *Reynolds number* flow occurring in the core. The Reynolds number, Re, is the ratio of inertial and viscous forces and is estimated to be $\mathrm{Re}\equiv \mathrm{Ro}/E\sim 10^9$ in Earth's core, where Ro is the Rossby number, a dimensionless measure of inertial force relative to the Coriolis force. Future studies of strongly turbulent ($\mathrm{Re}\gg 1$), rapidly rotating flows ($\mathrm{Ro}\ll 1$) in the presence of boundary topography will dispel present uncertainties about the strength of the convective topographic coupling mechanism.

We have shown that the adiabatic topographic torques and adiabatic gravitational torques act together to remove any misalignment between equilibrium position of the SIC relative to the mantle. These restoring torques are responsible for mantle-SIC gravitational oscillations. For an SIC uncoupled from the fluid in the adjacent TC, we estimate a gravitational oscillation period of the mantle-SIC system to be 4.1 years. If strong EM coupling exists between the TC and the SIC, the gravitational oscillation

period increases to 8.9 years. Both of these oscillation periods are in qualitative agreement with the semi-decadal LOD variations.

The above estimates of the gravitational oscillation period vary significantly depending on the physical assumptions under which they are derived. For example, few mantle models exist which explicitly estimate how the mantle gravity field perturbs gravitational equipotentials in the core, described here by the parameter $\widehat{\mathcal{A}}$ in (8c). Following Buffett (1996), we make use of two models to estimate $\widehat{\mathcal{A}}$ and they differ by a factor of roughly 2. Lastly, the period of gravitational oscillations and Γ_z^G depends on the thermo-mechanical properties of the SIC (Buffett 1997, Aurnou and Olson 2000, Dumberry and Mound 2010). To date all models have focused on viscous relaxation of the SIC back toward its equilibrium position. No detailed treatment has been carried out that elucidates how a displaced SIC relaxes back to its equilibrium alignment through melting and freezing. Relevant material appears in Fearn *et al.* (1981), Morse (1986), Alboussièrre *et al.* (2010) and Monnereau *et al.* (2010).

Electromagnetic processes also appears capable of explaining the LOD signal: a simple model of torsional waves traversing Earth's outer core gives periods of order 6 years; see (26a). The more complex models developed in the preceding section, based on the seminal work of Braginsky (1970), show that the magnetic torque, Γ_z^M, due to currents leaking from the core into the mantle is proportional to $\widehat{\Sigma}\widehat{\mathcal{B}}^2$, where $\widehat{\Sigma}$ is the mantle conductance and $\widehat{\mathcal{B}}$ is the field strength on the CMB. Further, we have developed a model for the MDL that exists below the CMB. Significant ohmic diffusion occurs in this layer, which appears capable of damping torsional waves as effectively as dissipation in the lowermost mantle, as discussed in section 8.3. The magnetic torque is shown to be able to reach the target torque of 10^{18} Nm. The associated ohmic dissipation in the mantle and MDL is responsible for damping the waves and is roughly proportional to $\widehat{\Sigma}\widehat{\mathcal{B}}^2$. This poses a magnetic coupling paradox: a large value of $\widehat{\Sigma}\widehat{\mathcal{B}}^2$ creates large torques but damps the waves too rapidly; small $\widehat{\Sigma}\widehat{\mathcal{B}}^2$ leads to small damping but weak torques. Our results also indicate that the inner core is strongly coupled to the TC fluid on decadal time scales. Similar to our estimates of ${\Gamma_z}^T$ and Γ_z^G, our assessments of Γ_z^M vary significantly with the detailed assumptions of the underlying physics.

We have shown that the topographic, gravitational, and magnetic torques all have significant uncertainties in their amplitudes. Within these uncertainties Γ_z^T, Γ_z^G and Γ_z^M all appear capable of explaining the semi-decadal LOD signals. These coupling processes may therefore be convolved. The recent model of Buffett *et al.* (2009) allows for this convolution and argues that the gravitational torque is dominant. In contrast, Gillet *et al.* (2010) identify a decadal oscillation in a time-dependent model of the geomagnetic field, from which they infer that torsional oscillations in the outer core fluid can explain the LOD observations without strong gravitational coupling. Improvements in data and modeling of Earth's rotation (e.g. Gross 2009), the geomagnetic field (e.g. Hulot *et al.* 2002, Jackson 2003), core seismology (e.g. Dai and Song 2008), and the time-variations in the gravity field (e.g. Velicogna and Wahr 2006) will all prove important in testing these core-mantle coupling arguments.

This article has focused on explaining variations in LOD that are due to internal coupling between the mantle and core. This coupling produces changes primarily in the axial angular rotation rate, Ω_z, on semi-decadal time scales. Detailed measurements now exist of variations in Earth's full rotation vector on many time scales

(e.g. Gross 2007), with different frequencies and directional components providing information on different geophysical phenomena (e.g. Mathews *et al*. 2002). Furthermore, measurements of the magnetic field and of the components of the angular velocity now exist for other planets (e.g. Margot *et al*. 2007, Uno *et al*. 2009), and will improve in quality in the coming decades. Such measurements will encourage the development of improved models of deep interior structure and dynamics in planetary bodies throughout the solar system (e.g. Tyler 2008, Noir *et al*. 2009, Goldreich and Mitchell 2010).

Acknowledgements

We wish to thank Richard Gross, Richard Holme and Andrew Jackson for sharing their insights and their data. We also thank Bruce Buffett and Andrew Soward for their helpful advice. We are also grateful to the referees for their thoughtful comments, particularly Dominique Jault who provided detailed criticisms of both revisions. PHR thanks the National Science Foundation for support under grant EAR-091104, and JMA thanks it for support under the aegis of the NSF Geophysics Program.

References

Abarca del Rio, R., Gambis, R. and Salstein, D.A., Interannual signals in length of day and atmospheric angular momentum. *Ann. Geophys.* 2000, **18**, 347–364.

Abramowitz, M. and Stegun, I.A. (Eds.), *Handbook of Mathematical Functions with Formulas, Graphs and Mathematical Tables*, National Bureau of Standards Applied Mathematics Series 55, 1953, (Dover: New York).

Alboussière, T., Deguen, R. and Melzani, M., Melting induced stratification above the Earth's inner core due to convective translation. *Nature* 2010, **466**, 744–747.

Anufriyev, A.P. and Braginsky, S.I., Effect of irregularities of the boundary of the Earth's core on the speed of the fluid and on the magnetic field, III. *Geomag. Aeron.* 1977, **17**, 742–750.

Aurnou, J.M., Planetary core dynamics and convective heat transfer scaling. *Geophys. Astrophys. Fluid Dyn.* 2007, **101**, 327–345.

Aurnou, J.M., Brito, D. and Olson, P.L., Mechanics of inner core super-rotation. *Geophys. Res. Lett.* 1996, **23**, 3401–3403.

Aurnou, J.M., Brito, D. and Olson, P.L., Anomalous rotation of the inner core and the toroidal magnetic field. *J. Geophys. Res.* 1998, **103**, 9721–9738.

Aurnou, J.M. and Olson, P.L., Control of inner core rotation by electromagnetic, gravitational and mechanical torques. *Phys. Earth Planet. Inter.* 2000, **117**, 111–121.

Bardina, J., Ferziger, J.H. and Reynolds, W.C., Improved sub-grid scale models for large-eddy simulations. *Am. Inst. Aeron. Acoust. J.* 1980, **34**, 1111–1119.

Bergman, M.I., Estimates of Earth's inner core grain size. *Geophys. Res. Lett.* 1998, **25**, 1593–1596.

Bradshaw, P., Possible origin of Prandtl's mixing length theory. *Nature* 1974, **249**, 138–139.

Braginsky, S.I., Torsional magnetohydrodynamic vibrations in the Earth's core and variations in day length. *Geomag. Aeron.* 1970, **10**, 1–8.

Braginsky, S.I., Short-period geomagnetic secular variation. *Geophys. Astrophys. Fluid Dyn.* 1984, **30**, 1–78.

Braginsky, S.I., Dynamics of the stably stratified ocean at the top of the core. *Phys. Earth planet. Inter.* 1999, **111**, 21–34.

Braginsky, S.I. and Meytlis, V.P., Local turbulence in the Earth's core. *Geophys. Astrophys. Fluid Dynam.* 1990, **55**, 71–87.

Braginsky, S.I. and Roberts, P.H., Equations governing convection in Earth's core and the Geodynamo. *Geophys. Astrophys. Fluid Dyn.* 1995, **79**, 1–97.

Braginsky, S.I. and Roberts, P.H., Anelastic and Boussinesq approximations. In *Encyclopedia of Geomagnetism and Paleomagnetism*, edited by D. Gubbins and E. Herrero-Bervera, pp. 11–19, 2007 (Springer: Heidelberg).

Buffett, B.A., Gravitational oscillations in the length of day. *Geophys. Res. Lett.* 1996, **23**, 2279–2282.

Buffett, B.A., Geodynamic estimates of the viscosity of the Earth's inner core. *Nature* 1997, **388**, 571–573.
Buffett, B.A., Free oscillations in the length of day: inferences on physical properties near the core–mantle boundary. *Geodynamics* 1998, **28**, 153–165.
Buffett, B.A., Chemical stratification at the top of Earth's core: constraints from nutation observations. *Earth Planet. Sci. Lett*. 2010, **296**, 367–372.
Buffett, B.A. and Christensen, U.R., Magnetic and viscous coupling at the core-mantle boundary; inferences from observations of the Earth's nutations. *Geophys. J. Int*. 2007, **171**, 145–152.
Buffett, B.A., Mathews, P.M. and Herring, T.A., Modeling of nutation and precession: effects of electromagnetic coupling. *J. Geophys. Res*. 2002, **107**, 2070–2083.
Buffett, B.A., Mound, J. and Jackson, A., Inversion of torsional oscillations for the structure and dynamics of Earth's core. *Geophys. J. Int*. 2009, **177**, 878–890.
Calkins, M.A., Noir, J., Eldredge, J.D. and Aurnou, J.M., Axisymmetric simulations of libration-driven fluid dynamics in a spherical shell geometry. *Phys. Fluids* 2010, **22**, 086602.
Cao, A. and Romanowicz, B., Hemispheric transition of seismic attenuation at the top of Earth's inner core. *Earth Planet. Sci. Lett*. 2004, **228**, 243–253.
Chen, B., Li, J. and Hauck II, S.A., Non-ideal liquidus curve in the Fe-S system and Mercury's snowing core. *Geophys. Res. Lett*. 2008, **35**, L07201.
Christensen, U.R. and Aubert, J., Scaling properties of convection-driven dynamos in rotating spherical shells and application to planetary magnetic fields. *Geophys. J. Int*. 2006, **166**, 97–114.
Cushman-Roisin, B., Beyond eddy diffusion: an alternative model for turbulent dispersion. *Environ. Fluid Mech*. 2008, **8**, 543–549.
Dai, W. and Song, X., Detection of motion and heterogeneity in Earth's liquid outer core. *Geophys. Res. Lett*. 2008, **35**, L16311.
Davidson, P.A., *An Introduction to Magnetohydrodynamics*, 2001 (Cambridge, UK: Cambridge University Press).
Davidson, P.A., *Turbulence*, 2004 (Oxford, UK: Oxford University Press).
Davies, G.F., Mantle regulation of core cooling: a geodynamo without core radioactivity? *Phys. Earth Planet. Inter*. 2007, **160**, 215–229.
de Wijs, G.A., Kresse, G., Vočadlo, I., Dobson, D.P., Alfè, D., Gillan, M.J. and Price, G.D., The viscosity of liquid iron at the physical conditions of Earth's core. *Nature* 1998, **392**, 805–807.
Defraigne, P., Dehant, V. and Wahr, J., Internal loading of an inhomogeneous compressible mantle with phase boundaries. *Geophys. J. Int*. 1996, **125**, 173–192.
Deleplace, B. and Cardin, P., Viscomagnetic torque at the core-mantle boundary. *Geophys. J. Int*. 2006, **167**, 557–566.
Deuss, A., Irving, J.C.E. and Woodhouse, J.H., Regional variation of inner core anisotropy from seismic normal mode observations. *Science* 2010, **328**, 1018–1020.
Dickey, J.O. and de Viron, O., Leading modes of torsional oscillations within the Earth's core. *Geophys. Res. Lett*. 2009, **36**, 45302–45305.
Dormy, E., Roberts, P.H. and Soward, A.M., Core, Boundary layers. In *Encyclopedia of Geomagnetism and Paleomagnetism*, edited by D. Gubbins and E. Herrero Bervera, pp. 111–116, 2007 (Springer: Heidelberg).
Dormy, E. and Soward, A.M. (Eds.), *Mathematical Aspects of Natural Dynamos*, pp. 142–145, 2007 (London: Taylor and Francis).
Duck, P.W. and Foster, M.R., Spin-up of homogeneous and stratified fluids. *Annu. Rev. Fluid Mech*. 2001, **33**, 231–263.
Dumberry, M., Torsional waves. In *Dynamos*, edited by P. Cardin and L.F. Cugliandolo, pp. 383–401, 2007 (Elsevier: Amsterdam).
Dumberry, M., Decadal variations in gravity caused by a tilt of the inner core. *Geophys. J. Int*. 2008, **172**, 921–933.
Dumberry, M. and Mound, J., Inner core-mantle gravitational locking and the super-rotation of the inner core. *Geophys. J. Int*. 2010, **181**, 806–817.
Dziewonski, A.M. and Anderson, D.L., Preliminary reference Earth model. *Phys. Earth Planet. Inter*. 1981, **25**, 297–356.
Fearn, D.R., Loper, D.E. and Roberts, P.H., Structure of the Earth's inner core. *Nature* 1981, **292**, 232–233.
Fearn, D.R. and Proctor, M.R.E., Dynamically consistent magnetic fields produced by differential rotation. *J. Fluid Mech*. 1987, **178**, 521–534.
Finlay, C.C., Dumberry, M., Chulliat, A. and Pais, M.A., *Space Sci. Rev*. 2010, **155**, 177–218.
Forte, A.M., Woodward, R.J. and Dziewonski, A.M., Joint inversion of seismic and geodynamic data for models of three-dimensional mantle heterogeneity. *J. Geophys. Res*. 1994, **99**, 21857–21877.
Frost, D.J., Asahara, Y., Rubie, D.C., Miyajima, N., Dubrovinsky, L.S., Holzapfel, C., Ohtani, E., Miyahara, M. and Sakai, T., Partitioning of oxygen between Earth's mantle and core. *J. Geophys. Res*. 2010, **115**, B02202.
Gillet, N., Jault, D., Canet, E. and Fournier, A., Fast torsional waves and strong magnetic field within the Earth's core. *Nature* 2010, **465**, 74–77.

Glatzmaier, G.A. and Roberts, P.H., A three-dimensional convective dynamo solution with rotating and finitely conducting inner core and mantle. *Phys. Earth Planet. Inter.* 1995, **91**, 63–75.
Glatzmaier, G.A. and Roberts, P.H., Rotation and magnetism of the Earth's inner core. *Science* 1996a, **274**, 1887–1892.
Glatzmaier, G.A. and Roberts, P.H., An anelastic evolutionary geodynamo simulation driven by compositional and thermal convection. *Physica D* 1996b, **97**, 81–94.
Goldreich, P.M. and Mitchell, J.L., Elastic ice shells and synchronous moons: implications for cracks on Europa and non-synchronous rotation on Titan. *Icarus* 2010, **209**, 631–638.
Gross, R.S., A combined length-of-day series spanning 1832–1997: LUNAR97. *Phys. Earth Planet. Inter.* 2001, **123**, 65–76.
Gross, R.S., Earth rotation variations – long period. In *Physical Geodesy*, edited by T.A. Herring, *Treatise on Geophysics*, Vol. 3, pp. 239–294, 2007 (Elsevier: Amsterdam).
Gross, R.S., Ocean tidal effects on Earth rotation. *J. Geodyn.* 2009, **48**, 219–225.
Gubbins, D., Masters, T.G. and Nimmo, F., A thermochemical boundary layer at the base of Earth's outer core and independent estimate of core heat flux. *Geophys. J. Int.* 2008, **174**, 1007–1018.
Heimpel, M.H., Aurnou, J.M and Wicht, J., Simulation of equatorial and high latitude jets on Jupiter in a deep convection model. *Nature* 2005, **438**, 193–196.
Hejda, P. and Reshetnyak, M., Effects of anisotropy in geostrophic turbulence. *Phys. Earth Planet. Inter.* 2009, **177**, 152–160.
Hide, R., Interaction between the earth's liquid core and solid mantle. *Nature* 1969, **222**, 1055–1956.
Hide, R., A note on topographic core-mantle coupling. *Phys. Earth Planet. Inter.* 1998, **109**, 91–92.
Hide, R., Boggs, D.H. and Dickey, J.O., Angular momentum fluctuations within the Earth's liquid core and torsional oscillations of the core-mantle system. *Geophys. J. Int.* 2000, **143**, 777–786.
Hide, R., Clayton, R.W., Hager, B.H., Speith, M.A. and Voorhies, C.V., Topographic core-mantle coupling and fluctuations in Earth's rotation. In *Relating Geophysical Structures and Processes: The Jeffreys Volume*, edited by K. Aki and R. Dmowska, Geophysics. Monograph Series, Vol. 76, pp. 107–120, 1993 (AGU, Washington, DC).
Hide, R. and James, I.N., Differential rotation produced by potential vorticity mixing in a rapidly rotating fluid. *Geophys. J. R. Astron. Soc.* 1983, **74**, 301–312.
Hollerbach, R., What can the observed rotation of the Earth's inner core reveal about the state of the outer core? *Geophys. J. Int.* 1998, **135**, 564–572.
Holme, R. and de Viron, O., Geomagnetic jerks and a high-resolution length-of-day profile for core studies. *Geophys. J. Int.* 2005, **160**, 435–439.
Hulot, G., Eymin, C., Langlais, B., Mandea, M. and Olsen, N., Small-scale structure of the geodynamo inferred from Oersetd and Magsat satellite data. *Nature* 2002, **416**, 620–623.
Ishihara, T., Gotoh, T. and Kaneda, Y., Study of high Reynolds number isotropic turbulence by direct numerical simulation. *Annu. Rev. Fluid Mech.* 2009, **41**, 165–180.
Jackson, A., Time-dependency of tangentially geostrophic core surface motions. *Phys. Earth Planet. Inter.* 1997, **103**, 293–311.
Jackson, A., Intense equatorial flux spots on the surface of Earth's core. *Nature* 2003, **424**, 760–763.
Jacobs, J.A., The Earth's inner core. *Nature* 1953, **172**, 297–298.
Jault, D., Electromagnetic and topographic coupling, and LOD variations. In *Earth's Core and lower Mantle*, edited by C.A. Jones, A.M. Soward and K. Zhang, pp. 56–76, 2003 (Taylor and Francis: London).
Jault, D., Model-Z by computation and Taylor's condition. *Geophys. Astrophys. Fluid Dynam.* 1995, **79**, 99–124.
Jault, D., Gire, C. and Le Mouël, J.-L., Westward drift, core motions and exchanges of angular momentum between core and mantle. *Nature* 1988, **333**, 353–356.
Jault, D. and Le Mouël, J.-L., The topographic torque associated with a tangentially geostrophic motion at the core surface and inferences on the flow inside the core. *Geophys. Astrophys. Fluid Dynam.* 1989, **48**, 273–296.
Jault, D. and Le Mouël, J.-L., Exchange of angular momentum between the core and mantle. *J. Geomag. Geoelectr.* 1991, **43**, 111–129.
Jault, D. and Le Mouël, J.-L., Comment on 'On the dynamics of topographic core-mantle coupling' by Weijia Kuang and Jeremy Bloxham. *Phys. Earth Planet. Inter.* 1999, **114**, 211–215.
Jeans, J.H., *The Mathematical Theory of Electricity and Magnetism*, 5th ed., 1925 (Cambridge, UK: Cambridge University Press).
Johnson, H. and Doerring, C.R., Comparison of turbulent thermal convection between conditions of constant temperature and constant flux. *Phys. Rev. Lett.* 2009, **102**, 064501.
Kawai, K. and Tsuchiya, T., Temperature profile in the lowermost mantle from seismological and mineral physics joint modeling. *Proc. Nati. Acad. Sci.* 2009, **106**, 22119–22123.
Kennett, B.L.N., Engdahl, E.R. and Buland, R., Constraints on seismic velocities in the Earth from traveltimes. *Geophys. J. Int.* 1995, **122**, 108–124.
King, E.M., Soderlund, K.M., Aurnou, J.M., Christensen, U.R. and Wicht, J., Convective heat transfer in planetary dynamo models. *Geochem. Geophys. Geosyst.* 2010, **11**, Q05007–Q05021.

Kuang, W. and Bloxham, J., The effect of boundary topography on motions in the Earth's core. *Geophys. Astrophys. Fluid Dyn.* 1993, **72**, 161–195.
Kuang, W. and Bloxham, J., On the dynamics of topographic core-mantle coupling. *Phys. Earth Planet. Inter.* 1997, **99**, 289–294.
Kuang, W.-J. and Chao, B.F., Topographic core-mantle coupling in geodynamo modeling. *Geophys. Res. Lett.* 2001, **28**, 1871–1874.
Landau, L.D. and Lifshitz, E.M., *Statistical Physics*, 3rd ed., Vol. 1, 1980 (Oxford: Pergamon Press).
Landau, L.D. and Lifshitz, E.M., *Fluid Mechanics*, 2nd ed., 1987 (Oxford: Pergamon Press).
Lay, T., Hernlund, J. and Buffett, B.A., Core-mantle boundary heat flow. *Nature Geo.* 2008, **1**, 25–32.
Le Mouël, J.L., Narteau, C., Greff-Lefftz, M. and Holschneider, M., Dissipation at the core-mantle boundary on a small-scale topography. *J. Geophys. Res.* 2006, **111**, B04413.
Loper, D.E., General solution for the linearized Ekman-Hartmann layer on a spherical boundary. *Phys. Fluids* 1970, **13**, 2995–2998.
Loper, D.E., The gravitationally powered dynamo. *Geophys. J. R. Astron. Soc.* 1978, **54**, 389–404.
Loper, D.E., Turbulence and small-scale dynamics in the core. In *Core Dynamics*, edited by P.L. Olson, *Treatise on Geophysics*, Vol. 8, pp. 187–206, 2007 (Elsevier: Amsterdam).
Loper, D.E. and Roberts, P.H., A study of conditions at the inner core boundary of the Earth. *Phys. Earth Planet. Inter.* 1981, **24**, 302–307.
Margot, J.L., Peale, S.J., Jurgens, R.F., Slade, M.A. and Holin, I.V., Large longitude libration of Mercury reveals a molten core. *Science* 2007, **316**, 710–714.
Mathews, P.M., Herring, T.A. and Buffett, B.A., Nutation and precession: new nutation series for nonrigid Earth and insights into the Earth's interior. *J. Geophys. Res.* 2002, **107**, 2068–2093.
Matsui, H. and Buffett, B.A., Sub-grid scale model for convection-driven dynamos in a rotating plane layer. *Phys. Earth Planet. Inter.* 2005, **153**, 108–123.
Matsushima, M., Nakajima, T. and Roberts, P.H., The anisotropy of local turbulence in Earth's core. *Earth Planets Space* 1999, **51**, 277–286.
Merrill, R., McElhinny, M.W. and McFadden, P.L., *The Magnetic Field of the Earth*, 1998 (San Diego: Academic Press).
Monnereau, M., Calvet, M., Margerin, L. and Souriau, A., Lopsided growth of Earth's inner core. *Science* 2010, **328**, 1014–1017.
Morse, S.A., Adcumulus growth of the inner core. *Geophys. Res. Lett.* 1986, **13**, 1466–1469.
Mound, J.E. and Buffett, B.A., Interannual oscillations in length of day: implications for the structure of the mantle and core. *J. Geophys. Res.* 2003, **108**, 2334–2350.
Mound, J.E. and Buffett, B.A., Mechanisms of core-mantle angular momentum exchange and the observed spectral properties of torsional oscillations. *J. Geophys. Res.* 2005, **110**, B08103–B08115.
Müller, U. and Bühler, L., *Magnetofluiddynamics in Channels and Containers*, 2001 (Heidelberg: Springer).
Niu, F.L. and Wen, L.X., Hemispherical variations in seismic velocity at the top of the Earth's inner core. *Nature* 2001, **410**, 1081–1084.
Noir, J., Hemmerlin, F., Wicht, J., Baca, S.M. and Aurnou, J.M., An experimental and numerical study of librationally driven flow in planetary cores and subsurface oceans. *Phys. Earth Planet. Inter.* 2009, **173**, 141–152.
Ohta, K., Onada, S., Hirose, K., Sinmyo, R., Shimizu, K., Saya, N., Ohishi, Y. and Yasuhara, A., The electrical conductivity of post-perovskite in Earth's D″ layer. *Science* 2008, **320**, 89–91.
Olsen, N. and Mandea, M., Rapidly changing flows in the Earth's core. *Nature Geosci.* 2008, **1**, 390–394.
Olver, F.W.J., Lozier, D.W., Boisvert, R.F. and Clark, C.W., *NIST Handbook of Mathematical Functions*, 2010 (Cambridge, UK: University Press).
Ricard, Y., Physics of mantle convection, In *Mantle dynamics*, edited by D. Bercovici, *Treatise on Geophysics*, Vol. 7, pp. 31–87, 2007 (Elsevier: Amsterdam).
Roberts, P.H. and Lowes, F.J., Earth currents of deep internal origin. *J. Geophys. Res.* 1961, **66**, 1243–1254.
Roberts, P.H. and Soward, A.M., Magnetohydrodynamics of the Earth's core. *Annu. Rev. Fluid Mech.* 1972, **4**, 117–154.
Roberts, P.H., Yu, S.J. and Russell, C.T., On the 60-year signal from the core. *Geophys. Astrophys. Fluid Dyn.* 2007, **101**, 11–35.
Rogers, T.M. and Glatzmaier, G.A., Angular momentum transport by gravity waves in the solar interior. *Geophys. Astrophys. Fluid Dyn.* 2006, **653**, 756–764.
Sakuraba, A. and Roberts, P.H., Generation of a strong magnetic field using uniform heat flux at the surface of the core. *Nature Geosci.* 2009, **2**, 802–805.
Schubert, G., Turcotte, D.L. and Olson, P., *Mantle Convection in the Earth and Planets*, 2001 (Cambridge, UK: University Press).
Secco, R.A. and Schloessin, H.H., The electrical resistivity of solid and liquid Fe at pressure up to 7 GPa. *J. Geophys. Res.* 1989, **94**, 5887–5894.
Song, X.D. and Richards, P.G., Seismological evidence for differential rotation of the Earth's inner core. *Nature* 1996, **382**, 221–224.

Souriau, A., Deep earth structure – the Earth's core. In *Seismology and Structure of the Earth*, edited by B.A. Romanowicz and A.M. Dziewonski, *Treatise on Geophysics*, Vol. 1, pp. 655–693, 2007 (Elsevier: Amsterdam).
Speith, M.A., Hide, R., Clayton, R.W., Hager, B.H. and Voorhies, C.V., Topographic coupling of core and mantle, and changes in the length of the day. *EOS, Trans. Am. Geophys. Un.* 1986, **67**, 908.
Sprague, M., Julien, K., Knobloch, E. and Werne, J., Numerical simulation of an asymptotically reduced system for rotationally constrained convection. *J. Fluid Mech.* 2006, **551**, 141–174.
Stacey, F.D. and Davis, P.M., *Physics of the Earth*, 4th ed., 2008 (Cambridge, UK: Cambridge University Press).
Stellmach, S. and Hansen, U., Cartesian convection driven dynamos at low Ekman number. *Phys. Rev. E* 2004, **70**, 056312.
Tanaka, S., Constraints on the core-mantle boundary topography from, *P4KP-PcP* differential travel times. *J. Geophys. Res.* 2010, **115**, B04310–B04323.
Tanaka, S. and Hamaguchi, H., Degree one heterogeneity and hemispherical variation of anisotropy in the inner core from PKP(BC)–PKP(DF) times. *J. Geophys. Res.* 1997, **102**, 2925–2938.
Taylor, J.B., The magnetohydrodynamics of a rotating fluid and the Earth's dynamo problem. *Proc. R. Soc. Lond., A* 1963, **274**, 274–283.
Tyler, R.H., Strong ocean tidal flow and heating on moons of the outer planets. *Nature* 2008, **456**, 770–773.
Uno, H., Johnson, C.L., Anderson, B.J., Korth, H. and Solomon, S.C., Modeling Mercury's internal magnetic field with smooth inversions. *Earth Planet. Sci. Lett.* 2009, **285**, 328–339.
van Orman, J.A., On the viscosity and creep mechanism of Earth's inner core. *Geophys. Res. Lett.* 2004, **31**, L20606–L20610.
Velicogna, I. and Wahr, J., Acceleration of Greenland ice mass loss in spring 2004. *Nature* 2006, **443**, 329–331.
Venet, L., Duffar, T. and Deguen, R., Grain structure of the Earth's inner core. *C. R. Geosci.* 2009, **341**, 513–516.
Wahr, J. and deVries, D., The possibility of lateral structure inside the core and its implications for nutation and Earth tide observations. *Geophys. J. Int.* 1989, **99**, 511–519.
Wahr, J., Swenson, S. and Velicogna, I., Accuracy of GRACE mass estimates. *Geophys. Res. Lett.* 2006, **33**, L06401–L06405.
Wicht, J. and Christensen, U.R., Torsional oscillations in dynamo simulations. *Geophys. J. Int.* 2010, **181**, 1367–1380.
Yoshida, S., Sumita, I. and Kumazawa, M., Growth model of the inner core coupled with outer core dynamics and the resulting elastic anisotropy. *J. Geophys. Res.* 1996, **101**, 28085–28103.
Yoshino, T., Laboratory electrical conductivity measurement of mantle minerals. *Surv. Geophys.* 2010, **31**, 163–206.
Zatman, S. and Bloxham, J., Torsional oscillations and the magnetic field within the Earth's core. *Nature* 1997, **388**, 760–763.
Zhang, K. and Schubert, G., Magnetohydrodynamics in rapidly rotating spherical systems. *Annu. Rev. Fluid Mech.* 2000, **32**, 409–433.
Zhang, S. and Jin, J, *Computation of Special Functions*, 1996 (New York: Wiley).

Appendix A: A simple core model

We discuss spherical and aspherical models of the core throughout this manuscript. For illustrative purposes, in this appendix we construct a simple spherical reference state that represents the FOC reasonably well.

By (2d,e) and (3a)

$$\rho_a^s = -\mathrm{d}p_a^s/\mathrm{d}\Phi_a^s. \quad \text{where } \nabla^2\Phi_a^s = 4\pi G\rho_a(\Phi_a^s). \tag{A.1a,b}$$

This nonlinear system is easily solved if it is assumed that p_a^s depends quadratically on Φ_a^s:

$$p_a^s = p_0 - \rho_0\Phi_a^s + F(\Phi_a^s)^2, \quad \rho_a^s = \rho_0 - 2F\Phi_a^s, \tag{A.1c,d}$$

where p_0^s, ρ_0 and F are constants. This implies that

$$p_a^s = P_0 + (\rho_a^s)^2/4F, \quad \text{where } P_0 = p_0 - \rho_0^2/4F, \tag{A.1e,f}$$

and (A.1b,d) give

$$(r\Phi_a^s)'' = 4\pi G\rho_0 r - 8\pi GF(r\Phi_a^s), \tag{A.1g}$$

so that

$$\Phi_a^s = \frac{\rho_0}{2F} + \frac{(L\sin ar + N\cos ar)}{r}, \quad \text{where } a = \sqrt{(8\pi GF)}, \tag{A.1h,i}$$

L and N are constants. It then follows from (A.1d) that

$$\rho_a^s = -2F(L\sin ar + N\cos ar)/r. \tag{A.1j}$$

According to the PREM model of Dziewonski and Anderson (1981) and ak135 of Kennett *et al.* (1995), $p(r_o) = 136$ (135) GPa, $p(r_i) = 329$ (328) GPa, $\rho(r_o) = 9.90$ $(9.89) \times 10^3\,\mathrm{kg\,m^{-3}}$ and $\rho(r_i) = 12.2$ (12.2) $\mathrm{g\,cm^{-3}}$, where the ak135 values are in brackets. We fitted the PREM values to (A.1e) by choosing

$$F = 6.4646 \times 10^{-5}\,\mathrm{kg\,m^{-5}\,s^2}, \quad P_0 = -243.5\,\mathrm{GPa}, \tag{A.2a,b}$$

so that $a = 3.2927 \times 10^{-7}\,\mathrm{m^{-1}}$. The PREM values of $\rho(r_o)$ and $\rho(r_i)$ above and (A.1j) determined the constants L and N as

$$L = -2.9233 \times 10^{14}\,\mathrm{m^3\,s^{-2}}, \quad N = -5.5139 \times 10^{11}\,\mathrm{m^3\,s^{-2}}. \tag{A.2c,d}$$

The resulting $\widehat{g}^{\,s}(r_o) = 10.66\,\mathrm{m\,s^{-2}}$, $\widetilde{g}^{\,s}(r_i) = 4.58\,\mathrm{m\,s^{-2}}$, and $\Delta\Phi_a^s = \Phi_a^s(r_o) - \Phi_a^s(r_i) = 1.750 \times 10^7\,\mathrm{m^2\,s^{-2}}$ may be compared with the values from the PREM and ak135: $\widehat{g}\,(r_o) = 10.68$ (10.68) $\mathrm{m\,s^{-2}}$, $\widetilde{g}(r_i) = 4.4$ (4.4) $\mathrm{m\,s^{-2}}$, and $\Delta\Phi_a = 1.741$ $(1.742) \times 10^7\,\mathrm{m^2\,s^{-2}}$. Without doubt, a better fit to the core could be obtained by recognizing that in reality ρ_a^s depends nonlinearly on Φ_a^s; see Figure A1. However, the model would no longer be simple and (A.lb) would then have to be integrated numerically. It is also doubtful whether the differences between our values and those of PREM or aka135 are geophysically significant.

Appendix B: Dissipative torsional waves

The derivation of the equation governing torsional waves is reviewed here, with emphasis on diffusive effects within the SIC and its bounding walls, Since we shall disregard all except magnetic torques, electrical conductivity is totally responsible for the coupling of the waves to the walls and for their dissipation. We split off the waves from the underlying Taylor state by using the representation (26b), with $\boldsymbol{v}^{\mathrm{A}}$ replaced by $\boldsymbol{v}$; similarly for other variables. We simplify initially by ignoring the existence of the inner core.

Consider first the main effect of viscosity on the waves. One might at first think that this will damp the waves on a time scale of $\tau_\nu = r_o^2/\nu = \Omega^{-1}E^{-1} \approx 10^{11}$ yr. This time is gigantic because of the smallness of the Ekman number $E = \nu/\Omega r_o^2 \approx 10^{-15}$ (or 10^{-9} if a turbulent viscosity is assumed, though here we assume laminar flow). In fact, τ_ν is

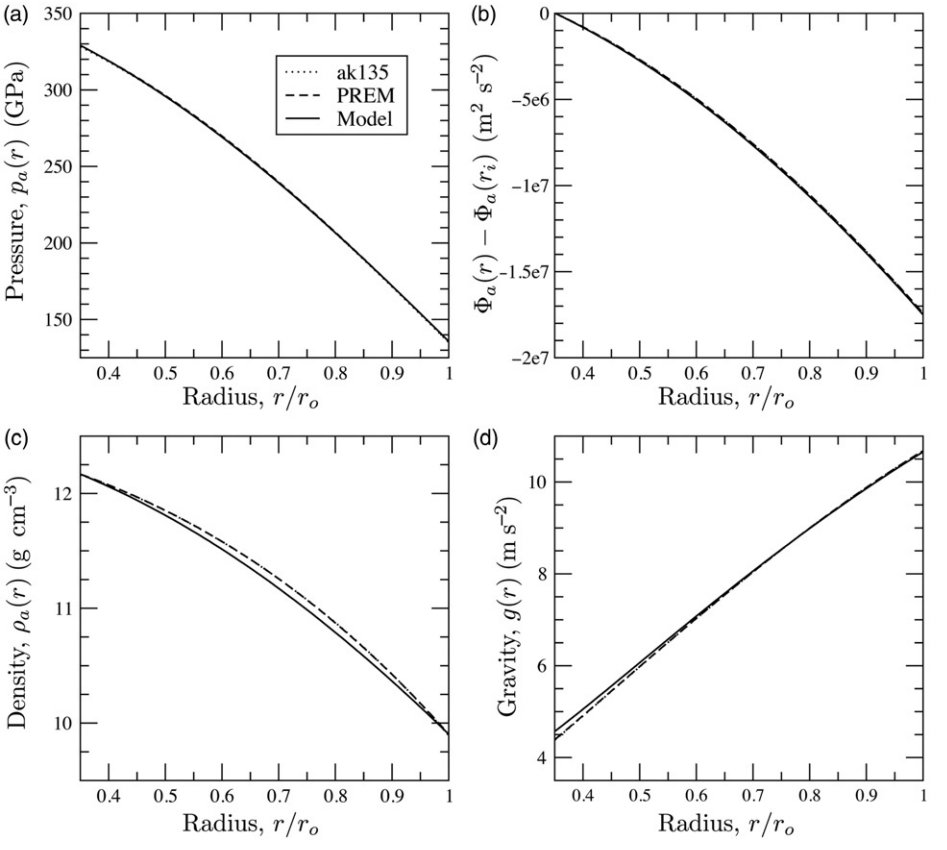

Figure A1. Radial profiles of (a) pressure, (b) gravitational potential, (c) density, and (d) gravity for ak135 and PREM plotted versus our adiabatic core model.

irrelevant for phenomena forced on time scales short compared with τ_ν. Then the potency of viscosity is restricted almost entirely to an Ekman layer of thickness $d_\nu = \sqrt{(\nu/\Omega)} \approx 10\,\text{cm}$, within which the viscous dissipation per unit volume is enhanced by a factor of order $(r_o/d_\nu)^2$. As this boundary layer occupies a fraction d_ν/r_o of the fluid volume, the total dissipation is increased only by a factor of about r_o/d_ν as $d_\nu \to 0$. Correspondingly, the time scale of wave damping is reduced by the same factor to roughly $\tau_{\text{SU}} = \tau_\nu d_\nu/r_o \approx 3 \times 10^5\,\text{yr}$. Since this is again much longer than τ_{A}, it continues to make sense to take $E = 0$ when studying torsional wave propagation.

Similar arguments apply when we consider wave damping by ohmic resistivity. One might at first think that resistivity will damp the waves on a time scale of $\tau_\eta = r_o^2/\eta \approx 10^5\,\text{yr}$, but this is untrue; τ_η, is irrelevant for phenomena forced on time scales short compared with τ_η. Because the Lundquist number,

$$\lambda = V_{\text{A}} r_o/\eta = \Lambda/Ro_M = \tau_\eta/\tau_{\text{A}}, \tag{B.1a}$$

is large ($\approx 2 \times 10^4$), ohmic diffusion operates almost entirely in an MDL at the CMB. Its characteristic thickness is

$$d_\eta = r_o \lambda^{-1/2} = \sqrt{(\eta \tau_A)} \approx 20\,\text{km}. \tag{B.1b}$$

As $\lambda \to \infty$, ohmic dissipation per unit volume within the layer increases by an $O((r_o/d_\eta)^2)$ factor but the volume in which this happens is reduced by an $O(r_o/d_\eta)$ factor, so that the net effect is an enhanced dissipation by an $O(r_o/d_\eta)$ factor. The time scale of wave damping is curtailed by the same factor to roughly $\tau_\eta d_\eta / r_o \approx 300$ yr. Although little credence can be placed on this rough order of magnitude estimate, it establishes that the core alone, independently of the mantle, creates ohmic damping of torsional waves that cannot be safely ignored. It should be emphasized that Coriolis and Lorentz forces operate in the MDL too; see below. The structure of the MDL was first discussed by Braginsky (1970).

It should be stressed that, although the field in a non-conducting mantle adjusts instantly to changing conditions in the core and does not oppose them, the adjustment requires that an MDL exists. As established above, the total ohmic dissipation in the core is greatly increased by the MDL from what it would be in its absence. We call this *enhanced dissipation*. A highly conducting mantle would grip the field that threads it and, as in the skin effect, induce a response in the upper core. The ohmic losses in the MDL might then be even greater. The significant point is however that enhanced dissipation occurs within the core even when $\widehat{\sigma}$ is small (or zero), and then exceeds ohmic losses in the mantle.

When viscous and ohmic diffusion are both significant, the boundary layer is said to be of EH type. Most theory is aimed at applications in which conditions outside the layer are quasi-steady. The frequency of torsional waves is, however, so high that the theory requires generalization, a topic to which appendix D is devoted. When, as for the case of Earth's core, the magnetic Prandtl number, $P_m = \nu/\eta$ is tiny, the EH layer has a double structure, in which a layer of Ekman type is a thin film adjacent to the boundary and embedded within the much thicker MDL. Loper (1970) gives an analysis based on $P_m \to 0$; see also Dormy and Soward (2007) or appendix D. When it is assumed (as we do here) that $E = 0$, the film disappears, as does viscous core-mantle coupling. All thoughts of satisfying the correct, no-slip conditions on the boundary are abandoned and $\boldsymbol{v}_H$ is nonzero there. The task of satisfying the magnetic boundary conditions is left to the MDL.

What is attempted below is an asymptotic treatment of torsional wave transmission, in which $E = 0$ and $\varepsilon \to 0$, where

$$\varepsilon = \lambda^{-1/2} \ (= d_\eta / r_o). \tag{B.2}$$

Outside the core, the magnetic and electric fields of the wave will be denoted by $\widehat{\boldsymbol{b}}(\boldsymbol{r})$ and $\widehat{\boldsymbol{e}}(\boldsymbol{r})$, so that on the outer edge of the MDL (the CMB, denoted by $\widehat{S}$), they are $\widehat{\boldsymbol{b}}(\boldsymbol{r}_o)$ and $\widehat{\boldsymbol{e}}(\boldsymbol{r}_o)$, where $\boldsymbol{r}_o$ is a general point on $\widehat{S}$. Beneath the MDL, a region we call "the mainstream", where ohmic dissipation is neglected, the magnetic and electric fields of the wave will be denoted by $\boldsymbol{b}(\boldsymbol{r})$ and $\boldsymbol{e}(\boldsymbol{r})$. On the inner edge, S, of the MDL (the one further from the CMB), they are $\boldsymbol{b}(\boldsymbol{r}_o)$ and $\boldsymbol{e}(\boldsymbol{r}_o)$ and differ substantially from $\widehat{\boldsymbol{b}}(\boldsymbol{r}_o)$ and $\widehat{\boldsymbol{e}}(\boldsymbol{r}_o)$, because of their high frequency. (In contrast, the slowly varying $\boldsymbol{B}^m$ is continuous.) The MDL smoothes out the discontinuities in magnetic and electric

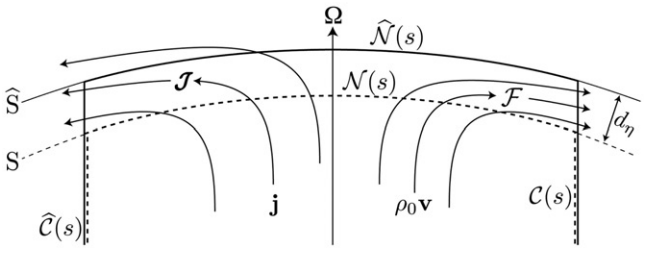

Figure B1. Schematic cross-sectional view of the MDL and the northern spherical cap $\widehat{\mathcal{N}}(s)$ of the geostrophic cylinder $\widehat{\mathcal{C}}(s)$. The inner edge of the layer (dashed) is the sphere $r = r_o - d_\eta$ and, where it lies outside $\mathcal{N}(s)$ and $\widehat{\mathcal{S}}(s)$, it is denoted by S; it defines another, shortened geostrophic cylinder $\mathcal{C}(s)$ (also shown dashed) in which magnetic diffusion is negligible and which is capped by $\mathcal{N}(s)$ and $\mathcal{S}(s)$. The outward (or inward) flow of current $\boldsymbol{j}$ and mass $\rho_0\boldsymbol{v}$ into the MDL is concentrated into a surface current $\boldsymbol{\mathcal{J}}$ and a surface momentum flux $\boldsymbol{\mathcal{F}}$. The former can penetrate the mantle if it is conducting, as indicated in the figure. The rim, $\mathcal{R}_N(s)$, is the part of $\widehat{\mathcal{C}}$ lying between $\widehat{\mathrm{S}}$ and S and is not labeled. The MDL is only part of the EH layer; the other Ekman-type part is much thinner for $P_m \ll 1$, and is not shown.

fields. In section 3.2, geostrophic cylinders $\widehat{\mathcal{C}}(s)$ were introduced, closed by spherical caps $\widehat{\mathcal{N}}(s)$ and $\widehat{\mathcal{S}}(s)$ on $\widehat{\mathrm{S}}$. It will be helpful to introduce the adjacent spherical caps, $\mathcal{N}(s)$ and $\mathcal{S}(s)$ on S. Figure B1 shows $\mathcal{N}(s)$ as the end of a slightly shortened geostrophic cylinder $\mathcal{C}(s)$.

Some terminology should be clarified here. In section 8.3 and above, we used the adjectives "outer" and "inner", meaning shallower and deeper within the Earth. This follows common engineering practice, but contradicts the usage of asymptotic analysis, where "outer" refers to the mainstream and "inner" to the boundary layer. Although asymptopia is basic to boundary layer theory, the engineering description is often found helpful, as for example in figure B1 which illustrates the coming text. In asymptopia the boundary layer part, $\boldsymbol{b}'$, of the wave's magnetic field, $\breve{\boldsymbol{b}} = \boldsymbol{b} + \boldsymbol{b}'$, is not a function of r, but depends instead on a stretched/scaled coordinate, $\xi = (r_o - r)/d_\eta$. In the $\varepsilon \to 0$ limit, $\partial_r \boldsymbol{b}' = \mathrm{O}(\varepsilon^{-1}\boldsymbol{b}') \gg \boldsymbol{b}'$ but $\partial_\xi \boldsymbol{b}' = \mathrm{O}(\boldsymbol{b}')$, so that $\boldsymbol{b}'$ undergoes a finite change when ξ increases from 0 to a finite value during which $r = r_o(1-\varepsilon)$ is essentially unchanged. The MDL is completely "crossed" as ξ increases from 0 to ∞, and $\boldsymbol{b}'$ changes from $\widehat{\boldsymbol{b}}(\boldsymbol{r}_o) - \boldsymbol{b}(\boldsymbol{r}_o)$ at the CMB to its mainstream core value $\mathbf{0}$. Its "lower boundary", S, is not a sharp surface at all, even though ε is said to be "the boundary layer thickness". When below we say we integrate the s-component of the velocity over $\mathcal{C}(s)$, we mean that we are ignoring the MDL and integrating v_s alone; integration over $\widehat{\mathcal{C}}(s)$ will imply that the full $v_s + v_s'$ is integrated, but the physical domain of integration is the same.

Boundary layer variables vanish "outside the boundary layer", which in asymptopia means, for example,

$$\boldsymbol{v}'(\xi) \to 0, \quad \text{as } \xi \to \infty, \tag{B.3}$$

for fixed ε. All variables depend on ε and are expanded in powers of ε, though usually we retain only the first (or "leading") terms of the expansions; in some cases we must keep the first two terms, e.g., $\boldsymbol{v} = \boldsymbol{v}^{(0)} + \varepsilon\boldsymbol{v}^{(1)} + \mathrm{O}(\varepsilon^2)$.

To leading order, (11d) and (B.3) imply $\partial_\xi b_r'^{(0)} = 0$, giving

$$b_r'^{(0)} = 0, \quad \text{so that} \quad \boldsymbol{b}'^{(0)} = \boldsymbol{b}_{\mathrm{H}}'^{(0)}. \tag{B.4a,b}$$

The analogous statements for the electric field are untrue because the total electric charge generated by the wave in the MDL is nonzero, but (18b) and (11h) establish

$$v_r'^{(0)} = 0, \quad j_r'^{(0)} = 0, \quad \text{so that } \boldsymbol{v}'^{(0)} = \boldsymbol{v}_{\mathrm{H}}'^{(0)}, \quad \boldsymbol{j}'^{(0)} = \boldsymbol{j}_{\mathrm{H}}'^{(0)}. \tag{B.4c,d,e,f}$$

At the next order in the ε expansion of the MDL, (18b) shows that

$$\partial_\xi v_r'^{(1)} = r_o \boldsymbol{\nabla}_{\mathrm{H}} \cdot \boldsymbol{v}_{\mathrm{H}}'^{(0)}, \quad \text{which implies } v_r'^{(1)}(\xi) = -r_o \int_\xi^\infty \boldsymbol{\nabla}_{\mathrm{H}} \cdot \boldsymbol{v}_{\mathrm{H}}'^{(0)} \mathrm{d}\xi, \tag{B.5a,b}$$

by (B.3). (The surface divergence, $\boldsymbol{\nabla}_{\mathrm{S}} \cdot \boldsymbol{v}_{\mathrm{S}}$, is defined for example in Dormy *et al.* (2007), both geometrically and as $\boldsymbol{n} \cdot (\boldsymbol{\nabla} \times (\boldsymbol{n} \times \boldsymbol{v}) + c\boldsymbol{v})$, where c is the Gaussian curvature. For the sphere $\widehat{\mathrm{S}}$, this gives $\boldsymbol{\nabla}_{\mathrm{H}} \cdot \boldsymbol{v}_{\mathrm{H}} = \mathbf{1}_r \cdot (\boldsymbol{\nabla} \times (\mathbf{1}_r \times \boldsymbol{v}) + 2\boldsymbol{v}/r_o) \approx \mathbf{1}_r \cdot \boldsymbol{\nabla} \times (\mathbf{1}_r \times \boldsymbol{v})$, by (B.4c,e).) As $\breve{v}_r$ $(= v_r + v_r')$ vanishes on $\widehat{\mathrm{S}}$, the mainstream mass flux out of S and into the MDL is, to leading order,

$$\rho_0 v_r^{(1)}(\boldsymbol{r}_o) = -\rho_0 v_r'^{(1)}(0) = \rho_0 r_o \int_0^\infty \boldsymbol{\nabla}_{\mathrm{H}} \cdot \boldsymbol{v}_{\mathrm{H}}'^{(0)} \, \mathrm{d}\xi = \boldsymbol{\nabla}_{\mathrm{H}} \cdot \boldsymbol{\mathcal{F}}, \tag{B.5c}$$

where

$$\boldsymbol{\mathcal{F}} = \rho_0 r_o \int_0^\infty \boldsymbol{v}_{\mathrm{H}}'^{(0)} \, \mathrm{d}\xi \tag{B.5d}$$

is the tangential mass flux ($\mathrm{kg\,m^{-1}\,s^{-1}}$) in oscillatory jets of fluid that carry mass along the MDL on the τ_{A} time scale. (This is analogous to oscillatory jets in an Ekman layer that are induced when the boundary is librating, Calkins *et al.* 2010.) Equation (B.5c) expresses the fact that these jets are fed by the radial mainstream flow on S. The mass flux, $f_{\mathcal{N}}$, from $\mathcal{C}(s)$ across $\mathcal{N}(s)$ is the mass expelled per second through the northern "rim", $\mathcal{R}_{\mathcal{N}}(s)$, of $\widehat{\mathcal{C}}(s)$ so that

$$f_{\mathcal{N}} = s \oint (\mathcal{F}_\theta)_{\mathcal{R}_{\mathcal{N}}} \mathrm{d}\phi = \rho_0 \int_{\mathcal{N}(s)} v_r^{(1)}(\boldsymbol{r}_o) \mathrm{d}a. \tag{B.5e}$$

The radial mainstream flow across $\mathcal{N}(s)$ and $\mathcal{S}(s)$ shares the basic torsional wave periodicity and, by mass conservation, causes the radius s of $\mathcal{C}(s)$ to pulsate slightly.

In a similar way, the second term in the expansion of (11h) gives

$$j_r'^{(1)}(\xi) = -r_o \int_\xi^\infty \boldsymbol{\nabla}_{\mathrm{H}} \cdot \boldsymbol{j}_{\mathrm{H}}'^{(0)} \mathrm{d}\xi, \quad \text{and} \quad j_r^{(1)}(\boldsymbol{r}_o) - \widehat{j}_r^{(1)}(\boldsymbol{r}_o) = -j_r'^{(1)}(\boldsymbol{r}_o) = \boldsymbol{\nabla}_{\mathrm{H}} \cdot \boldsymbol{\mathcal{J}}, \tag{B.6a,b}$$

where $j_r^{(1)}$ is the current flow out of S and $\widehat{j}_r^{(1)}(\boldsymbol{r}_o)$ is the current flow into the mantle (if electrically conducting). In (B.6b), $\boldsymbol{\mathcal{J}}$ is the surface current, i.e. the net horizontal current flowing in the MDL. Since $\mu_0 \boldsymbol{j}'^{(1)} = \mathbf{1}_r \times \partial_r \boldsymbol{b}_{\mathrm{H}}'^{(0)} = -r_o \mathbf{1}_r \times \partial_\xi \boldsymbol{b}_{\mathrm{H}}'^{(0)}$, this is given by

$$\mu_0 \boldsymbol{\mathcal{J}} = -\int_0^\infty \mathbf{1}_r \times \partial_\xi \boldsymbol{b}_{\mathrm{H}}'^{(0)} r_o \mathrm{d}\xi = \mathbf{1}_r \times \boldsymbol{b}_{\mathrm{H}}'^{(0)}(0) = \mathbf{1}_r \times [\widehat{\boldsymbol{b}}^{(0)}(\boldsymbol{r}_o) - \boldsymbol{b}^{(0)}(\boldsymbol{r}_o)]_{\mathrm{H}}. \tag{B.6c}$$

Analogous to (B.5e) is the expression for the flux of current through $\mathcal{R}_{\mathcal{N}}(s)$:

$$i_N = s \oint (\mathcal{J}_\theta)_{\mathcal{R}_{\mathcal{N}}} \mathrm{d}\phi = \int_{\mathcal{N}(s)} [j_r^{(1)}(\boldsymbol{r}_o) - \widehat{j}_r^{(1)}(\boldsymbol{r}_o)] \mathrm{d}a. \tag{B.6d}$$

Henceforth, the superscripts $^{(0)}$ and $^{(1)}$ are omitted but implied, and $O(\varepsilon^2)$ terms are ignored.

As argued in section 3.2, wave dynamics requires the inertial force to be retained in the equation of motion, so that

$$\rho_0(\partial_t \breve{\boldsymbol{V}} + 2\boldsymbol{\Omega} \times \breve{\boldsymbol{V}}) = -\boldsymbol{\nabla} p_c + \breve{\boldsymbol{J}} \times \breve{\boldsymbol{B}}, \tag{B.7}$$

where $\breve{\boldsymbol{B}}$ and $\breve{\boldsymbol{J}} = \mu_0^{-1}\boldsymbol{\nabla} \times \breve{\boldsymbol{B}}$ are the total field and current, and $\breve{\boldsymbol{V}}$ is the total fluid velocity. Their principal parts are $\boldsymbol{B}^{\mathrm{m}}$, $\boldsymbol{J}^{\mathrm{m}}$, and $\boldsymbol{V}^{\mathrm{m}}$ of the Taylor state, and are considered time-independent because $\tau_{\mathrm{mac}} \gg \tau_{\mathrm{A}}$. Also included are contributions $\breve{\boldsymbol{b}}$ $(=\boldsymbol{b}+\boldsymbol{b}')$, $\breve{\boldsymbol{j}}$ $(=\boldsymbol{j}+\boldsymbol{j}')$ and $\breve{\boldsymbol{v}}$ $(=\boldsymbol{v}+\boldsymbol{v}')$ from the wave, where $\boldsymbol{v} = s\zeta \mathbf{1}_\phi$. The wave is treated as a perturbation, i.e. squares and products of wave variables are discarded. The buoyancy force has been omitted from (B.7) because it does not affect the wave dynamics.

The dynamics of the MDL are governed by (B.7), with $\boldsymbol{\nabla} = \mathbf{1}_r \partial_r$, to leading order in ε. The dominant term of (B.7) is $\partial_r p_c' = 0$, so that $p_c' = p_c'(\theta, \phi, t)$. At the next order

$$\rho_0(\partial_t \boldsymbol{v}_{\mathrm{H}}' + 2\Omega_r \mathbf{1}_r \times \boldsymbol{v}_{\mathrm{H}}') = -\boldsymbol{\nabla}_{\mathrm{H}} p_c' - B_r^{\mathrm{m}} \mathbf{1}_r \times \boldsymbol{j}_{\mathrm{H}}'. \tag{B.8a}$$

When this is integrated across the MDL, the contribution from p_c' is negligible, so that

$$\partial_t \boldsymbol{\mathcal{F}} + 2\Omega_r \mathbf{1}_r \times \boldsymbol{\mathcal{F}} = -B_r^{\mathrm{m}} \mathbf{1}_r \times \boldsymbol{\mathcal{J}}, \quad \text{or} \quad B_r^{\mathrm{m}} \boldsymbol{\mathcal{J}} = \mathbf{1}_r \times \partial_t \boldsymbol{\mathcal{F}} - 2\Omega_r \boldsymbol{\mathcal{F}}. \tag{B.8b,c}$$

From this and (B.5e)

$$2\Omega s(f_{\mathcal{N}} + f_{\mathcal{S}}) = 2\Omega s^2 \oint (\mathcal{F}_\theta)_{\mathcal{N}\&\mathcal{S}} \mathrm{d}\phi = -\frac{r_o s^2}{z_1} \oint \left(B_r^{\mathrm{m}} \mathcal{J}_\theta + \frac{\partial \mathcal{F}_\phi}{\partial t} \right)_{\mathcal{N}\&\mathcal{S}} \mathrm{d}\phi, \tag{B.8d}$$

since $\Omega/\Omega_r = r_o/z_1$. Here $_{\mathcal{N}\&\mathcal{S}}$ means the sum of values on the latitude circles where $\widehat{\mathcal{C}}$ meets $\widehat{\mathrm{S}}$, in the northern and southern rims, $\mathcal{R}_{\mathcal{N}}$ and $\mathcal{R}_{\mathcal{S}}$.

The Lorentz force, $\boldsymbol{\mathcal{J}} \times \boldsymbol{B}^{\mathrm{m}}$, is responsible for driving flow within the MDL. The torque it creates on the MDL lying between $\widehat{\mathcal{N}}$ and $\mathcal{N}$ is

$$\gamma_{\mathcal{N}}^M = \oint_{\mathcal{N}} \boldsymbol{r} \times (\boldsymbol{\mathcal{J}} \times \boldsymbol{B}^{\mathrm{m}}) \mathrm{d}a = \oint_{\mathcal{N}} (\boldsymbol{r} \cdot \boldsymbol{B}^{\mathrm{m}}) \boldsymbol{\mathcal{J}} \mathrm{d}a, \quad \text{or} \quad \gamma_{\mathcal{N}}^M = \oint_{\mathcal{N}} r B_r^{\mathrm{m}} \mathbf{1}_r \times (\widehat{\boldsymbol{b}} - \boldsymbol{b})_{\mathrm{H}} \mathrm{d}a. \tag{B.9a,b}$$

The ratio of the two terms on the right-hand side of (B.8c) is of order $\omega_{\mathrm{A}}/\Omega$, so the first term is negligible (except very near the equator). Then, by (B.8c) and (B.9a),

$$2\Omega_r \boldsymbol{\mathcal{F}} = -B_r^{\mathrm{m}} \boldsymbol{\mathcal{J}}, \quad \text{and} \quad \gamma_{\mathcal{N}}^M = -2 \oint_{\mathrm{S}} (\boldsymbol{r} \cdot \boldsymbol{\Omega}) \boldsymbol{\mathcal{F}} \mathrm{d}a. \tag{B.9c,d}$$

Consider next the dynamics of $\mathcal{C}(s)$. The ϕ-component of (B.7) gives

$$\rho_0 s(\partial_t v_\phi + 2\Omega v_s) = -\partial_\phi p_c + s(\boldsymbol{J} \times \boldsymbol{B})_\phi. \tag{B.10a}$$

It was shown in section 3.2 that the integral of $2\Omega\rho_s s \breve{v}_s$ over $\widehat{\mathcal{C}}(s)$ vanishes, by mass conservation. When however $2\Omega\rho_s s v_s$ is integrated over $\mathcal{C}(s)$, the integral does not vanish, because of the flux through the caps $\mathcal{N}$ and $\mathcal{S}$. Instead mass conservation requires that

$$\rho_0 \int_{\mathcal{C}} v_s \, \mathrm{d}s + f_{\mathcal{N}} + f_{\mathcal{S}} = 0. \tag{B.10b}$$

By using this and $v_\phi = s\zeta$, we obtain from (B.10a),

$$\rho_0 \widehat{A} s^2 \partial_t \zeta - 2\Omega s(f_{\mathcal{N}} + f_{\mathcal{S}}) = \int_{\mathcal{C}} s(\boldsymbol{J} \times \boldsymbol{B})_\phi \, \mathrm{d}s, \tag{B.10c}$$

where $\widehat{A}(s) = 4\pi s z_1$ is the area of $\mathcal{C}(s)$ (which is asymptotically the same as that of $\widehat{\mathcal{C}}(s)$), and $z_1 = \surd(r_o^2 - s^2)$. The right-hand side of (B.10a) gives

$$\int_{\mathcal{C}} s(\boldsymbol{J} \times \boldsymbol{B})_\phi \mathrm{d}a = \partial_s \Gamma^M_{\mathcal{I},z}(s,t), \tag{B.10d}$$

where $\Gamma^M_{\mathcal{I},z}(s,t)$ is the magnetic torque on the interior, $\mathcal{I}(s)$, of $\mathcal{C}(s)$. From the equivalence of (45g,h), we have

$$\mu_0 \Gamma^M_{\mathcal{I},z}(s,t) = s \int_{\mathcal{C}(s)} B_s B_\phi \, \mathrm{d}a + \int_{\mathcal{N}\&\mathcal{S}} s B_r B_\phi \, \mathrm{d}a. \tag{B.10e}$$

If the same equivalence (45g,h) is applied to $\boldsymbol{B}^{\mathrm{m}}$, (B.10e) gives an alternative expression of Taylor's condition (21c) for magnetostrophic flows:

$$s \int_{\mathcal{C}(s)} B^{\mathrm{m}}_s B^{\mathrm{m}}_\phi \, \mathrm{d}a + \int_{\mathcal{N}\&\mathcal{S}} s B^{\mathrm{m}}_r B^{\mathrm{m}}_\phi \, \mathrm{d}a = 0. \tag{B.10f}$$

When we substitute (B.10e) into (B.10d), we face terms of the form

$$I_{\mathcal{N}} = \partial_s \int_{\mathcal{N}(s)} s B_r B_\phi \, \mathrm{d}a, \tag{B.11a}$$

where $\mathrm{d}a = r_o s \, \mathrm{d}\theta \, \mathrm{d}\phi$. As $\theta(s) = \sin^{-1}(s/r_o)$, we have $\mathrm{d}\theta = \mathrm{d}s/z_1$. It follows that

$$I_{\mathcal{N}} = \frac{r_o s^2}{z_1} \oint (B_r B_\phi)_{\mathcal{N}} \, \mathrm{d}\phi. \tag{B.11b}$$

We can now write (B.10c) as

$$\mu_0 \rho_0 \widehat{A} s^2 \frac{\partial \zeta}{\partial t} - 2\Omega \mu_0 s(f_{\mathcal{N}} + f_{\mathcal{S}}) = \frac{\partial}{\partial s}\left(s \int_{\mathcal{C}(s)} B_s B_\phi \, \mathrm{d}a \right) + \frac{r_o s^2}{z_1} \oint (B_r B_\phi)_{\mathcal{N}\&\mathcal{S}} \, \mathrm{d}\phi. \tag{B.11c}$$

This applies only to $\mathcal{C}$, in which $\boldsymbol{b}' = \boldsymbol{0}$ and $\boldsymbol{B} = \boldsymbol{B}^{\mathrm{m}} + \boldsymbol{b}$.

We can now combine the dynamics of the MDL and $\mathcal{C}(s)$ by eliminating $2\Omega s(f_{\mathcal{N}} + f_{\mathcal{S}})$ between (B.11c) and (B.8d):

$$\mu_0 \frac{\partial \breve{M}_{\widehat{\mathcal{C}}}}{\partial t} = \frac{\partial}{\partial s}\left(s \int_{\mathcal{C}(s)} B_s B_\phi \, \mathrm{d}a \right) + \frac{r_o s^2}{z_1} \oint (B_r \widehat{B}_\phi)_{\widehat{\mathcal{N}}\&\widehat{\mathcal{S}}} \mathrm{d}\phi, \tag{B.12a}$$

where $\breve{M}_{\widehat{\mathcal{C}}}(s,t)\mathrm{d}s$ is the axial angular momentum between $\widehat{\mathcal{C}}(s + \mathrm{d}s)$ and $\widehat{\mathcal{C}}(s)$:

$$\breve{M}_{\widehat{\mathcal{C}}}(s,t) = s^2 \left[\rho_0 \widehat{A} \zeta + \frac{r_o}{z_1} \oint (\mathcal{F}_\phi)_{\widehat{\mathcal{N}}\&\widehat{\mathcal{S}}} \mathrm{d}\phi \right]. \tag{B.12b}$$

The surface integral in (B.12a) is over $\widehat{\mathcal{N}}$ and $\widehat{\mathcal{S}}$ on which $\boldsymbol{B} = \boldsymbol{B}^{\mathrm{m}} + \boldsymbol{b} + \boldsymbol{b}'$; the corresponding surface integral in (B.11c) was over $\mathcal{N}$ and $\mathcal{S}$ on which $\boldsymbol{B} = \boldsymbol{B}^{\mathrm{m}} + \boldsymbol{b}$.

When (B.12a) is integrated over all s, the first term on its right-hand vanishes and the remainder gives

$$\partial_t \breve{M}_z = -\widehat{\Gamma}_z^M, \quad \text{where } \widehat{\Gamma}_z^M = -\mu_0^{-1} \oint_{\widehat{\mathrm{S}}} sB_r \widehat{B}_\phi \, \mathrm{d}a \tag{B.12c,d}$$

is the axial torque on the mantle, which vanishes if the mantle is insulating. In contrast, the corresponding integral over $\mathcal{N}$ and $\mathcal{S}$ gives the axial torque on S:

$$\Gamma_z^M = -\mu_0^{-1} \oint_{\widehat{\mathrm{S}}} sB_r B_\phi \, \mathrm{d}a, \tag{B.12e}$$

which is generally unequal to $\widehat{\Gamma}_z^M$ and nonzero. The difference supplies the angular momentum ejected from the rims of $\widehat{\mathcal{C}}$.

The part of $\breve{M}_{\widehat{\mathcal{C}}}$ due to the momentum of the rims is smaller than the rest; it was previously ignored in approximating (B.8c) by (B.9c). If it is again ignored in $\breve{M}_{\widehat{\mathcal{C}}}$, the result (B.12c) coincides with the equation that could have been derived at the outset had (B.10a) been integrated over $\widehat{\mathcal{C}}$ instead of $\mathcal{C}$. This would however have concealed the importance of the MDL and its associated enhanced dissipation. This dissipation is made good by a Poynting flux, $\boldsymbol{P} = \mu_0^{-1} \boldsymbol{E} \times \boldsymbol{B}$, across S, which has a non-fluctuating part from the mainstream wave of $\boldsymbol{p} = \mu_0^{-1} \boldsymbol{e} \times \boldsymbol{b}$. Its radial component, $p_r = sB_r^{\mathrm{m}} \zeta b_\phi$, passes energy to the MDL, part of which it transmits to the mantle, the remainder countering the ohmic losses of the MDL, which are $\mathrm{O}(|\mathcal{J}|^2/\sigma d_\eta)$ per unit area.

When $\boldsymbol{B} = \boldsymbol{B}^{\mathrm{m}} + \breve{\boldsymbol{b}}$ is substituted into (B.12a) and $\mathcal{F}_\phi$ is ignored (see above), the terms quadratic in $\boldsymbol{B}^{\mathrm{m}}$ disappear by (B.10f). The terms linear in $\breve{\boldsymbol{b}}$ give

$$\mu_0 \rho_0 \widehat{A} s^2 \frac{\partial \zeta}{\partial t} = \frac{\partial}{\partial s} \left[s \int_{\mathcal{C}(s)} (B_\phi^{\mathrm{m}} b_s + B_s^{\mathrm{m}} b_\phi) \mathrm{d}a \right] + \frac{r_o s^2}{z_1} \oint (B_\phi^{\mathrm{m}} b_r + B_r^{\mathrm{m}} \overline{h}_\phi)_{\mathcal{N}\&\mathcal{S}} \, \mathrm{d}\phi, \tag{B.13a}$$

$$\widehat{\Gamma}_z^M(t) = -\mu_0^{-1} \oint_{\mathrm{S}} s(B_\phi^{\mathrm{m}} b_r + B_r^{\mathrm{m}} \widehat{b}_\phi) \mathrm{d}a. \tag{B.13b}$$

Further progress depends on being able to re-express $\boldsymbol{b}$ and $\widehat{b}_\phi$ in terms of ζ. This requires application of EM theory only. As ohmic diffusion can be ignored in the mainstream core, and as the wave amplitude is small,

$$\boldsymbol{e} = -\boldsymbol{v} \times \boldsymbol{B}^{\mathrm{m}} - \boldsymbol{V}^{\mathrm{m}} \times \boldsymbol{b}. \tag{B.14a}$$

The emf $\boldsymbol{V}^{\mathrm{m}} \times \boldsymbol{b}$ appears to be somewhat smaller than $\boldsymbol{v} \times \boldsymbol{B}^{\mathrm{m}}$ in the geophysical context. Their ratio is of order $A^{\mathrm{m}}[b/v\sqrt{(\mu_0 \rho_0)}]^{-1}$, where A is the Alfvén number (17d), for which we previously estimated 0.01. As in an Alfvén wave, $v = \mathrm{O}[b/\sqrt{(\mu_0 \rho_0)}]$, so that $\boldsymbol{V}^{\mathrm{m}} \times \boldsymbol{b}$ is only about 1% of $\boldsymbol{v} \times \boldsymbol{B}^{\mathrm{m}}$. This, combined with the fact that the inclusion of $\boldsymbol{V}^{\mathrm{m}} \times \boldsymbol{b}$ in $\boldsymbol{e}$ adds severe complications, encourages the neglect of this emf. Its retention would invalidate (25). After abandoning $\boldsymbol{V}^{\mathrm{m}} \times \boldsymbol{b}$, we have

$$\boldsymbol{e} = -\boldsymbol{v} \times \boldsymbol{B}^{\mathrm{m}}, \quad \partial_t \boldsymbol{b} = \boldsymbol{\nabla} \times (\boldsymbol{v} \times \boldsymbol{B}^{\mathrm{m}}) = sB_s^{\mathrm{m}} \partial_s \zeta \mathbf{1}_\phi - \zeta \partial_{1\phi} \boldsymbol{B}^{\mathrm{m}}, \tag{B.14b,c}$$

the latter being the induction equation given by the former and Faraday's law ($\partial_t \boldsymbol{b} = -\boldsymbol{\nabla} \times \boldsymbol{e}$); in (B.14c), $\partial_{1\phi}$ means differentiation with respect to ϕ holding the unit

vectors fixed. More explicitly, the cylindrical components of (B.14c) are

$$\frac{\partial b_s}{\partial t}=-\zeta\frac{\partial B_s^{\rm m}}{\partial\phi},\quad \frac{\partial b_\phi}{\partial t}=sB_s^{\rm m}\frac{\partial\zeta}{\partial s}-\zeta\frac{\partial B_\phi^{\rm m}}{\partial\phi},\quad \frac{\partial b_z}{\partial t}=-\zeta\frac{\partial B_z^{\rm m}}{\partial\phi}. \tag{B.14d,e,f}$$

Its spherical components are

$$\frac{\partial b_r}{\partial t}=-\zeta\frac{\partial B_r^{\rm m}}{\partial\phi},\quad \frac{\partial b_\theta}{\partial t}=-\zeta\frac{\partial B_\theta^{\rm m}}{\partial\phi},\quad \frac{\partial b_\phi}{\partial t}=sB_s^{\rm m}\frac{\partial\zeta}{\partial s}-\zeta\frac{\partial B_\phi^{\rm m}}{\partial\phi}. \tag{B.14g,h,i}$$

In taking the time derivative of (B.13a), we may set $\partial_t\boldsymbol{B}^{\rm m}=\boldsymbol{0}$, as already noted. Other simplifications arise because, by (B.14d,e),

$$B_\phi^{\rm m}\frac{\partial b_s}{\partial t}+B_s^{\rm m}\frac{\partial b_\phi}{\partial t}=s(B_s^{\rm m})^2\frac{\partial\zeta}{\partial s}-\frac{\partial}{\partial\phi}[\zeta B_s^{\rm m}B_\phi^{\rm m}], \tag{B.14j}$$

the last term of which vanishes on integration over ϕ, as does the last term in

$$B_\phi^{\rm m}\frac{\partial b_r}{\partial t}+B_r^{\rm m}\frac{\partial b_\phi}{\partial t}=sB_r^{\rm m}B_s^{\rm m}\frac{\partial\zeta}{\partial s}-\frac{\partial}{\partial\phi}[\zeta B_r^{\rm m}B_\phi^{\rm m}], \tag{B.14k}$$

obtained from (B.14g,i). Recalling that $\breve{b}_\phi=b_\phi+b'_\phi$, we then obtain the wave equation in the form

$$\frac{\partial^2\zeta}{\partial t^2}=\frac{1}{s^2\widehat{A}(s)}\frac{\partial}{\partial s}\left[s^2\widehat{A}(s)V_{\rm A}^2(s)\frac{\partial\zeta}{\partial s}\right]+\widehat{N}(s)s\frac{\partial\zeta}{\partial s}+K(s,t), \tag{B.15a}$$

where (24d) defines $\widehat{N}(s)$; the torsional wave velocity, $V_{\rm A}(s)$, is given below (24c) and

$$K(s,t)=\frac{r_o}{\mu_0\rho_0\widehat{A}z_1}\oint[B_r^{\rm m}\partial_t b'_\phi]_{\widehat{\mathcal{N}}\&\widehat{\mathcal{S}}}\,{\rm d}\phi. \tag{B.15b}$$

For other ways of deriving the wave equation, see Braginsky (1970), Roberts and Soward (1972) and Jault (2003), who also includes mantle topography. The results of these investigations differ from the one given here.

Our derivation of (B.15a) has confirmed a conclusion adumbrated in section 3.2: the canonical (25) lacks $\widehat{N}(s)$; it also lacks $K(s,t)$. Because

$$\widehat{N}(s)\sim V_A^2(r_o)/z_1^2\sim -V_A^2(r_0)\widehat{A}'(s)/r_o\widehat{A}(s),\quad \text{for } s\to r_o, \tag{B.15c}$$

the singularity of (B.15a) at $s=r_o$ arises only from $K(s,t)$. This term did not appear in the simplified discussion of section 3.2 as it was deeply hidden in (23g,h). Despite first appearances, (B.15a) is a homogeneous equation, because b'_ϕ and therefore K is a linear functional of $\zeta(s,t)$. A more convenient form of (B.15a) replaces b'_ϕ by the actual field $\widehat{b}_\phi$ on S, by the substitution $\boldsymbol{b}'=\breve{\boldsymbol{b}}-\boldsymbol{b}$, giving

$$\frac{\partial^2\zeta}{\partial t^2}=\frac{1}{s^2\widehat{A}(s)}\frac{\partial}{\partial s}\left[s^2\widehat{A}(s)V_{\rm A}^2(s)\frac{\partial\zeta}{\partial s}\right]+\widehat{H}(s)\zeta+L(s,t), \tag{B.15d}$$

where

$$\widehat{H}(s)=\frac{r_o}{\mu_0\rho_0\widehat{A}z_1}\oint[B_r^{\rm m}\partial_\phi B_\phi^{\rm m}]_{\widehat{\mathcal{N}}\&\widehat{\mathcal{S}}}\,{\rm d}\phi,\quad L(s,t)=\frac{r_o}{\mu_0\rho_0\widehat{A}z_1}\oint[B_r^{\rm m}\partial_t\breve{b}_\phi]_{\widehat{\mathcal{N}}\&\widehat{\mathcal{S}}}\,{\rm d}\phi. \tag{B.15e,f}$$

Except for L, the coefficients in (B.15d–f) are immediately given by $\boldsymbol{B}^{\mathrm{m}}$ (assumed known). It is more troublesome to determine L.

On multiplying (B.15d) by $\rho_0 s^2 \widehat{A}(s)$ and integrating over s, it is seen that, for the torque on the core,

$$\partial_t \breve{\Gamma}_z^M = \int_0^{r_o} \rho_0 s^2 \widehat{A}[\widehat{H}(s)\zeta + L(s,t)]\mathrm{d}s. \tag{B.15g}$$

The same result apart from sign is obtained from (B.14g) and the time derivative of (B.13b), as required by conservation of the total angular momentum: $\breve{M}_z + \widehat{M}_z$.

We first look at consequences of ignoring mantle conduction, which implies the field in the mantle is a potential field. We write its principal and wave parts as $\boldsymbol{B}^{\mathrm{m}*}$ and $\boldsymbol{b}^*$, where

$$\partial_t \boldsymbol{b}^* = -\boldsymbol{\nabla} u, \quad \boldsymbol{B}^{\mathrm{m}*} = -\boldsymbol{\nabla} W. \tag{B.16a,b}$$

and

$$\nabla^2 u = 0, \quad \nabla^2 W = 0, \quad \text{and} \quad u, W \to 0, \quad \text{for } r \to \infty. \tag{B.16c,d,e}$$

The mantle fields are uniquely determined from the core fields by

$$b_r^* = \breve{b}_r, \quad B_r^{\mathrm{m}*} = \breve{B}_r^{\mathrm{m}}, \quad \text{on } \widehat{\mathrm{S}}. \tag{B.16f,g}$$

These radial components are identical to b_r and B_r^{m} on S, below the MDL, and in fact, by (20a), all components of $\breve{\boldsymbol{B}}^{\mathrm{m}}$ are continuous through the MDL, although $\boldsymbol{b}_{\mathrm{H}}^*(\widehat{\mathrm{S}}) \neq \boldsymbol{b}_{\mathrm{H}}(\mathrm{S})$, the discontinuity determining $\mathcal{J}$. Since $\widehat{\boldsymbol{\Gamma}}^M = \boldsymbol{0}$ when the mantle is insulating, the integral (B.15g) of $\widehat{H}\zeta + L$ over $\widehat{\mathrm{S}}$ vanishes. Nevertheless $\widehat{H}\zeta + L$ is nonzero on $\widehat{\mathrm{S}}$. This is because angular momentum can, and generally will, be transported from one geostrophic cylinder to another by the potential field, as already noted in section 8.3. Because the field strength is so much weaker in the mantle than the core, it is likely that this coupling is dwarfed by the local coupling of adjacent cylinders within the core, except possibly near the core equator. For the same reason, it may be speculated that L could be omitted without seriously marring the accuracy of solutions of (B.15d). Though this would remove the main practical obstacle in solving (B.15d) simply, it also, by eliminating the angular momentum transfer in the mantle, upsets the angular momentum balance of the core, so that (B.18h) below is no longer true. In appendix C, this is demonstrated by an example in which $\widehat{H}$ too has only a small effect. Nevertheless, we shall see below that the surface terms $\widehat{H}$ and L are influential for a conducting mantle.

There are two cases in which it is easy to make progress. First, if $\boldsymbol{B}^{\mathrm{m}}(=\overline{\boldsymbol{B}}^{\mathrm{m}})$ is axisymmetric and we ignore the singularity at $s=0$ of (B.15d), then (B.14g,h) show that $\overline{\boldsymbol{b}} = \overline{b}_\phi \boldsymbol{1}_\phi$ is entirely zonal, so that, by (B.16f), $\overline{b}_r = 0$ on the CMB. Therefore, $\overline{\boldsymbol{b}}^* \equiv \boldsymbol{0}$ and $\overline{b}_\phi^* = 0$ on $\widehat{\mathrm{S}}$, implying that $L=0$; similarly $\overline{B}_\phi^{\mathrm{m}} = 0$ on $\widehat{\mathrm{S}}$ so that $\widehat{H} = 0$. Second,

$$\zeta(s,t) = \zeta_0 = \text{constant} \tag{B.17a}$$

is, for any $\widehat{\boldsymbol{B}}^{\mathrm{m}}$, a solution of (B.15d). (Note: despite the constancy of ζ, generally $\boldsymbol{b}$ is time dependent through the asymmetry of $\boldsymbol{B}^{\mathrm{m}}$.) When (B.17a) holds, (B.14g) shows that

$$\partial_r u = -\zeta_0 \partial_{r\phi}^2 W \quad \text{on } r = r_o. \tag{B.17b}$$

Therefore, everywhere in $\widehat{\mathrm{V}}$,

$$u = -\zeta_0 \partial_\phi W \quad \text{so that } \partial_t \boldsymbol{b}^* = -\zeta_0 \partial_{1\phi} \boldsymbol{B}^{\mathrm{m}*}, \tag{B.17c,d}$$

giving $\widehat{H}\zeta_0 + L = 0$. We call this mode "exceptional". Its physical significance is that the system is neutrally stable with respect to a transformation $\zeta \to \zeta +$ constant, because so far coupling between mantle and core has been excluded, i.e. ζ is arbitrary to an additive constant. There is no MDL for the exceptional mode for which, as (B.17d) shows,

$$\boldsymbol{b}^*(s, \phi, z, t) = \boldsymbol{B}^{\mathrm{m}*}(s, \phi - \zeta_0 t, z). \tag{B.17e}$$

The added ζ_0 makes the potential field co-rotate with the core. For other normal modes however (B.14g) gives

$$b_r^* = B_r^*(s, \phi - \zeta(s)\mathrm{e}^{-\mathrm{i}\omega t}, z), \tag{B.17f}$$

and, because of the s-dependence of ζ, there is no reason to expect (B.17f) will create a potential field, $\boldsymbol{b}^*$ on $\widehat{\mathrm{S}}$ that is continuous with $\boldsymbol{b}$ on S. This is even clearer when $\overline{\boldsymbol{B}}^{\mathrm{m}}$ is axisymmetric; then $\overline{\boldsymbol{b}}^* \equiv \boldsymbol{0}$ but b_ϕ is generally nonzero on S. This shows that an MDL generally exists at the CMB, together with its enhanced ohmic dissipation. As indicated below (B.1b), the total dissipation increases by a factor of order $r_o/\sqrt{(\eta\omega)}$, which is significant but not large enough to vitiate the following argument which is valid only to leading order in ε.

We seek normal mode solutions of (B.15d) in which $\zeta(s, t) \to \zeta(s)\mathrm{e}^{-\mathrm{i}\omega t}$, so that

$$\frac{\mathrm{d}}{\mathrm{d}s}\left[s^2 \widehat{A}(s) V_{\mathrm{A}}^2 \frac{\mathrm{d}\zeta}{\mathrm{d}s}\right] + \omega^2 s^2 \widehat{A}(s)\zeta = s^2 \widehat{A}(s)\widehat{H}(s)\zeta + \frac{s^2}{\mu_0 \rho_0 z_1} \oint [B_r^{\mathrm{n}} \partial_t \overline{h}_\phi]^{\widehat{\ }}_{\mathcal{N}\&\mathcal{S}} \mathrm{d}\phi. \tag{B.18a}$$

As shown in appendix D, all solutions of (B.15d) for any axisymmetric field, $\overline{\boldsymbol{B}}^{\mathrm{m}}$, are singular. We exclude that case here, and can then assume that ζ is bounded at $s = r_o$ *and* $s = 0$. [If we ignore the singular $\zeta(0)$ for $\overline{\boldsymbol{B}}^{\mathrm{m}}$, the terms below in $Z_{\alpha,\beta}$ do not appear because $\overline{\boldsymbol{b}}^* \equiv \boldsymbol{0}$.] When the mantle is an insulator, (B.15d) defines a self-adjoint eigenvalue problem. To see this, one proceeds in the usual manner: Let ζ_α and ζ_β be two eigenfunctions, It follows from (B.18a) that

$$\omega_\alpha^2 \int_0^{r_o} s^2 \widehat{A}(s)\zeta_\alpha \zeta_\beta \mathrm{d}s = \int_0^{r_o} s^2 \widehat{A}(s) V_A^2 \frac{\mathrm{d}\zeta_\alpha}{\mathrm{d}s}\frac{\mathrm{d}\zeta_\beta}{\mathrm{d}s}\mathrm{d}s + \frac{1}{\mu_0\rho_0}\left[\oint_{\widehat{\mathrm{S}}} s B_r^{\mathrm{m}} \partial_\phi B_\phi^{\mathrm{m}}\, \zeta_\alpha \zeta_\beta \mathrm{d}s + Z_{\alpha,\beta}\right], \tag{B.18b}$$

where, by the same argument as was used to establish the equivalence of (B.13a,b),

$$Z_{\alpha,\beta} = \oint_{\widehat{\mathrm{S}}}\left[\frac{s^2}{z_1}\zeta_\beta \oint [B_r^{\mathrm{m}} \partial_t \overline{h}_{\alpha,\phi}]^{\widehat{\ }}_{\mathcal{N}\&\mathcal{S}} \mathrm{d}\phi\right]\mathrm{d}s = \oint_{\widehat{\mathrm{S}}} s B_r^{\mathrm{m}} \zeta_\beta\, \partial_t \overline{h}_{\alpha,\phi}\, \mathrm{d}a. \tag{B.18c}$$

Using (B.14g) and (B.16a,f), we obtain

$$\begin{aligned} Z_{\alpha,\beta} &= -\oint_{\widehat{\mathrm{S}}} B_r^{\mathrm{n}} \zeta_\beta\, \partial_\phi u_\alpha\, \mathrm{d}a \\ &= \oint_{\widehat{\mathrm{S}}} (\zeta_\beta \partial_\phi B_r^{\mathrm{n}}) u_\alpha\, \mathrm{d}a = -\oint_{\widehat{\mathrm{S}}} u_\alpha \partial_t b_{\beta,r}\, \mathrm{d}a = -\oint_{\widehat{\mathrm{S}}} u_\alpha \partial_t b_{\beta,r}^*\, \mathrm{d}a = \oint_{\widehat{\mathrm{S}}} u_\alpha \partial_r u_\beta\, \mathrm{d}a. \end{aligned} \tag{B.18d}$$

Therefore it follows from (B.16c,e) and Green's theorems that

$$Z_{\alpha,\alpha} = -\oint_{\widehat{\mathrm{S}}} u_\alpha \boldsymbol{n}\cdot\nabla u_\alpha \,\mathrm{d}a = -\int_{\widehat{\mathrm{V}}} (\nabla u_\alpha)^2 \,\mathrm{d}v = \omega_\alpha^2 \int_{\widehat{\mathrm{V}}} b^{*2}\,\mathrm{d}v, \tag{B.18e}$$

$$Z_{\alpha,\beta} - Z_{\beta,\alpha} = -\oint_{\widehat{\mathrm{S}}} \boldsymbol{n}\cdot(u_\alpha\nabla u_\beta - u_\beta\nabla u_\alpha)\mathrm{d}a = -\int_{\widehat{\mathrm{V}}} (u_\alpha\nabla^2 u_\beta - u_\beta\nabla^2 u_\alpha)\mathrm{d}v = 0. \tag{B.18f}$$

This establishes that (B.18a) defines a self-adjoint eigenvalue problem, that ω^2 is real and that, for $\omega_\alpha \neq \omega_\beta$, the eigenfunctions are orthogonal:

$$\int_0^{r_o} s^2 \widehat{A}(s)\zeta_\alpha\zeta_\beta \,\mathrm{d}s = 0. \tag{B.18g}$$

On taking ζ_β to be the exceptional mode ζ_0, (B.18g) shows that the angular momentum of every other mode vanishes:

$$M_{z,\alpha} = \int_0^{r_o} s^2 \widehat{A}(s)\zeta_\alpha(s)\mathrm{d}s = 0. \quad \text{for all } \alpha \neq 0. \tag{B.18h}$$

Taken to the next order in ε, this argument shows that ω has an $\mathrm{O}(\varepsilon)$ imaginary part.

Suppose next that the mantle is electrically conducting. The core and mantle are then linked together as one system of fixed total angular momentum $\boldsymbol{M}+\widehat{\boldsymbol{M}}$. Assume, as in section 8.2, that conduction is confined to a layer at the bottom of the mantle of thickness d, above which the mantle is insulating. Although the general results (B.15a–g) continue to apply, L now depends on the mantle conductivity and how it is modeled. For simplicity, we shall adopt the thin layer approximation developed in section 8.2, despite its possible limitations. A new notation is required: $\widehat{\boldsymbol{b}}$ will be the field within the conducting layer, and $\boldsymbol{b}^* = -\nabla w^*$ will be the potential field in the insulating region above it.

The thin layer approximation (52d) gives

$$\widehat{\boldsymbol{b}}_{\mathrm{H}} = \boldsymbol{b}^*_{\mathrm{H}} + \mu_0\widehat{\Sigma}(\mathbf{1}_r \times \widehat{\boldsymbol{e}}_{\mathrm{H}} + sB_r^{\mathrm{m}}\widehat{\zeta}\mathbf{1}_\phi), \quad \text{on } r = r_o, \tag{B.19a}$$

where $\widehat{\zeta}$ $(= \widehat{\Omega})$ is the angular velocity of the mantle. Appendix D contains an analysis of the MDL on the CMB. Assuming that the Elsasser number at the CMB is small, it is shown there that,

$$\widehat{\boldsymbol{b}}_{\mathrm{H}} + \mu_0\Sigma\,\mathbf{1}_r\times\widehat{\boldsymbol{e}}_{\mathrm{H}} = \boldsymbol{b}_{\mathrm{H}} + \mu_0\Sigma\,\mathbf{1}_r\times\boldsymbol{e}_{\mathrm{H}} \quad \text{on } r = r_o, \tag{B.19b}$$

where Σ is the (complex) core conductance. Both $\widehat{\boldsymbol{b}}_{\mathrm{H}}$ and $\widehat{\boldsymbol{e}}_{\mathrm{H}}$ can be obtained from (B.19a,b) but only $\widehat{\boldsymbol{b}}_{\mathrm{H}}$ is needed to evaluate L and $\widehat{\boldsymbol{\Gamma}}^M$. Using also (B.13d),

$$\widehat{\boldsymbol{b}}_{\mathrm{H}} = \Upsilon\boldsymbol{b}^*_{\mathrm{H}} + \widehat{\Upsilon}\,[\boldsymbol{b}_{\mathrm{H}} - \mu_0\Sigma s B_r^{\mathrm{m}}(\zeta - \widehat{\zeta})\mathbf{1}_\phi] \quad \text{on } r = r_o, \tag{B.19c}$$

where $\boldsymbol{b}_{\mathrm{H}}$ is given by (B.14c) and

$$\Upsilon = \frac{\Sigma}{\Sigma+\widehat{\Sigma}}, \quad \widehat{\Upsilon} = \frac{\widehat{\Sigma}}{\Sigma+\widehat{\Sigma}} = 1-\Upsilon, \quad \Upsilon\widehat{\Sigma} = \widehat{\Upsilon}\Sigma = \frac{\Sigma\widehat{\Sigma}}{\Sigma+\widehat{\Sigma}}. \tag{B.19d,e,f}$$

According to (B.19a,b), $|\Upsilon|$ and $|\widehat{\Upsilon}|$ are approximately the fractions of the total ohmic dissipation, due to the MDL and the mantle, respectively.

We now use (B.19c) to transform (B.15d) into a form that makes the effects of mantle conduction more apparent:

$$\widehat{H}(s)\zeta + L(s,t) = \widehat{H}_m(s)\zeta + \widehat{N}_m(s)s\partial_s\zeta + L_m(s,t) - \widehat{D}(s)\partial_t(\zeta - \widehat{\zeta}), \tag{B.20a}$$

where, by (B.14c),

$$\widehat{H}_m = \Upsilon\widehat{H}, \quad \widehat{N}_m = \widehat{\Upsilon}\,\widehat{N}, \quad L_m = \widehat{\Upsilon}\,L, \quad \widehat{D}(s) = \frac{r_o s}{\rho_0 \widehat{A} z_1}\,\Upsilon\,\widehat{\Sigma}\oint[(B_r^{\mathrm{m}})^2]_{\mathcal{N}\&\mathcal{S}}\,\mathrm{d}\phi. \tag{B.20b,c,d}$$

Substitution into (B.15d–f) gives

$$\frac{\partial^2\zeta}{\partial t^2} + \widehat{D}\frac{\partial}{\partial t}(\zeta - \widehat{\zeta}) = \frac{1}{s^2\widehat{A}}\frac{\partial}{\partial s}\left[s^2\widehat{A}V_A^2\frac{\partial\zeta}{\partial s}\right] + \widehat{H}_m\zeta + \widehat{N}_m s\partial_s\zeta + L_m. \tag{B.21a}$$

Of particular interest is the term in $\widehat{D}$ on the left-hand side of (B.21a), which couples the wave to the mantle and leads to ohmic loss. To derive the equation of motion of the mantle,

$$\widehat{C}\partial_t\widehat{\zeta} = \widehat{\Gamma}_z^M, \tag{B.21b}$$

we must evaluate $\widehat{\Gamma}_z^M$. Knowledge of b_ϕ^* is not required since the field above the conducting layer does not contribute. By (B.15g) and (B.20a),

$$\frac{\partial\widehat{\Gamma}_z^M}{\partial t} = \Upsilon\widehat{\Sigma}\oint_{\widehat{\mathrm{S}}} s^2(B_r^{\mathrm{m}})^2\frac{\partial}{\partial t}(\zeta - \widehat{\zeta})\mathrm{d}a - \frac{1}{\mu_0}\oint_{\widehat{\mathrm{S}}} sB_r^{\mathrm{m}}\left[\widehat{\Upsilon}sB_s^{\mathrm{m}}\frac{\partial\zeta}{\partial s} + \Upsilon\zeta\frac{\partial B_\phi^{\mathrm{m}}}{\partial\phi}\right]\mathrm{d}a. \tag{B.21c}$$

Consistent with angular momentum conservation, (B.20a–c) imply that $\partial_t^2(\widehat{C}\,\widehat{\zeta} + M_z) = 0$. The first of the simplifications, mentioned below (B.16f,g), concerns axisymmetric $\overline{\boldsymbol{B}}^{\mathrm{m}}$ but, though $\overline{b}_\phi^* = 0$ again holds, $\widehat{\overline{b}}_\phi$ is generally nonzero and generates a torque $\widehat{\Gamma}_z^M$. The second simplification applies in the sense that $\zeta = \widehat{\zeta} =$ constant satisfies (B.16f,g). Now see section 8.3.

Everything so far in this appendix has ignored the existence of the SIC. We now aim to rectify that omission, at least partially. The SIC is magnetically coupled to the mantle and FOC, so that $\boldsymbol{M} + \widehat{\boldsymbol{M}} + \widetilde{\boldsymbol{M}}$ is fixed, as in (28e). Of serious concern is the possibility of intense magnetic coupling of the SIC to the fluid in the TC. To simplify the discussion, we shall totally ignore the MDL on the CMB and core-mantle coupling.

As pointed out in section 3.2, there are now two geostrophic cylinders, $\mathcal{C}^N$ and $\mathcal{C}^S$, to the north and south of the SIC; $\mathcal{C}^N$ is closed by spherical caps $\widehat{\mathcal{N}}$ on the CMB and $\widetilde{\mathcal{S}}$ on the ICB, defined by $0 < \theta_1(s) = \sin^{-1}(s/r_o) < \frac{1}{2}\pi$ and $0 < \theta_2(s) = \sin^{-1}(s/r_i) < \frac{1}{2}\pi$, respectively; see figure 3(b). The area of $\mathcal{C}^N$ is $\widetilde{A} = 2\pi s z_{12}$, where $z_{12} = z_1 - z_2$ and $z_2 = \sqrt{(r_i^2 - s^2)}$. A geostrophic average on $\mathcal{C}^N$ is now defined by, for example,

$$\{\!\{V_\phi\}\!\}^N = \frac{1}{\widetilde{A}(s)}\int_{\mathcal{C}^N(s)} V_\phi\,\mathrm{d}a, \tag{B.22}$$

which replaces (22a) for $s < r_i$.

We shall focus on the coupling across $\widetilde{\mathcal{S}}$. The field, $\widetilde{\boldsymbol{b}}$ and electric current, $\widetilde{\boldsymbol{j}}$, in the SIC generated by the torsional wave are significant only in a layer at the top of the SIC whose thickness, $\widetilde{d}_\eta = (\frac{1}{2}\omega_A\mu_0\widetilde{\sigma})^{-1/2}$, is of order 10 km. As this is small compared with the thickness, r_i, of the conducting region, the high frequency approximation of section 8.2 is an accurate replacement for the thin layer approximation.

The boundary layer at the bottom of the FOC is quite different from the one at its top because the Elsasser number, Λ, at the ICB is probably O(1) or greater. The boundary layer is analyzed in appendix D, where its horizontal electric and magnetic fields are joined continuously to $\widetilde{\boldsymbol{e}}_{\mathrm{H}}$ and $\widetilde{\boldsymbol{b}}_{\mathrm{H}}$ of the SIC using (53g). Appendix D deals with general Λ, but concentrates on $\Lambda \gg 1$, for which (D.12f) holds. Transformed from the SIC reference frame, it is

$$\widetilde{b}_\phi = b_\phi + \Lambda^{-1/2}\mu_0\widetilde{\Sigma} s B_r^{\mathrm{m}}(\zeta^N - \widetilde{\zeta}), \quad \text{on } r = r_i, \tag{B.23}$$

where $\widetilde{\zeta}$ is the angular velocity of the SIC and ζ^N refers to $\mathcal{C}^N$. Following the same procedure as before, we find that

$$\frac{\partial^2 \zeta^N}{\partial t^2} + \widetilde{D}(s)\frac{\partial}{\partial t}(\zeta^N - \widetilde{\zeta}) = \frac{1}{s^2\widetilde{A}(s)}\frac{\partial}{\partial s}\left[s^2\widetilde{A}(s)V_A^{N2}(s)\frac{\partial \zeta^N}{\partial s}\right] + \widetilde{H}_m(s)\zeta^N, \tag{B.24a}$$

where $V_A^{N2}(s) = \{\!\{V_{\mathrm{A}}^2\}\!\}^N$ and

$$\widetilde{D}(s) = \frac{r_i s}{\rho_0 \widetilde{A} z_2}\Lambda^{-1/2}\widetilde{\Sigma}\oint [(B_r^{\mathrm{m}})^2]_{\widetilde{\mathcal{S}}}\,\mathrm{d}\phi, \quad \widetilde{H}_m(s) = -\frac{r_i}{\mu_0\rho_0\widetilde{A}z_2}\oint [B_r^{\mathrm{m}}\partial_\phi B_\phi^{\mathrm{m}}]_{\widetilde{\mathcal{S}}}\,\mathrm{d}\phi. \tag{B.24b,c}$$

The equations governing ζ^S in $\mathcal{C}^S$ are similar. The equation of motion of the SIC is

$$\widetilde{C}\partial_t\widetilde{\zeta} = \widetilde{\Gamma}_z^M, \tag{B.24d}$$

where the torque on the SIC follows from (B.23), which gives

$$\frac{\partial \widetilde{\Gamma}_z^M}{\partial t} = \Lambda^{-1/2}\widetilde{\Sigma}\left[\int_{\widetilde{\mathcal{S}}}(sB_r^{\mathrm{m}})^2\frac{\partial}{\partial t}(\zeta^N - \widetilde{\zeta})\mathrm{d}a + \int_{\widetilde{\mathcal{N}}}(sB_r^{\mathrm{m}})^2\frac{\partial}{\partial t}(\zeta^S - \widetilde{\zeta})\mathrm{d}a\right] + \frac{1}{\mu_0}\oint_{\widetilde{\mathrm{S}}} sB_r^{\mathrm{m}}\frac{\partial B_\phi^{\mathrm{m}}}{\partial \phi}\,\zeta\,\mathrm{d}a, \tag{B.24e}$$

where the first two integrals on the right-hand side are over the northern and southern hemispheres of the ICB. Now see section 8.4.

Derivation of (23b) *and* (24b)

The following gives steps leading from (23a) to (23b). Equation (11c) shows that

$$\mu_0\partial_t\{\!\{(\boldsymbol{J}\times\boldsymbol{B})\}\!\}_\phi = \{\!\{(\nabla\times\boldsymbol{\mathcal{Q}})\times\boldsymbol{B} + (\nabla\times\boldsymbol{B})\times\boldsymbol{\mathcal{Q}}\}\!\}_\phi, \quad \text{where } \boldsymbol{\mathcal{Q}} = \partial_t\boldsymbol{B}. \tag{B.25a,b}$$

Use the vector identity

$$(\nabla\times\boldsymbol{\mathcal{Q}})\times\boldsymbol{B} + (\nabla\times\boldsymbol{B})\times\boldsymbol{\mathcal{Q}} = \boldsymbol{B}\cdot\nabla\boldsymbol{\mathcal{Q}} + \boldsymbol{\mathcal{Q}}\cdot\nabla\boldsymbol{B} - \nabla(\boldsymbol{B}\cdot\boldsymbol{\mathcal{Q}}), \tag{B.25c}$$

the last term in which vanishes when (B.25c) is substituted into (B.25a) and the implied ϕ-integration is carried out. The induction equation (11g) can be written

$$\boldsymbol{\mathcal{Q}} = \boldsymbol{\mathcal{R}} + \boldsymbol{\mathcal{S}}, \quad \text{where } \boldsymbol{\mathcal{R}} = \nabla\times(\boldsymbol{v}\times\boldsymbol{B}), \quad \boldsymbol{\mathcal{S}} = \nabla\times(\boldsymbol{V}^{\mathrm{m}}\times\boldsymbol{B}) + \eta\nabla^2\boldsymbol{B}. \tag{B.25d,e,f}$$

When (B.25e) is substituted into (B.25c), and (B.14g–i) is used, it is found that

$$[\boldsymbol{B}\cdot\nabla\boldsymbol{\mathcal{R}} + \boldsymbol{\mathcal{R}}\cdot\nabla\boldsymbol{B}]_\phi = \left(\boldsymbol{B}\cdot\nabla + \frac{B_s}{s}\right)\left(s\frac{\partial\zeta}{\partial s}B_s\right) - \zeta\frac{\partial}{\partial\phi}\left(\boldsymbol{B}\cdot\nabla + \frac{B_s}{s}\right)B_\phi, \tag{B.25g}$$

the last term in which vanishes when (B.25g) is substituted into (B.25a). Insertion of (B.25d,g) into (B.25a) gives

$$\mu_0 \partial_t \{\!\{(\boldsymbol{J}\times\boldsymbol{B})\}\!\}_\phi = s\left[\alpha(s,t)\frac{\partial^2\zeta}{\partial s^2}+\beta(s,t)\frac{\partial\zeta}{\partial s}-R(s,t)\right], \tag{B.25h}$$

where α, β and R are given by (23c–e). Equations (23a,b) are now seen to be equivalent.

For the derivation of (24b), we first use the definition (22a) of the geostrophic average of any $X(s,\phi,z)$ to show that

$$\begin{aligned}\frac{1}{\widehat{A}}\frac{\partial}{\partial s}\{\!\{\widehat{A}X\}\!\} &= \frac{1}{\widehat{A}}\frac{\partial}{\partial s}\oint\int_{-z_1}^{z_1} Xs\,\mathrm{d}\phi\,\mathrm{d}z \\ &= \frac{1}{\widehat{A}}\oint\int_{-z_1}^{z_1}\left(s\frac{\partial X}{\partial s}+X\right)\mathrm{d}\phi\,\mathrm{d}z-\frac{s^2}{\widehat{A}z_1}\oint[X(s,\phi,z_1)+X(s,\phi,-z_1)]\mathrm{d}\phi.\end{aligned} \tag{B.26a}$$

Therefore, if $Y=X/s$,

$$\left\{\!\!\left\{\frac{\partial Y}{\partial s}\right\}\!\!\right\} = \frac{s}{\widehat{A}}\frac{\partial}{\partial s}\left\{\!\!\left\{\frac{\widehat{A}}{s}Y\right\}\!\!\right\}+\frac{s^2}{\widehat{A}z_1}\oint[Y(s,\phi,z_1)+Y(s,\phi,-z_1)]\mathrm{d}\phi. \tag{B.26b}$$

Now use (11d) to transform β, given by (23d) as follows

$$\beta(s,t) = \left\{\!\!\left\{\nabla\cdot(B_s\boldsymbol{B})+\frac{2B_s^2}{s}\right\}\!\!\right\} = \left\{\!\!\left\{\frac{\partial B_s^2}{\partial s}+\frac{1}{s}\frac{\partial(B_sB_\phi)}{\partial\phi}+\frac{\partial(B_sB_z)}{\partial z}+\frac{3B_s^2}{s}\right\}\!\!\right\}$$

$$= \left\{\!\!\left\{\frac{1}{s^2}\frac{\partial}{\partial s}\left(s^3B_s^2\right)\right\}\!\!\right\}+\frac{s}{\widehat{A}}\oint(B_sB_z)_{-z_1}^{z_1}\mathrm{d}\phi. \tag{B.26c}$$

Applying (B.26b) with $Y=B_s^2$. we simplify (B.26c) to

$$\beta(s,t) = \frac{1}{s^2\widehat{A}}\left(s^2\widehat{A}\{\!\{B_s^2\}\!\}\right)+\mu_0\rho_0 s\widehat{N}(s,t), \tag{B.26d}$$

where $\widehat{N}(s,t)$ is defined in (24d). Equation (24b) follows.

Appendix C: Solutions of the canonical wave equation

This appendix discusses solutions of (25). These are expressed as a sum of normal modes in which $\zeta\propto \mathrm{e}^{-\mathrm{i}\omega t}$. The self-adjoint form of (54) is

$$\frac{\mathrm{d}}{\mathrm{d}\xi}\left[L(\xi)V^2(\xi)\frac{\mathrm{d}\zeta}{\mathrm{d}\xi}\right]+c^2L(\xi)\zeta=0, \quad \text{where } L(\xi)=\xi^3(1-\xi^2)^{1/2}(\geq 0), \tag{C.1a,b}$$

and we have introduced non-dimensional variables by

$$s=r_o\xi, \quad V_A(s)=UV(\xi), \quad \omega=(U/r_o)c, \tag{C.1c,d,e}$$

U being a characteristic Alfvén velocity. Equation (C.1a) admits the exceptional solution

$$c = 0, \quad \zeta(\xi, t) = \zeta_0 = \text{constant}. \tag{C.1f,g}$$

For the non-exceptional solutions, an attractive alternative to (C.1a) is

$$\frac{\mathrm{d}M}{\mathrm{d}\xi} = L(\xi)\zeta, \quad \frac{\mathrm{d}\zeta}{\mathrm{d}\xi} = -\frac{c^2 M}{L(\xi)V^2(\xi)}, \tag{C.2a,b}$$

(Braginsky 1970). Thus M is the angular momentum of the wave about Oz. Because $L(0) = L(1) = 0$, (C.1a) has singular points at $\xi = 0$ and $\xi = 1$ that are regular, except in artificial cases. The solutions are physically meaningful only if ζ and M are bounded at these points. This requirement determines the eigenvalues c which are all real, as demonstrated in appendix B. For the non-exceptional eigensolutions, (C.2b) implies that

$$M(0) = 0, \quad M(1) = 0, \tag{C.2c,d}$$

the first of which shows, via (C.2b), that

$$M(\xi) = \int_0^\xi \xi^3 (1 - \xi^2)^{1/2} \zeta(\xi) \mathrm{d}\xi. \tag{C.2e}$$

Two conclusions can be drawn: (i) the exceptional eigensolution carries all the angular momentum, M, of the wave about Oz; (ii) except for that solution, every eigenfunction, ζ, has at least one zero within $0 < s < 1$. It follows from (C.2a) that, if $\zeta(0) \neq 0$, then $M \sim \mathrm{O}(\xi^4)$ for $\xi \to 0$, so that (C.2b) shows that $\mathrm{d}\zeta/\mathrm{d}\xi = \mathrm{O}(\xi)$, provided that $V(0) \neq 0$ but, if $V(0) = \mathrm{O}(\xi)$ for $\xi \to 0$, then $\mathrm{d}\zeta/\mathrm{d}\xi$ is singular at $\xi = 0$. The singularity at $\xi = 1$ is usually milder: if $\zeta(1) \neq 0$, (C.2a) shows that $M \sim \mathrm{O}((1-\xi)^{3/2})$ for $\xi \to 1$ so that, by (C.2b), $\mathrm{d}\zeta/\mathrm{d}\xi = \mathrm{O}((1-\xi)^2)$ provided that $V(1) \neq 0$ while, if $V(\xi) = \mathrm{O}((1-\xi)^{1/2})$, then $\mathrm{d}\zeta/\mathrm{d}\xi = \mathrm{O}(1-\xi)$.

Equation (C.1a) can be solved semi-analytically if V_A is constant; we take $V = 1$. On making the change of variables

$$\mu = \sqrt{(1 - \xi^2)}, \quad \zeta = (1 - \mu^2)^{-1/2} S_{m,n}(\mu), \tag{C.3a,b}$$

(C.1a) becomes the case $m = 1$, $\lambda_{m,n} = 2$ of the equation governing the well-studied angular oblate spheroidal wave functions, $S_{m,n}(\mu, c)$, which satisfy

$$\frac{\mathrm{d}}{\mathrm{d}\mu}\left[(1 - \mu^2)\frac{\mathrm{d}S_{m,n}}{\mathrm{d}\mu}\right] + \left(\lambda_{m,n} + c^2\mu^2 - \frac{m^2}{1 - \mu^2}\right) S_{m,n} = 0\,; \tag{C.3c}$$

see Chapter 21 of Abramowitz and Stegun (1953) or Chapter 30 of Olver *et al.* (2010). According to sub-paragraph 21.7.19 of the former $(1 - \mu^2)^{-1/2} S_{1.n}(\mu)$ is O(1) for $\mu \to 1$, i.e. $\zeta(\xi)$ is bounded for $\xi \to 0$ but, if n is even, $S_{1.n}$ is odd in μ, so that $\zeta(\xi)$ is $\mathrm{O}((1 - \xi^2)^{1/2})$ for $\xi \to 1$. Therefore only the odd n solutions are of interest and, for these, $\zeta(\xi)$ is O(1) for $\xi \to 1$; $n = 1$ is the exceptional solution.

In most contexts where (C.3c) arises, solutions $\lambda_{m,n}$ are sought for given c, but here the objective is inverted: to find c for given $\lambda_{m,n} = 2$. Solutions are required that are bounded at $\mu = 1$ (i.e. $\xi = 0$). If $c = 0$, then $S_{m,n}(\mu) = P_n^m(\mu)$ and $\lambda_{m,n} = n(n+1)$. For

Table C1. Eigenvalues c in the case $V=1$.

n	c	n	c
3	5.2759462	5	8.6300525
7	11.8698525	9	15.0693190
11	18.2494245	13	21.4186323
15	24.5810610	17	27.7389696
19	30.8937060	21	34.0461267

$n=m=1$, this gives the eigenfunction $S_{1,1}=(1-\mu^2)^{1/2}$, which recovers the exceptional solution (C.1f,g).

The first 10 non-exceptional eigenvalues ($n=3-21$, $m=1$) are listed in table C1. They were derived using programs devised by Zhang and Jin (1996) that are available on the web. Mode n has $\frac{1}{2}(n-1)$ zeros within the interval $0<\xi<1$.

It appears likely that, for any non-constant $V(\xi)$, the eigenvalues can be found only by numerical integration of (C.1a). The required solution should be bounded at both the singularities $s=0$ and $s=1$. The general solution of (C.1a) is a linear combination of two independent solutions:

$$\zeta(\xi)=a_1\zeta_1(\xi)+a_2\zeta_2(\xi). \tag{C.4a}$$

In most cases, one of the independent solutions, say $\zeta_1(\xi)$, is bounded at $\xi=1$ and the other is unbounded. Selecting therefore $a_2=0$, one seeks to express ζ_1 as a linear combination,

$$\zeta_1(\xi)=a_3\zeta_3(\xi)+a_4\zeta_4(\xi), \tag{C.4b}$$

where one of these solutions, say $\zeta_3(\xi)$, is bounded at $\xi=0$ and the other is unbounded. The eigencondition for c is then $a_4=0$. This method of solution fails completely if neither $\zeta_3(\xi)$ nor $\zeta_4(\xi)$ is bounded at $\xi=0$. Then the eigenvalue problem is non-integrable. The danger of this happening is real, as the following important example shows.

For all axisymmetric $\boldsymbol{B}$ ($=\bar{\boldsymbol{B}}$), the singularity of (C.1a) at $\xi=0$ is non-integrable because $V(0)=0$. To see this, let $V'(0)=c_0>0$ so that

$$V(\xi)=c_0\xi+\mathrm{O}(\xi^2), \quad \text{for } \xi\to 0. \tag{C.5a}$$

Solutions of (C.1a) are asymptotically equivalent as $\xi\to 0$ to those of

$$\frac{\mathrm{d}^2\zeta}{\mathrm{d}\xi^2}+\frac{5}{\xi}\frac{\mathrm{d}\zeta}{\mathrm{d}\xi}+\left(\frac{c}{c_0}\right)^2\frac{\zeta}{\xi^2}=0, \tag{C.5b}$$

an equation homogeneous in ξ. For $c>2c_0$, its solution is

$$\zeta=(2\pm \mathrm{i}c')\xi^{-2}\exp(\pm \mathrm{i}c'\log\xi), \quad M=\xi^2\exp(\mathrm{i}c'\log\xi), \tag{C.5c,d}$$

where $c'=\sqrt{[(c/c_0)^2-4]}$; if $c<2c_0$,

$$\zeta=(2\pm c'')\xi^{-2\pm c''}, \quad M=\xi^{2\pm c''}, \tag{C.5e,f}$$

Table C2. Eigenvalues c for the case (C.6b).

n	c	n	c
1	20.716312	2	34.579955
3	47.836658	4	60.875695
5	73.810609	6	86.687341
7	99.528169	8	112.345244
9	125.145771	10	137.934298

Table C3. Eigenvalues c for the augmented case (C.6b).

n	c	n	c
1	20.204870	2	34.269159
3	47.606276	4	60.690445
5	73.654746	6	86.552320
7	99.408780	8	112.238055
9	125.048391	10	137.844992

where $c'' = \surd[4 - (c/c_0)^2]$. Both ζs are unacceptably singular as $\xi \to 0$. The existence of this singularity was noted by Fearn and Proctor (1987) who surmised that it is logarithmic and can be removed by reinstating viscosity. This matter is taken up below. We now consider asymmetric $\boldsymbol{B}$ for which $V(0) \neq 0$. It may be worth noticing that the addition of an axisymmetric field to an asymmetric field, such as (C.6b) below, does not change its nonzero value of $V(0)$ and therefore does not re-introduce the singularities of totally axisymmetric $\bar{\boldsymbol{B}}$.

In the toroidal/poloidal representation,

$$\boldsymbol{B} = \boldsymbol{\nabla} \times (\mathcal{T}\boldsymbol{r}) + \boldsymbol{\nabla} \times \boldsymbol{\nabla} \times (\mathcal{P}\boldsymbol{r}), \tag{C.6a}$$

where $\boldsymbol{r}$ is the radius vector. If the mantle is an insulator, the toroidal scalar, $\mathcal{T}$, vanishes on $\widehat{\mathrm{S}}$ and the poloidal scalar, $\mathcal{P}$, is such that $\boldsymbol{B}$ is continuous with a source-free potential field in the mantle. A field that is totally toroidal but asymmetric can transmit torsional waves but, because $\mathcal{T}(r_o, \theta, \phi) = 0$, (C.1a) then has a singularity at $s = r_o$ that is generally non-integrable. We confine attention here to asymmetric poloidal fields, and focus on the particular case

$$\mathcal{P} = r(5 - 3r^2)\sin\theta\cos\phi, \tag{C.6b}$$

for which the external field is an equatorial dipole of unit strength, and

$$V^2(\xi) = \frac{2}{5}(61 - 62\xi^2 + 21\xi^4), \tag{C.6c}$$

so that $V^2(0) = 122/5$ and $V(1) = 2\surd 2$. Because these are both nonzero, the regular singularity of (C.1a) at $\xi = 0$ is as mild as the one at $\xi = 1$. The required solution and its derivative are required to be O(1) at both end points and this determines the

eigenvalues, the first 10 of which are listed in table C2 (labeled differently from table C1). Mode n has $n-1$ zeros of ζ within the interval $0<\xi<1$.

Appendix B points out that (25) is not the correct torsional wave equation when $\boldsymbol{B}$ is asymmetric and should be replaced by (B.15d). When (25) is augmented by the $\widehat{H}(s)$ of (B.15e), the eigenvalues for the example (C.6a) are reduced by roughly 2.5% for $n=1$, decreasing to 0.06% for $n=10$, See table C3. Augmentation of (25) by the $L(s, t)$ term of (B.15f) would require more labor than would be justified here, but a symptom from which the importance of the missing L term can be assessed is available. When L is assumed to be zero, (B.15d) fails to preserve angular momentum; (C.2d) is not satisfied. The magnitude of the error decreases with increasing n. In the case of (C.6b) it was found that, for solutions normalized by $\zeta(0)=1$, $|M(1)|$ decreases from about 5×10^{-3} for $n=1$ to 3×10^{-5} for $n=10$.

Finally, we return to the singularity of (C.1a) when $V(0)=0$ and (C.5a) holds. It was shown above that (C.1a)) then has no valid solutions, although numerical integration will often find c. This verisimilitude of success evaporates if the truncation level is increased, when it is found that the spurious "solution" becomes increasingly pathological near $\xi=0$, and the eigenvalues fail to converge. Fearn and Proctor (1987) speculated that the singularity can be removed by restoring viscous forces, see also Jault (1995).

It was shown by Roberts and Soward (1972) that, in dimensional variables, the principal effect of introducing viscosity, ν, is to transform

$$\frac{\partial^2\zeta}{\partial t^2} \quad \text{into} \quad \frac{\partial^2\zeta}{\partial t^2}+\frac{(\nu\Omega r_o)^{1/2}}{(r_o^2-s^2)^{3/4}}\frac{\partial\zeta}{\partial t} \tag{C.7a}$$

in (25). As already mentioned in appendix B, the additional term creates wave damping on the spin-up time scale $E^{1/2}\tau_\nu$, where E is the Ekman number (15b). Terms that are of order E are neglected in the transition (C.7a) but become significant near $s=0$, where they transform

$$\frac{\partial\zeta}{\partial t} \quad \text{into} \quad \frac{\partial\zeta}{\partial t}-\frac{\nu}{s}\frac{\partial\zeta}{\partial s} \tag{C.7b}$$

in (B.13a). The torsional wave equation that was previously asymptotic to (C.5b) for $\xi\to0$ becomes instead asymptotic to

$$\frac{\mathrm{d}^2\zeta}{\mathrm{d}\chi^2}+\left(5-\frac{\mathrm{i}\varsigma}{\chi^2}\right)\frac{1}{\chi}\frac{\mathrm{d}\zeta}{\mathrm{d}\chi}+\varsigma^2\frac{\zeta}{\chi^2}=0. \tag{C.7c}$$

We have here replaced (C.1c–e) by

$$s=[(\nu|\omega|)^{1/2}/\bar{V}_A'(0)]\chi, \quad \omega=\varsigma|\omega|, \tag{C.7d,e}$$

where $\bar{V}_A'(0)>0$ and we may anticipate that $\mathrm{Im}(\varsigma)<0$.

The method of dominant balance shows that two solutions of (C.7c) exist for which

$$\zeta_3(\xi)=1+\mathrm{O}(\chi^2), \quad \zeta_4(\xi)\sim\xi^{-2}\exp(-\mathrm{i}\varsigma/2\chi^2), \quad \text{for } \chi\to0. \tag{C.8a,b}$$

The unusual character of ζ_4 raises doubts about whether it is admissible; ζ_4 and all its derivatives, vanish as $\chi\to0$ when $\mathrm{Im}(\varsigma)<0$. If it is admitted, both solutions (C.8a,b) are bounded as $\chi\to0$, and a further boundary condition is needed to close the eigenvalue problem. This could be the rejection of ζ_3 or ζ_4. No attempt is made here to take the analysis further but it is plausible that, if $\zeta=\mathrm{O}(1)$ for $\xi=\mathrm{O}(1)$, then

$\zeta = \mathrm{O}(V_\mathrm{A}^2/\nu|\omega|) \gg 1$ for $\chi = \mathrm{O}(1)$. It is clear however that viscosity broadens the concept of what is physically acceptable for $s \to 0$.

Appendix D: Magnetic diffusion layers in the fluid core

Because of their time-dependence, torsional waves are coupled to the mantle and SIC by EH layers that differ from the quasi time-independent EH layers treated by, for example, Dormy *et al.* (2007) and Dormy and Soward (2007). This appendix generalizes their analysis.

The point was made in section 3.2 that the magnetostrophic approximation is valid only for large length scales: $\mathcal{L} \gg V_\mathrm{A}/\Omega$. This inequality is not satisfied by the thicknesses of the EH layers on the CMB and ICB considered in this appendix, for which the distinction between geostrophic and non-geostrophic motions becomes meaningless, and Coriolis forces again become significant. The fluid motions in the torsional waves are of the form (19a) only in the main body of the core, outside the diffusion layers. Using a terminology common in boundary layer theory, we call this the *mainstream*. Considering first the EH layer on the CMB, we use the mantle frame and write the mainstream velocity, electric field and magnetic field as $\boldsymbol{v}$, $\boldsymbol{e}$ and $\boldsymbol{b}$, where

$$\boldsymbol{v} = s(\zeta - \widehat{\zeta})\mathbf{1}_\phi, \quad \boldsymbol{e} = -\boldsymbol{v} \times \boldsymbol{B}^\mathrm{m}, \quad \partial_t \boldsymbol{b} = sB_s^\mathrm{m}\partial_s\zeta\mathbf{1}_\phi - (\zeta - \widehat{\zeta})\partial_{1\phi}\boldsymbol{B}^\mathrm{m}, \tag{D.1a,b,c}$$

and $\widehat{\zeta}$ is the mantle's angular velocity; as before the $_1$ in $\partial_{1\phi}$ means that the unit vectors are held fixed in the ϕ-differentiation.

The velocity, electric field, and magnetic field in the boundary layers will be denoted by $\boldsymbol{v} + \boldsymbol{v}'$, $\boldsymbol{e} + \boldsymbol{e}'$, and $\boldsymbol{b} + \boldsymbol{b}'$, so that the boundary layer parts, $\boldsymbol{v}'$, $\boldsymbol{e}'$ and $\boldsymbol{b}'$, vanish in the mainstream:

$$\boldsymbol{v}', \ \boldsymbol{e}', \ \boldsymbol{b}' \ \to 0, \quad \text{as } \xi \to \infty, \tag{D.1d}$$

where ξ is a stretched coordinate for the distance, $r_o - r$, from CMB. Therefore (suppressing the dependence of θ and ϕ)

$$\widehat{\boldsymbol{b}}(r_o) = \boldsymbol{b}(r_o) + \boldsymbol{b}'(r_o), \quad \text{etc.} \tag{D.1e}$$

The equations governing $\boldsymbol{v}'$, $\boldsymbol{e}'$ and $\boldsymbol{b}'$ are obtained by subtracting the equations governing the mainstream $\boldsymbol{v}$, $\boldsymbol{e}$ and $\boldsymbol{b}$ from the equations governing the total fields $\boldsymbol{v} + \boldsymbol{v}'$, $\boldsymbol{e} + \boldsymbol{e}'$ and $\boldsymbol{b} + \boldsymbol{b}'$, and by assuming $|\partial_r| \gg |\boldsymbol{\nabla}_\mathrm{H}|$. At leading order, the boundary layer is governed by

$$\rho_0(\partial_t \boldsymbol{v}'_\mathrm{H} + 2\Omega_r \mathbf{1}_r \times \boldsymbol{v}'_\mathrm{H}) = \mu_0^{-1} B_r^\mathrm{m} \partial_r \boldsymbol{b}'_\mathrm{H} + \rho_0 \nu \partial_r^2 \boldsymbol{v}'_\mathrm{H}, \tag{D.2a}$$

$$\partial_t \boldsymbol{b}'_\mathrm{H} = B_r^\mathrm{m} \partial_r \boldsymbol{v}'_\mathrm{H} + \eta \partial_r^2 \boldsymbol{b}'_\mathrm{H}. \quad \boldsymbol{e}'_\mathrm{H} = \mathbf{1}_r \times (B_r^\mathrm{m} \boldsymbol{v}' + \eta \partial_r \boldsymbol{b}')_\mathrm{H}. \tag{D.2b,c}$$

Solutions are sought that are proportional to $\exp(-\mathrm{i}\omega t)$. We introduce

$$\epsilon = \left|\frac{\omega}{2\Omega_r}\right| \ll 1, \quad \Lambda = \frac{B_r^{\mathrm{m}2}}{2|\Omega_r|\eta\mu_0\rho_0}, \quad \varsigma = \mathrm{sgn}(\omega), \quad \varpi = \mathrm{sgn}(\Omega_r), \tag{D.2d,e,f,g}$$

so that

$$\omega = \varsigma|\omega|, \quad \Omega_r = \varpi|\Omega_r|. \tag{D.2h,i}$$

We seek solutions of (D.2a,b) in the limit $\epsilon \to 0$.

We scale EM quantities to velocities and make r dimensionless by the transformations

$$r \to \left(\frac{\eta}{|\omega|}\right)^{1/2} r, \quad \boldsymbol{b}' \to \frac{B_r^{\mathrm{m}}}{(\eta|\omega|)^{1/2}}\boldsymbol{b}', \quad \boldsymbol{e}' \to B_r^{\mathrm{m}}\boldsymbol{e}', \quad \boldsymbol{j}' \to \sigma B_r^{\mathrm{m}}\boldsymbol{j}'. \tag{D.2j,k,l,m}$$

Equations (D.2a–c) become

$$-\mathrm{i}\varsigma\epsilon\boldsymbol{v}'_{\mathrm{H}} + \varpi\mathbf{1}_r \times \boldsymbol{v}'_{\mathrm{H}} = \Lambda\partial_r\boldsymbol{b}'_{\mathrm{H}} + \epsilon P_m\partial_r^2\boldsymbol{v}'_{\mathrm{H}}, \tag{D.3a}$$

$$-\mathrm{i}\varsigma\boldsymbol{b}'_{\mathrm{H}} = \partial_r\boldsymbol{v}'_{\mathrm{H}} + \partial_r^2\boldsymbol{b}'_{\mathrm{H}}, \quad \boldsymbol{e}'_{\mathrm{H}} = \mathbf{1}_r \times (\boldsymbol{v}' + \partial_r\boldsymbol{b}')_{\mathrm{H}}, \tag{D.3b,c}$$

where $P_m = \nu/\eta$ is the magnetic Prandtl number.

It is convenient to introduce

$$\mathbb{B}'^{\pm} = \boldsymbol{b}'_{\mathrm{H}} \pm \mathrm{i}\mathbf{1}_r \times \boldsymbol{b}'_{\mathrm{H}}, \quad \mathbb{E}'^{\pm} = \boldsymbol{e}'_{\mathrm{H}} \pm \mathrm{i}\mathbf{1}_r \times \boldsymbol{e}'_{\mathrm{H}}, \quad \mathbb{V}'^{\pm} = \boldsymbol{v}'_{\mathrm{H}} \pm \mathrm{i}\mathbf{1}_r \times \boldsymbol{v}'_{\mathrm{H}}, \tag{D.4a,b,c}$$

and to define $\widehat{\mathbb{B}}^{\pm}$, $\widehat{\mathbb{E}}^{\pm}$ and $\widehat{\mathbb{V}}^{\pm}$ similarly for the mantle and $\mathbb{B}^{\pm}$, $\mathbb{E}^{\pm}$ and $\mathbb{V}^{\pm}$ for the mainstream. It is clear that

$$\mathbf{1}_r \times \mathbb{B}'^{\pm} = \mp\mathrm{i}\mathbb{B}'^{\pm}, \tag{D.4d}$$

and similarly for the other variables. Equations (D.3a–c) may then be written as

$$(\epsilon P_m\partial_r^2 \pm \mathrm{i}\varpi)\mathbb{V}'^{\pm} = -\Lambda\partial_r\mathbb{B}'^{\pm}, \quad (\partial_r^2 + \mathrm{i}\varsigma)\mathbb{B}'^{\pm} = -\partial_r\mathbb{V}'^{\pm}, \tag{D.5a,b}$$

$$\mathbb{E}'^{\pm} = \mp\mathrm{i}(\mathbb{V}'^{\pm} + \partial_r\mathbb{B}'^{\pm}), \tag{D.5c}$$

where a term $\mathrm{i}\varsigma\epsilon\mathbb{V}'^{\pm}$ has been discarded from (D.5a) in comparison with $\pm\mathrm{i}\varpi\mathbb{V}'^{\pm}$; in other words, the inertial term in (D.2a) could have been omitted from the outset.

In the case of the EH layer at the CMB, we seek solutions proportional to

$$\exp[\lambda^{\pm}(r - r_o)], \quad \text{where } \mathrm{Re}(\lambda^{\pm}) > 0. \tag{D.5d,e}$$

Substituting into (D.5a,b), we obtain

$$\epsilon P_m\lambda^{\pm 4} - (\Lambda \mp \mathrm{i}\varpi)\lambda^{\pm 2} \mp \varsigma\varpi = 0, \tag{D.5f}$$

where the small term $-2\mathrm{i}\varsigma\epsilon P_m\lambda^{\pm 2}$ has been discarded in comparison with $\pm\mathrm{i}\varpi\lambda^{\pm 2}$.

In the limit $\epsilon \to 0$, the roots of (D.5f) are of two types:

- *Inner EH layer*, $\lambda = \mathrm{O}(\epsilon^{-1/2})$.
  To leading order in ϵP_m, one root of (D.5f) is

$$\lambda^{\pm 2} = (\Lambda \mp \mathrm{i}\varpi)/\epsilon P_m, \tag{D.6a}$$

  and (D.5a–c) give

$$\mathbb{V}'^{\pm} = -\lambda_{\mathrm{I}}^{\pm}\mathbb{B}'^{\pm}, \quad \mathbb{E}'^{\pm} = \mathbf{0}. \tag{D.6b,c}$$

  From (D.6a), we select $\lambda_{\mathrm{I}}^{\pm}$ with positive real part:

$$\lambda_{\mathrm{I}}^{\pm} = (2\epsilon P_m)^{-1/2}\{[(\Lambda^2 + 1)^{1/2} + \Lambda]^{1/2} \mp \mathrm{i}\varpi[(\Lambda^2 + 1)^{1/2} - \Lambda]^{1/2}\}. \tag{D.6d}$$

In dimensional terms, this gives

$$\lambda_1^{\pm} = \begin{cases} (1 \mp \mathrm{i}\varpi)/d_E, & \text{if } \Lambda \ll 1 , \\ 1/d_H, & \text{if } \Lambda \gg 1 , \end{cases} \tag{D.6e}$$

where d_E and d_H are the thicknesses of EH layers:

$$d_E = (\nu/|\Omega_r|)^{1/2}, \quad d_H = (\mu_0 \rho_0 \nu \eta)^{1/2}/|B_r^{\mathrm{m}}|, \tag{D.6f,g}$$

e.g. see chapter 3 of Dormy and Soward (2007).

- *Outer EH layer*, $\lambda = \mathrm{O}(1)$.
  To leading order in ϵP_m, the other root of (D.5f) is

$$\lambda^{\pm 2} = \mp \frac{\varsigma \varpi}{\Lambda \mp \mathrm{i}\varpi}, \tag{D.7a}$$

and (D.5a–c) give

$$\mathbb{V}'^{\pm} = \pm \mathrm{i}\varpi \Lambda \lambda_2^{\pm} \mathbb{B}'^{\pm}, \quad \mathbb{E}'^{\pm} = \varpi(\Lambda \mp \mathrm{i}\varpi)\lambda_2^{\pm} \mathbb{B}'^{\pm}. \tag{D.7b,c}$$

From (D.7a), we select $\lambda_2^{\pm}$ with positive real part:

$$\lambda_2^{\pm} = \tfrac{1}{2}(1 - \mathrm{i}\varsigma)(1 \mp \mathrm{i}\varpi)\left\{ \left(\frac{(\Lambda^2+1)^{1/2} + \Lambda}{2(\Lambda^2+1)} \right)^{1/2} \pm \mathrm{i}\varpi \left(\frac{(\Lambda^2+1)^{1/2} - \Lambda}{2(\Lambda^2+1)} \right)^{1/2} \right\}. \tag{D.7d}$$

In dimensional terms, this gives

$$\lambda_2^{\pm} = \begin{cases} (1 - \mathrm{i}\varsigma)/d_\eta, & \text{if } \Lambda \ll 1 , \\ (1 - \mathrm{i}\varsigma)(1 \mp \mathrm{i}\varpi)/2d_{\mathrm{A}}, & \text{if } \Lambda \gg 1 , \end{cases} \tag{D.7e}$$

where d_η is the skin depth and d_{A} is an Alfvénic wave length for a time scale of $\epsilon^{1/2}/|\omega|$:

$$d_\eta = (2\eta/|\omega|)^{1/2}, \quad d_{\mathrm{A}} = |B_r^{\mathrm{m}}|/(2|\Omega_r \omega| \mu_0 \rho_0)^{1/2} = (\Lambda \eta/|\omega|)^{1/2}. \tag{D.7f,g}$$

It follows from (D.6b,c) and (D.7b,c) that, for some $\boldsymbol{C}_1^{\pm}(\theta, \phi)$ and $\boldsymbol{C}_2^{\pm}(\theta, \phi)$,

$$\mathbb{B}'^{\pm} = \boldsymbol{C}_1^{\pm} \mathrm{e}^{\lambda_1^{\pm}(r - r_o)} + \boldsymbol{C}_2^{\pm} \mathrm{e}^{\lambda_2^{\pm}(r - r_o)}, \quad \mathbb{E}'^{\pm} = \varpi(\Lambda \mp \mathrm{i}\varpi)\lambda_2^{\pm} \boldsymbol{C}_2^{\pm} \mathrm{e}^{\lambda_2^{\pm}(r - r_o)}, \tag{D.8a,b}$$

$$\mathbb{V}'^{\pm} = -\lambda_1^{\pm} \boldsymbol{C}_1^{\pm} \mathrm{e}^{\lambda_1^{\pm}(r - r_o)} \pm \mathrm{i}\varpi \Lambda \lambda_2^{\pm} \boldsymbol{C}_2^{\pm} \mathrm{e}^{\lambda_2^{\pm}(r - r_o)}. \tag{D.8c}$$

Therefore

$$\varpi(\Lambda \mp \mathrm{i}\varpi)\lambda_2^{\pm}(\mathbb{V}'^{\pm} + \lambda_1^{\pm} \mathbb{B}'^{\pm}) - (\lambda_1^{\pm} \pm \mathrm{i}\varpi \Lambda \lambda_2^{\pm}) \mathbb{E}'^{\pm} = \mathbf{0}. \tag{D.8d}$$

This is equivalent to $\boldsymbol{U}' = 0$, where

$$\boldsymbol{U}' = \varpi(\lambda_2^p + \mathrm{i}\lambda_2^m \mathbf{1}_r \times)(\Lambda \boldsymbol{v}' + \varpi \mathbf{1}_r \times \boldsymbol{v}')_{\mathrm{H}} + \varpi[(\lambda_1 \lambda_2)^p + \mathrm{i}(\lambda_1 \lambda_2)^m \mathbf{1}_r \times](\Lambda \boldsymbol{b}' + \varpi \mathbf{1}_r \times \boldsymbol{b}')_{\mathrm{H}}$$

$$-(\lambda_1^p + \mathrm{i}\lambda_1^m \mathbf{1}_r \times)\boldsymbol{e}'_{\mathrm{H}} - \mathrm{i}\varpi \Lambda(\lambda_2^p + \mathrm{i}\lambda_2^m \mathbf{1}_r \times)\boldsymbol{e}'_{\mathrm{H}}, \tag{D.8e}$$

and, for any $q^{\pm}$,

$$q^p = \tfrac{1}{2}(q^+ + q^-), \quad q^m = \tfrac{1}{2}(q^+ - q^-). \tag{D.8f,g}$$

This general result, which with minor changes, applies equally to the EH layer on the ICB, will not be pursued here. In the geophysical application, $(P_m\epsilon)^{1/2} \approx 10^{-5}$ and $|\lambda_2^{\pm}/\lambda_1^{\pm}| \ll 1$. By setting $\epsilon = 0$, we may ignore the inner boundary layer (equivalent to dropping $\rho_0 \nu \partial_r^2 \boldsymbol{v}'_{\mathrm{H}}$ from (D.2a) and ignoring the no-slip boundary conditions), and replace (D.8d) by

$$\varpi(\Lambda \mp \mathrm{i}\varpi)\lambda_2^{\pm}\mathbb{B}'^{\pm} - \mathbb{E}'^{\pm} = \mathbf{0}, \tag{D.9a}$$

which is equivalent to the condition $\boldsymbol{U}' = 0$, where

$$\boldsymbol{U}' = \varpi(\lambda_2^p + \mathrm{i}\lambda_2^m \mathbf{1}_r \times)(\Lambda \boldsymbol{b}'_{\mathrm{H}} + \varpi \mathbf{1}_r \times \boldsymbol{b}'_{\mathrm{H}}) - \boldsymbol{e}'_{\mathrm{H}}. \tag{D.9b}$$

Quantities $\boldsymbol{U}$ and $\widehat{\boldsymbol{U}}$ analogous to $\boldsymbol{U}'$ are defined for the mainstream core and the mantle. They are useful because, according to (D.1d) and (D.8e), we have

$$\widehat{\boldsymbol{U}}(r_o) = \boldsymbol{U}(r_o) + \boldsymbol{U}'(r_o), \quad \text{where } \widehat{\boldsymbol{U}}(r_o) = \boldsymbol{U}(r_o). \tag{D.10a,b}$$

The second of these provides the required link across the outer EH layer.

For the mantle, a further simplification can be made. As already pointed out in appendix B, Λ is probably less than 0.1 at the CMB. We shall specialize to the case $\Lambda = 0$, in which Coriolis forces, but not Lorentz forces influence the structure of the outer boundary layer. To leading order, $\lambda_2^{\pm}$ is given by the upper of (D.7e), so that $\lambda_2^p = (1 - \mathrm{i}\varsigma)/d_\eta$ and $\lambda_2^m = 0$. Equation (D.9b) reduces, in the original unscaled units, to

$$\boldsymbol{U}' = (\mu_0 \Sigma)^{-1} \mathbf{1}_r \times \boldsymbol{b}'_{\mathrm{H}} - \boldsymbol{e}'_{\mathrm{H}}. \tag{D.11a}$$

This has a very simple interpretation; see appendix B. From (D.1a,b), we have

$$\boldsymbol{U} = (\mu_0 \Sigma)^{-1} \mathbf{1}_r \times \boldsymbol{b}_{\mathrm{H}} + s(\zeta - \widehat{\zeta}) B_r^{\mathrm{m}} \mathbf{1}_\theta. \tag{D.11b}$$

The thin layer approximation of section 8.2 gives on the CMB

$$\widehat{\boldsymbol{U}} = (\mu_0 \Sigma)^{-1} \mathbf{1}_r \times \widehat{\boldsymbol{b}}_{\mathrm{H}} + (\mu_0 \widehat{\Sigma})^{-1} \mathbf{1}_r \times (\widehat{\boldsymbol{b}} - \boldsymbol{b}^*)_{\mathrm{H}}. \tag{D.11c}$$

By applying (D.10b), the desired connection across the MDL between the mantle and core is established:

$$\widehat{\boldsymbol{b}}_{\mathrm{H}} = \frac{1}{\Sigma + \widehat{\Sigma}} (\widehat{\Sigma} \boldsymbol{b} + \Sigma \boldsymbol{b}^*)_{\mathrm{H}} - \frac{\mu_0 \Sigma \widehat{\Sigma}}{\Sigma + \widehat{\Sigma}} s(\zeta - \widehat{\zeta}) B_r^{\mathrm{m}} \mathbf{1}_\phi. \tag{D.11d}$$

The technique used to derive (D.11d) can be used to establish the connection between the FOC and SIC across the EH layer on the ICB. We now work in the reference frame rotating with the SIC. To satisfy (D.11d), the stretched boundary layer coordinate, ξ, now measures distance, $r - r_i$, from the ICB. The signs of $\lambda_1^{\pm}$ and $\lambda_2^{\pm}$ must therefore be reversed to give them negative real parts. Apart from this, (D.8e) is unchanged, as we again take the limit $\epsilon \to 0$. As already pointed out in appendix B, Λ probably exceeds 1 at the ICB, and should not be neglected. We specialize (D.9b) to the case $\Lambda \gg 1$.

To leading order in Λ^{-1}, the lower of (D.7e) gives, with the indicated reversed sign,

$$\lambda_2^p = -(1 - \mathrm{i}\varsigma)/d_A, \quad \lambda_2^m = \mathrm{i}\varpi(1 - \mathrm{i}\varsigma)/d_A. \tag{D.12a,b}$$

In the original unscaled units, (D.9b) becomes

$$\boldsymbol{U}' = -\frac{\varpi}{\mu_0 \Sigma}\left(\frac{\Lambda}{2}\right)^{1/2}(\boldsymbol{b}' + \varpi \mathbf{1}_r \times \boldsymbol{b}')_{\mathrm{H}} - \boldsymbol{e}'_{\mathrm{H}}. \tag{D.12c}$$

The corresponding $\boldsymbol{U}$ for the mainstream core is

$$\boldsymbol{U} = -\frac{\varpi}{\mu_0 \Sigma}\left(\frac{\Lambda}{2}\right)^{1/2}(\boldsymbol{b} + \varpi \mathbf{1}_r \times \boldsymbol{b})_{\mathrm{H}} - s(\zeta - \widetilde{\zeta})B_r^{\mathrm{m}}\mathbf{1}_\theta. \tag{D.12d}$$

The high frequency approximation of section 8.2 gives on the ICB

$$\widetilde{\boldsymbol{U}} = -\frac{\varpi}{\mu_0 \Sigma}\left(\frac{\Lambda}{2}\right)^{1/2}(\widetilde{\boldsymbol{b}} + \varpi \mathbf{1}_r \times \widetilde{\boldsymbol{b}})_{\mathrm{H}} - \frac{1}{\mu_0 \widetilde{\Sigma}}\mathbf{1}_r \times \widetilde{\boldsymbol{b}}_{\mathrm{H}}. \tag{D.12e}$$

For $\Lambda \gg 1$, the last term in (D.12e) is negligible in comparison with the first term on the right-hand side of (D.12d), By applying (D.10b) now to the ICB instead of the CMB, the desired connection across the EH layer between the SIC and the mainstream is established as

$$\widetilde{b}_\phi - b_\phi = -\varpi(\widetilde{b}_\theta - b_\theta) = \Lambda^{-1/2}\mu_0 \Sigma s(\zeta - \widetilde{\zeta})B_r^{\mathrm{m}}. \tag{D.12f}$$

This entire analysis breaks down at the equator, where the inner and outer EH boundary layers have singularities. This situation is familiar in non-magnetic contexts for Ekman layers on closed surfaces, and we have followed the standard practice of assuming the singularities are passive and ignorable. There may also be difficulties on any null flux curve, such as the magnetic equator, where $B_r^{\mathrm{m}} = 0$. We disregarded these too.

Appendix E: Gravitational and magnetic interactions

This appendix generalizes some of the results reported in appendix B of Braginsky and Roberts (1995) on gravitation theory and extends them to EM theory. The notation will differ from that in the main text in one significant respect. In the main text, $\widehat{\boldsymbol{g}}(\boldsymbol{r})$, $\breve{\boldsymbol{g}}(\boldsymbol{r})$, and $\widetilde{\boldsymbol{g}}(\boldsymbol{r})$ are the gravitational fields when $\boldsymbol{r}$ lies in the mantle, FOC, and SIC, respectively; see for example (7a). Here however they are the gravitational fields produced by the density sources $\widehat{\rho}$, $\breve{\rho}$, and $\widetilde{\rho}$, so that, for example, $\boldsymbol{g}(\boldsymbol{r}) = \widehat{\boldsymbol{g}}(\boldsymbol{r}) + \breve{\boldsymbol{g}}(\boldsymbol{r}) + \widetilde{\boldsymbol{g}}(\boldsymbol{r})$, for any point $\boldsymbol{r}$ wherever situated. Similarly, $\widehat{\boldsymbol{B}}(\boldsymbol{r})$, $\breve{\boldsymbol{B}}(\boldsymbol{r})$, and $\widetilde{\boldsymbol{B}}(\boldsymbol{r})$ will be the magnetic fields produced by the individual sources, $\widehat{\boldsymbol{J}}$, $\breve{\boldsymbol{J}}$, and $\widetilde{\boldsymbol{J}}$.

If the gravitational source ρ of $\boldsymbol{g}$ is nonzero only within a region V′, Poisson's equation (2g) gives the gravitational potential and field at any $\boldsymbol{r}$ inside or outside V′ as

$$\Phi(\boldsymbol{r}) = -G\int_{\mathrm{V}'}\frac{\rho(\boldsymbol{r}')}{|\boldsymbol{r} - \boldsymbol{r}'|}\mathrm{d}v, \quad \boldsymbol{g}(\boldsymbol{r}) = -G\int_{\mathrm{V}'}\frac{\boldsymbol{r} - \boldsymbol{r}'}{|\boldsymbol{r} - \boldsymbol{r}'|^3}\rho(\boldsymbol{r}')\mathrm{d}v. \tag{E.1a,b}$$

By (E.1b), the force and torque exerted by the gravitational field created *by* the mass in volume V_1 *on* the mass in volume V_2 are

$$\boldsymbol{F}^G_{1\mathrm{on}2} = \int_{\mathrm{V}_2} \rho_2 \boldsymbol{g}_1 \mathrm{d}v = -G \int_{\mathrm{V}_1}\int_{\mathrm{V}_2} \frac{\boldsymbol{r}_1 - \boldsymbol{r}_2}{|\boldsymbol{r}_1 - \boldsymbol{r}_2|^3} \rho_1 \rho_2 \mathrm{d}v \mathrm{d}v = -\int_{\mathrm{V}_1} \rho_1 \boldsymbol{g}_2 \mathrm{d}v = -\boldsymbol{F}^G_{2\mathrm{on}1} \quad \text{(E.2a)}$$

$$\boldsymbol{\Gamma}^G_{1\mathrm{on}2} = \int_{\mathrm{V}_2} \boldsymbol{r}_2 \times \rho_2 \boldsymbol{g}_1 \mathrm{d}v = G \int_{\mathrm{V}_1}\int_{\mathrm{V}_2} \frac{\boldsymbol{r}_1 \times \boldsymbol{r}_2}{|\boldsymbol{r} - \boldsymbol{r}'|^3} \rho_1 \rho_2 \mathrm{d}v \mathrm{d}v = -\int_{\mathrm{V}_1} \boldsymbol{r}_1 \times \rho_1 \boldsymbol{g}_2 \mathrm{d}v = -\boldsymbol{\Gamma}^G_{2\mathrm{on}1}. \quad \text{(E.2b)}$$

In these reciprocity relations, ρ_1 etc stands for $\rho(\boldsymbol{r}_1)$ etc. By taking V_1 and V_2 to be the same volume, it is seen that the self-force and self-torque of a mass distribution on itself are zero.

These results have implications for the 3 component system of mantle, FOC, and SIC, e.g.

$$\widehat{\boldsymbol{\Gamma}}^G_a + \widetilde{\boldsymbol{\Gamma}}^G_a = \int_{\widehat{\mathrm{V}}} \widehat{\rho}_a \boldsymbol{r} \times \breve{\boldsymbol{g}}_a \mathrm{d}v + \int_{\widetilde{\mathrm{V}}} \widetilde{\rho}_a \boldsymbol{r} \times \breve{\boldsymbol{g}}_a \mathrm{d}v = -\int_{\breve{\mathrm{V}}} \breve{\rho}_a \boldsymbol{r} \times (\widehat{\boldsymbol{g}} + \widetilde{\boldsymbol{g}})_a \mathrm{d}v = -\int_{\breve{\mathrm{V}}} \breve{\rho}_a \boldsymbol{r} \times \boldsymbol{g}_a \mathrm{d}v. \quad \text{(E.3a)}$$

Therefore, by hydrostatic balance and (35c),

$$\widehat{\boldsymbol{\Gamma}}^G_a + \widetilde{\boldsymbol{\Gamma}}^G_c = -\int_{\breve{\mathrm{V}}} \boldsymbol{r} \times \boldsymbol{\nabla} p_a \mathrm{d}v = \breve{\boldsymbol{\Gamma}}^T_a = -\widehat{\boldsymbol{\Gamma}}^T_a - \widetilde{\boldsymbol{\Gamma}}^T_a, \quad \text{(E.3b)}$$

which confirms (39e) by a different method.

The integrals (E.2a,b) over volume can be usefully transformed into surface integrals, though at the expense of expressions that are harder to interpret than (37a,b). The transformation draws on the analogy between the theories governing Newtonian gravitation and electrostatics, the only difference between these theories being one of sign: like charges repel but all masses attract. Scalar formulations of the electrostatic force and torque are derived in §§193 and 194 of Jeans (1925). The vectorial formulations of the gravitational force and torque are derived in appendix B of Braginsky and Roberts (1995). To derive the gravitational stress tensor, we use (2e) to write

$$4\pi G \rho g_i = -g_i \nabla_j g_j = -\nabla_j (g_i g_j) - [\boldsymbol{g} \times (\boldsymbol{\nabla} \times \boldsymbol{g})]_i + g_j \nabla_i g_j. \quad \text{(E.4a)}$$

Equations (37c,d) then follow from (2c,d):

$$\rho g_i = \nabla_j S^G_{ij}, \quad \text{where } S^G_{ij} = -(4\pi G)^{-1}(g_i g_j - \tfrac{1}{2} g^2 \delta_{ij}) \quad \text{(E.4b,c)}$$

is the gravitational stress tensor. The gravitational "pressure", $-g^2/8\pi G$, in (E.4c) is also the gravitational energy density. Equations (E.4b,c) enable (37a,b) to be written as integrals over the surface, A, of V, see (37e,f).

The gravitational interaction between two bodies, V_1 and V_2, can be treated similarly. Alternative expressions for (E.2a,b) are

$$\boldsymbol{F}^G_{1\mathrm{on}2} = -\frac{1}{4\pi G} \oint_{\mathrm{S}_2} [(\boldsymbol{n}_2 \cdot \boldsymbol{g}_1)\boldsymbol{g}_2 + (\boldsymbol{n}_2 \cdot \boldsymbol{g}_2)\boldsymbol{g}_1 - (\boldsymbol{g}_1 \cdot \boldsymbol{g}_2)\boldsymbol{n}_2] \mathrm{d}a = -\boldsymbol{F}^G_{2\mathrm{on}1}, \quad \text{(E.5a)}$$

and

$$\boldsymbol{\Gamma}^G_{1\mathrm{on}2} = -\frac{1}{4\pi G} \oint_{\mathrm{S}_2} \boldsymbol{r} \times [(\boldsymbol{n}_2 \cdot \boldsymbol{g}_1)\boldsymbol{g}_2 + (\boldsymbol{n}_2 \cdot \boldsymbol{g}_2)\boldsymbol{g}_1 - (\boldsymbol{g}_1 \cdot \boldsymbol{g}_2)\boldsymbol{n}_2] \mathrm{d}a = -\boldsymbol{\Gamma}^G_{2\mathrm{on}1}. \quad \text{(E.5b)}$$

where $\boldsymbol{n}_2$ is the normal to the boundary, S_2, of V_2 directed outwards from V_2. The first step in deriving (E.5a) from (E.2a), and similarly (E.5b) from (E.2b), is to replace $\rho_2 \boldsymbol{g}_1$ by $\rho_2 \boldsymbol{g}_1 + \rho_1 \boldsymbol{g}_2$. The added term does not contribute to $\boldsymbol{F}^G_{1on2}$ or $\boldsymbol{\Gamma}^G_{1on2}$ because $\rho_1 = 0$ in V_2, but allows the transformation

$$4\pi G(\rho_2 \boldsymbol{g}_1 + \rho_1 \boldsymbol{g}_2)_i = -g_{2i}\nabla_j g_{1j} - g_{1i}\nabla_j g_{2j} = -\nabla_j (g_{1i}g_{2j} + g_{1j}g_{2i}) + \nabla_i (g_{1j}g_{2j}), \quad \text{(E.5c)}$$

from which (E.5a,b) follow.

Analogous results hold for the magnetic field, $\boldsymbol{B}$, on representing this by a vector potential $\boldsymbol{A}$ obeying the Coulomb gauge condition:

$$\boldsymbol{B} = \nabla \times \boldsymbol{A}, \quad \nabla \cdot \boldsymbol{A} = 0, \quad \text{(E.6a,b)}$$

$\mu_0/4\pi$, $\boldsymbol{J}$ and $\boldsymbol{A}$ replay the roles of $-G$, ρ and Φ above. The consequences are sufficiently similar to the gravitational results that only a shortened version of the EM results is given below. We consider $\boldsymbol{J}$ to be bounded everywhere, to vanish outside a volume V′ with surface S, and to obey

$$\nabla \cdot \boldsymbol{J} = 0, \quad \text{where } \boldsymbol{n} \cdot \boldsymbol{J} = 0 \text{ on S}, \quad \text{(E.6c,d)}$$

the first of which is a consequence of Ampère's law,

$$\nabla \times \boldsymbol{B} = \mu_0 \boldsymbol{J} \quad \text{and implies} \quad \nabla^2 \boldsymbol{A} = -\mu_0 \boldsymbol{J}. \quad \text{(E.6e,f)}$$

The solution to the vector Poisson equation (E.6f) is

$$\boldsymbol{A}(\boldsymbol{r}) = \frac{\mu_0}{4\pi}\int_{V'} \frac{\boldsymbol{J}(\boldsymbol{r}')\mathrm{d}v}{|\boldsymbol{r} - \boldsymbol{r}'|} \quad \text{and implies } \boldsymbol{B}(\boldsymbol{r}) = \frac{\mu_0}{4\pi}\int_{V'} \frac{\boldsymbol{J}(\boldsymbol{r}') \times (\boldsymbol{r} - \boldsymbol{r}')}{|\boldsymbol{r} - \boldsymbol{r}'|^3}\mathrm{d}v, \quad \text{(E.7a,b)}$$

which is the well-known Biot–Savart law. One way to derive the force and torque on the current distribution in V employs

$$(\boldsymbol{J} \times \boldsymbol{B})_i = [\boldsymbol{J} \times (\nabla \times \boldsymbol{A})]_i = J_j(\nabla_j A_i - \nabla_i A_j). \quad \text{(E.8a)}$$

Then, by (E.6c,d),

$$F^M_i = \int_V [J_j \nabla_i A_j - \nabla_j (A_i J_j)]\mathrm{d}v = \int_V J_j \nabla_i A_j \,\mathrm{d}v, \quad \text{(E.8b)}$$

$$\Gamma^M_i = \int_V \epsilon_{ijk} r_j J_\ell (\nabla_k A_\ell - \nabla_\ell A_k)\mathrm{d}v. \quad \text{(E.8c)}$$

Apply (E.7a) to $\boldsymbol{A}_1$ created by the current distribution $\boldsymbol{J}_1$ in V_1, and substitute it into (E.8c) to determine the force on $\boldsymbol{J}_2$ in V_2 due to $\boldsymbol{J}_1$:

$$\boldsymbol{F}^M_{1on2} = \frac{\mu_0}{4\pi}\int_{V_1}\int_{V_2} \frac{\boldsymbol{r}_1 - \boldsymbol{r}_2}{|\boldsymbol{r}_1 - \boldsymbol{r}_2|^3}(\boldsymbol{J}_1 \cdot \boldsymbol{J}_2)\mathrm{d}v\mathrm{d}v = -\boldsymbol{F}^M_{2on1}. \quad \text{(E.8d)}$$

Similarly when $\boldsymbol{A}_1$ is substituted into the second term in (E.8b), it can be simplified as follows:

$$\int_{V_1}\int_{V_2} (\boldsymbol{r}_2 \times \boldsymbol{J}_1)\boldsymbol{J}_2 \cdot \left(\frac{\boldsymbol{r}_1 - \boldsymbol{r}_2}{|\boldsymbol{r}_1 - \boldsymbol{r}_2|^3}\right)\mathrm{d}v\mathrm{d}v = \int_{V_1}\int_{V_2} (\boldsymbol{r}_2 \times \boldsymbol{J}_1)\nabla_2 \cdot \left(\frac{\boldsymbol{J}_2}{|\boldsymbol{r}_1 - \boldsymbol{r}_2|}\right)\mathrm{d}v\mathrm{d}v$$

$$= \int_{V_1} \left(\oint_{S_2} \frac{(\boldsymbol{r}_2 \times \boldsymbol{J}_1)\boldsymbol{n}_2 \cdot \boldsymbol{J}_2}{|\boldsymbol{r}_1 - \boldsymbol{r}_2|} \mathrm{d}a \right) \mathrm{d}v + \int_{V_1} \int_{V_2} \frac{\boldsymbol{J}_1 \times \boldsymbol{J}_2}{|\boldsymbol{r}_1 - \boldsymbol{r}_2|} \mathrm{d}v \, \mathrm{d}v. \tag{E.8e}$$

The surface integral vanishes by (E.6d). By combining the remnant with the first term on the right-hand side of (E.8b), we obtain

$$\boldsymbol{\Gamma}^M_{1\mathrm{on}\,2} = -\frac{\mu_0}{4\pi} \int_{V_1} \int_{V_2} \left(\frac{\boldsymbol{J}_1 \times \boldsymbol{J}_2}{|\boldsymbol{r}_1 - \boldsymbol{r}_2|} + \frac{\boldsymbol{r}_1 \times \boldsymbol{r}_2}{|\boldsymbol{r}_1 - \boldsymbol{r}_2|^3} (\boldsymbol{J}_1 \cdot \boldsymbol{J}_2) \right) \mathrm{d}v \mathrm{d}v = -\boldsymbol{\Gamma}^M_{2\mathrm{on}\,1}. \tag{E.8f}$$

By taking V_2 to be the same volume as V_1 in (E.8d,f), it follows that the self-force and self-torque on a volume current are zero.

The other way to derive the force and torque on the current distribution in V employs

$$\mu_0(\boldsymbol{J} \times \boldsymbol{B})_i = [(\boldsymbol{\nabla} \times \boldsymbol{B}) \times \boldsymbol{B}]_i = B_j(\nabla_j B_i - \nabla_i B_j) = \nabla_j (B_i B_j - \tfrac{1}{2} B^2 \delta_{ij}) = \mu_0 \nabla_j S^M_{ij}, \tag{E.9a}$$

which is the basis of the transformation of $\boldsymbol{F}^M$ and $\boldsymbol{\Gamma}^M$ into surface integrals used in section 8.1. It is also the basis of integrals analogous to (E.5a,b) for the magnetic force and torque that V_1 exerts on V_2:

$$\boldsymbol{F}^M_{1\mathrm{on}\,2} = \frac{1}{\mu_0} \oint_{S_2} [(\boldsymbol{n}_2 \cdot \boldsymbol{B}_1)\boldsymbol{B}_2 + (\boldsymbol{n}_2 \cdot \boldsymbol{B}_2)\boldsymbol{B}_1 - (\boldsymbol{B}_1 \cdot \boldsymbol{B}_2)\boldsymbol{n}_2] \mathrm{d}a = -\boldsymbol{F}^M_{2\mathrm{on}1}, \tag{E.9b}$$

$$\boldsymbol{\Gamma}^M_{1\mathrm{on}\,2} = \frac{1}{\mu_0} \oint_{S_2} \boldsymbol{r} \times [(\boldsymbol{n}_2 \cdot \boldsymbol{B}_1)\boldsymbol{B}_2 + (\boldsymbol{n}_2 \cdot \boldsymbol{B}_2)\boldsymbol{B}_1 - (\boldsymbol{B}_1 \cdot \boldsymbol{B}_2)\boldsymbol{n}_2] \mathrm{d}a = -\boldsymbol{\Gamma}^M_{2\mathrm{on}\,1}. \tag{E.9c}$$

An obvious advantage of (E.8d,f) over (E.9b,c) is that the former does not require $\boldsymbol{B}_1$ and $\boldsymbol{B}_2$ to be derived from given $\boldsymbol{J}_1$ and $\boldsymbol{J}_2$.